Egocentric Distance Encoding in the Posterior Parietal Cortex

Thesis by

Rajan Bhattacharyya

In Partial Fulfillment of the Requirements

For the Degree of

Doctor of Philosophy

California Institute of Technology

Pasadena, California

2009

(Defended August 29, 2008)

Acknowledgements

I wish to thank my advisor, Richard Andersen, for his time, guidance, and careful attention and mentorship all of these years. I wish to acknowledge my committee: Shin Shimojo, Pietro Perona, Christof Koch, and Joel Burdick for their time and thoughtful advice. Thank you also to: Grant Mulliken, EunJung Hwang, He Cui, for helpful comments on the journal manuscript submitted based on this thesis work; Zoltan Nadasdy, Rodrigo Quian-Quiroga, and Alexander Gail for useful discussions; Igor Kagan for discussions and assistance on MRI images; Kelsie Pejsa, Nicole Sammons, Lea Martel, J. Baer and C. Lindsell for help with animal handling and veterinary assistance; V. Shcherbatyuk for computer support; T. Yao for administrative assistance; and R. Panagua and M. Walsh for laboratory equipment construction. I also wish to thank Sam Musallam and Brian Corneil for training and the opportunity for hands-on experience in neurophysiology and the collection of data in the cortical prosthetics project, and to Bijan Pesaran for discussions and mentorship.

I owe Grant so much for my experience in the lab: discussions, lunches, and venting frustrations when losing the isolation of a neuron during recording! Grant and EunJung were wonderful officemates, and our many discussions on all our work were important to my thesis work, and so much else in life. Intellectual stimulation was always available at the kitchen table in the lab with so many lab members, and I am grateful to all of them. Tessa, besides getting me motivated to go to the gym, you also shaped me up for my first

job interview, and because of your help, it was a success. Michael Campos, my CNS classmate and friend, was always there to listen and help when I needed it. My dear labmate Asha Iyer always provided support and encouragement.

To my dear monkeys, Gizmo and Tarzan, who performed so well and made the study of egocentric distance in parietal cortex possible. Chewie and Gizmo were 2 of a kind, and will always hold a special place in my (and Grant's) heart and mind. I wish to thank my loving wife, Richa Amar, my parents Ranjan and Chitrita Bhattacharyya, and my in-laws Gulshan and Kumud Amar, who provided me all the love and support in the world through my work and beyond.

Abstract

Spatial perception and action in goal directed, visually guided reach movements requires the coordination between sensory information arriving in intrinsic reference frames that encode location in egocentric coordinates, and extrinsic reference frames that encode location in allocentric or object centered coordinates. Previous studies have shown that the parietal reach region (PRR) encodes the two dimensional location of frontoparallel reach targets in an eye centered reference frame in early movement plans (Batista 1999; Snyder et al. 2000). Performing a visually guided reach initially requires the ability to perceive the depth of a target in three dimensional space. Beyond that initial perception, however, reach plans may represent the egocentric distance of the target in different ways. To investigate how a reach target is represented in three dimensions, recordings were made of the spiking activity of PRR neurons from two rhesus macaques trained to fixate and perform memory reaches to targets at different depths. Reach and fixation targets were configured to explore whether neural activity directly reflects egocentric distance as the amplitude of the required motor command, which is the absolute depth of the target, or rather the relative depth of the target with reference to fixation depth.

This thesis shows that planning activity in PRR represents the depth of the reach target as a function of disparity and fixation depth, the spatial parameters important for encoding the egocentric distance of a reach goal in an eye centered reference frame. Most PRR neurons were found to be sensitive to the disparity of a reach target (82%), and vergence angle (74%) which determines fixation depth. Egocentric distance can be computed from

separate subpopulations of neurons encoding disparity and vergence angle in a subsequent processing stage, or represented in a single population of neurons that encode both disparity and vergence angle. Most PRR neurons carry both disparity and vergence angle signals, and comparisons of several modulation indices and the information carried in firing rates for each variable show a single homogenous PRR population encodes egocentric distance. The strength of modulation by disparity was maintained across vergence angle, where vergence angle gain modulates disparity tuning while preserving the location of peak tuning features in PRR neurons. PRR neurons code depth with respect to the fixation point, however, since the activity is gain modulated by vergence angle the absolute depth of the reach target can be decoded from the population activity. Neural activity in PRR shows a wide range of sensitivity to both target disparity and fixation depth that has never been previously tested in a reach task. The results demonstrate a specific role for PRR neurons in supporting eye-hand coordination when decoupling the effector from the point of gaze.

Table of Contents

List of Figures

List of Tables

Chapter 1 Introduction

Primates developed the ability to plan and perform complex actions using forelimbs that were essential to natural behaviors, ranging from feeding and locomotion to tool usage and gestural communication. The explosive expansion of the cerebral cortex in primates was the evolutionary platform to support these abilities (Allman 1999). An important primitive in the basis set of the primate action repertoire that supports these complex actions is the goal directed reach movement. Central to the performance of goal directed reaching is the interplay of perception and action. The theory of action-perception cycles, first described in the early twentieth century, discusses the critical interaction of perceptual processes necessary for sensorimotor behavior from the viewpoint of learning the consequences of motor action through observation during development (Piaget 1930). Neuroscience in the last two decades has revealed much about the neural pathways that are involved in visual perception and action that are central to goal directed, visually guided reach movements (Goodale and Milner 1992; Milner and Goodale 1995). Figure 1-1 shows a simplified side view of the human brain with some of the major sulci and areas in these pathways. Goal directed, visually guided reaches require an accurate estimate of the target location in three-dimensional space that necessitates the integration of depth cues. Knowledge of the distance of the target is necessary to end the reach at the appropriate depth. This thesis explores how neural activity in early reach plans reflects the distance to reach targets in depth.

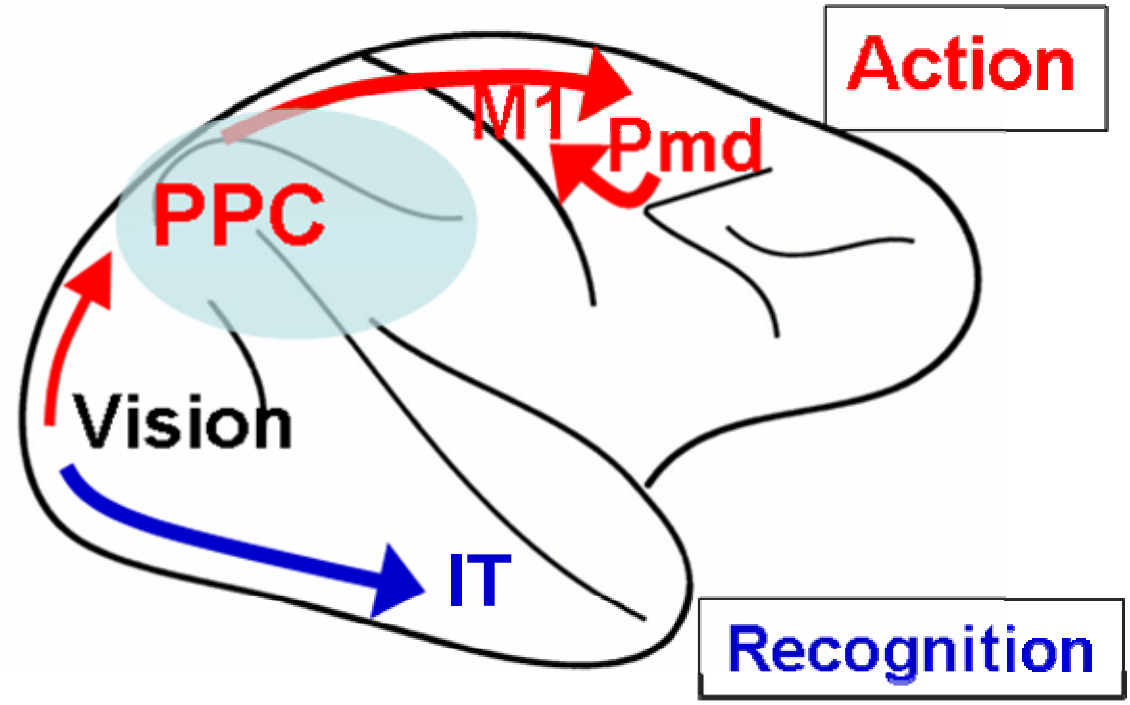

Figure 1-1 – Pathways for visually guided motor behaviors. Visual information enters the brain through the thalamus and arrives in the cortex in the occipital lobe, labeled "Vision". Processing occurs in the visual cortices, and the information bifurcates into 2 pathways, shown in blue and red. The dorsal/what pathway is shown in red, labeled "Action". Visual information enters the PPC, where it is combined with information from other modalities, such as proprioception (indicating body state). Simultaneously, visual information is processed in the ventral/what pathway, shown in blue and labeled "Recognition". Adapted from (Goodale and Milner 1992).

1.1 Dorsal and Ventral Streams in Visually Guided Reaching

Information from the early visual cortex in the occipital lobe initially feeds both dorsal and ventral pathways, where it is processed in the inferotemporal cortex (IT) to recognize objects in the visual scene (ventral stream), and in the posterior parietal cortex (PPC) to encode the locations of these targets in different reference frames (Andersen and Zipser 1988; Andersen, Snyder et al. 1993; Andersen 1994; Constantinidis and Steinmetz 2005) (dorsal stream). There is necessarily a high degree of interaction between the dorsal and

ventral pathways that supports perception and action (Himmelbach and Karnath 2005; Ellison and Cowey 2007; Krigolson, Clark et al. 2007), which rely on the network of frontal areas (not shown) related to executive control (Koechlin, Ody et al. 2003; Dias, McGinnis et al. 2006) and biasing attention and target selection (Buschman and Miller 2007). The final selection of a target, emanating from executive areas in the frontal cortex, is again used in the PPC in the formation of a final movement plan (Hasegawa 2000; Miller 2001; Rizzuto, Mamelak et al. 2005; Dias, McGinnis et al. 2006). An interplay of activity related to decision making exists between the PPC and frontal areas as evidenced by studies detailing neuronal tuning to choice related parameters in each area (Platt and Glimcher 1999; Dorris 2004; Cui and Andersen 2007).

The ventral ("what") pathway is implicated in the process of perceiving objects in the visual scene, shown in blue and labeled "Recognition". Though it is not clear whether the segmentation of the visual scene and identification of objects rely solely on the ventral pathway, there is a large body of evidence that suggests that inferotemporal cortex (IT) contains a neural representation of object categories (Ishai, Ungerleider et al.; Gross, Rocha-Miranda et al. 1972) and faces (Kiani, Esteky et al. 2005; Afraz, Kiani et al. 2006), and the medial temporal lobe encodes high level abstract representations of objects and individuals (Quiroga, Reddy et al. 2005).

The dorsal ("where") pathway is implicated in the perception of space and movement coordination, shown in red and labeled "Action". The PPC is a central element in the dorsal pathway, and receives and processes sources of information that relate the state of

the body and limbs, the location of objects, and the formation of motor plans (Andersen 1985; Andersen 1988; Andersen 1997; Jeannerod 1997). Movement plans are processed in the premotor cortex (Pmd – dorsal premotor area), where neural activity can represent goal information such as target location (Cisek and Kalaska 2002; Hoshi and Tanji 2002), information regarding the dynamics of the upcoming reach (Churchland, Santhanam et al. 2006), and target, hand, and eye positions relative to each other (Pesaran, Nelson et al. 2006). Finally, motor cortical areas (M1 – primary motor cortex) discharge to drive muscles and move the effector (Georgopoulos 1982; Georgopoulos, Schwartz et al. 1986; Georgopoulos 1988; Schwartz, Kettner et al. 1988; Mushiake, Tanatsugu et al. 1997; Koike, Hirose et al. 2006; Naselaris, Merchant et al. 2006).

1.2 Reference Frames and Multimodal Integration in the PPC

Sensory information arrives to the cerebral cortex in modality specific reference frames: information from the retinas arrives in an eye centered (or retinotopic) reference frame, information from the cochleas arrive in a head centered reference frame, touch and pressure information from the skin arrives in a somatotopic reference frame. Intrinsic reference frames such as those described above can be integrated into a higher order reference frame that is referenced to the subject (egocentric). Further, information can be represented in an extrinsic reference frame that is referenced to a feature outside of the subject that is view independent, such as a landmark in space (allocentric) or relative distances between objects (object centered).

Cognitive functions such as perception and action require coordinate transformations to combine sensory input that is initially represented in their intrinsic reference frames. For instance, auditory information (and localization) naturally occurs in a head centered reference frame in the early stages of processing in auditory cortex (Ahissar, Ahissar et al. 1992; Recanzone, Guard et al. 2000). The locations of sounds, however, are also represented in eye centered coordinates in the lateral intraparietal sulcus (LIP, in the PPC) (Stricanne, Andersen et al. 1996; Cohen and Andersen 2000; Cohen and Andersen 2000). Neurons in area LIP also exhibit body referenced modulation by neck proprioception, and show that this area contains a representation of target location that is suited to coordinate movements of the eyes and the head together to acquire the target (Snyder, Grieve et al. 1998). Recently, it has been shown that the spatial location of reach goals is encoded simultaneously in eye centered coordinates in the parietal reach region (PRR) and in both eye and hand coordinates in area 5 in the PPC instead of dynamically evolving in the different cortical areas, as would be expected in purely feed-forward processing (Buneo, Batista et al. 2008). These results provide evidence that a network of areas in the PPC supporting planned reaches and eye-hand coordination perform coordinate transformations continuously to maintain a synchronous representation of space in different reference frames.

Complex spatial navigation requires the ability to learn, store, and retrieve spatial configurations. The ability to plan routes within a spatial configuration is powerful if the locations are encoded with respect to it, allowing the flexible formation of plans without

any view point dependence. Spatial navigation requires coordinate transformations to build a world centered, or allocentric representation of space from sensory input in reference frames that is view dependent. The hippocampus has been implicated in learning and storing allocentric memories in spatial navigation tasks (Morris, Hagan et al. 1986; Kesner, Farnsworth et al. 1989; O'Keefe 1991; Gleason and Rothblat 1994; Galati, Lobel et al. 2000; Parslow, Morris et al. 2005; Schenk 2006), and facilitating in the transformation from egocentric to allocentric reference frames (Kesner, Farnsworth et al. 1989; Tamura, Ono et al. 1990; Holscher, Jacob et al. 2004; Zaehle, Jordan et al. 2007). The PPC contains allocentric representations of space in addition to egocentric ones. Area 7a in the PPC is modulated by vestibular inputs (present in active head movements), and represents visual target location in an allocentric reference frame (Snyder, Grieve et al. 1998). Area 7a projects to the parahippocampal region, which is implicated in the formation and recall of allocentric/topographical memories (Rolls, Robertson et al. 1997; Maguire, Frith et al. 1998; Hartley, Bird et al. 2007).

Both movement planning and the online control during movement execution of a visually guided reach relies on the feedback from the perception of body state (*e.g.*, limb location based on proprioception and a forward model), and the perception of the hand and target location in visual space (Clower, Hoffman et al. 1996; Connolly and Goodale 1999; Scheidt, Conditt et al. 2005; Sober and Sabes 2005). Anatomical studies detail the confluence of proprioceptive, somatosensory, auditory, and visual pathways in the PPC, making the position of the hands available in two different sensory modalities (Seltzer and Pandya 1980; Edward H. Yeterian 1985; Seltzer and Pandya 1986). The PPC brings

together information from the different senses to coordinate movements that are inherently in multiple reference frames, and employs coordinate transformations to combine information in a common reference frame (Andersen 1985; Andersen 1994; Andersen 1997; Andersen, Snyder et al. 1997; Sakata, Taira et al. 1997; Shipp, Blanton et al. 1998; Lewis and Van Essen 2000; Andersen 2003).

1.3 Egocentric Distance

Extrinsic reference frames represent spatial locations based on the computation of the distance of objects that are initially represented in an intrinsic reference frame. Visually guided reaching likely involves both extrinsic and intrinsic reference frames (Neggers, Van der Lubbe et al. 2006; Krigolson, Clark et al. 2007; Neely, Heath et al. 2008), however it is unknown where in the cerebral cortex the distance of targets is represented, and how it is represented. In this thesis, I hypothesize that early reach plans in the PRR represent target distance in an egocentric reference frame. It is possible to represent target distance in an egocentric reference frame explicitly as the absolute distance of the target from some body reference (*e.g.*, distance from head, trunk, hands), or a relative distance referenced to gaze position. Studies have examined the ability for humans to make perceptual estimates of depth, or distance, in a variety of tasks and conditions. Perceptual estimates of distance and visuomotor performance in walking tasks (Kudoh 2005) and reaching tasks (Dijkerman, Milner et al. 1996; Carey, Dijkerman et al. 1998; Baylis and Baylis 2001) indicate that a dissociation exists between depth/distance encoding between perceptual estimates and visuomotor tasks. In addition, high level

cognitive biases such as expectation affect the perceptual estimation of distance as expected but do not affect reach performance to targets in depth (Pagano and Isenhower 2008). These findings indicate that the encoding of target distance is dependent on both the task and the primary neural pathway involved in performing it.

Performance in memory reaches subsequent to intervening vergence eye movements are consistent with an egocentric reference frame that is referenced to gaze position, or a retinally based representation for reach target distance (Van Pelt and Medendorp 2008). Early reach plans in the PRR have been shown to encode the direction of an intended reach movement to eccentric targets on a single frontoparallel plane in an eye centered reference frame (Batista 1999; Snyder, Batista et al. 2000; Andersen 2002). It is not known whether reach plan activity in PRR contains a representation of target distance, and whether this distance is referenced to gaze position. This thesis examines whether firing rates of neurons in the PRR encode the egocentric distance of a reach target, and explores the representation of target distance as an absolute or relative distance referenced to viewing distance by varying the relationship between target depth, disparity, and vergence angle.

1.4 Depth Perception

The ability to sense the depth of visual stimuli has been examined for hundreds of years. A window into man's understanding of this particular aspect of vision is in the art of many cultures, for example, in the transition of the "flattened" descriptions of biblical scenes in the illuminated manuscripts of medieval Europe to the realism present in Renaissance era paintings (Livingstone 1990; Arnheim 2004). One of the earliest published works on the subject is by Charles Wheatstone and details the occurrence of perspective and retinal correspondence (Wheatstone 1838). Wheatstone examines the percepts created by various configurations of lines and objects using a stereoscope, discusses the findings of a bistable percept by Necker, and refutes the popular doctrine that images presented to each retina require physical correspondence to create a sense of stereoscopic depth with specific examples.

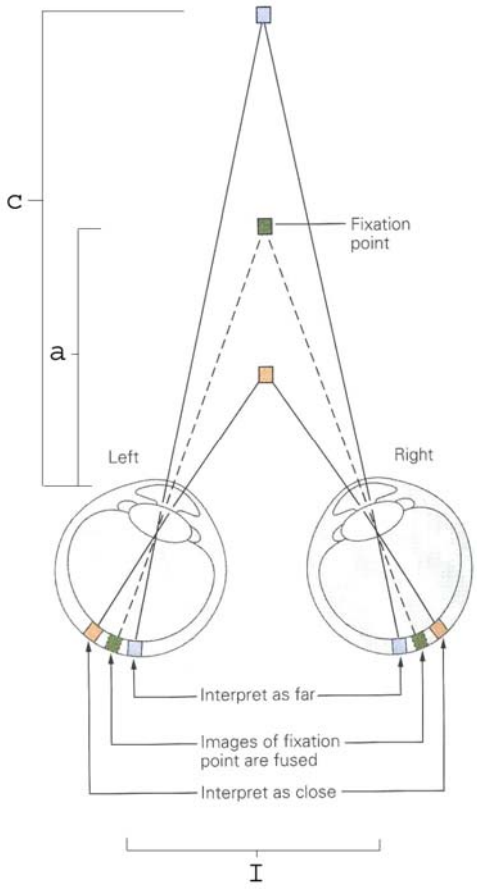

Figure 1-2 - Binocular Disparity (adapted from (Kandel 2000))

The ability to infer the depth of objects in a visual scene depends on many factors, and has made its study a popular topic. The sensation of depth in natural visual scenes is created from the combination of many informational elements. These informational elements, or depth cues, can provide

information that is directly due to physical circumstances, such as the separation of the eyes, or relational information that can prescribe the depth of one object relative to another. Another dimension is the changing information due to dynamics, where integration and cue combination occurs across time. An excellent discussion of depth cues can be found in (Palmer 1999). The influence of these factors has been examined through the study of human behavior (psychophysics) (Bulthoff, Edelman et al. 1995; Landy, Maloney et al. 1995; Gilaie-Dotan, Ullman et al. 2002; Knill 2003; Mather and Smith 2004), and more recently through imaging and physiology to directly examine the neural basis of depth perception (Poggio and Poggio 1984; Poggio 1995; DeAngelis 2000; Nishida, Hayashi et al. 2001; Cumming 2002; Gilaie-Dotan, Ullman et al. 2002; Brouwer, van Ee et al. 2005). In this thesis, experiments were designed to principally investigate the representation of static depth cues with a physiological basis: binocular disparity and vergence angle.

1.4.1 Binocular Disparity

The most studied depth cue in scientific literature has been binocular disparity, and refers to the differential position of points in the images projected on the two retinas. The relative positioning of the eyes imposes a tradeoff between the field of view and sense of binocular depth, as seen in the classic dichotomy

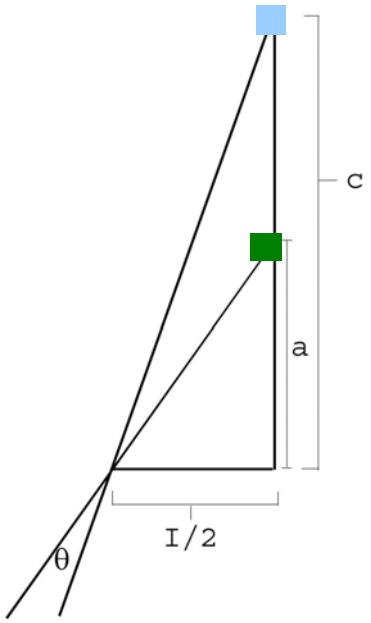

Figure 1-3 – Illustration for uncrossed disparity (blue target) when fixating (green target), see 1-1 and 1-2.

between the largely separated eyes of prey animals versus the frontal positioning of predatory ones. Frontward eyes are a significant feature in primates, where binocular vision increases acuity in the frontal field of view to benefit locomotion in the forest canopy, where life depends on the accurate estimate of the distance to the next branch to grasp (Allman 1999). In reference to this thesis topic, the positioning of the eyes/interocular distance has implications in reaching because it linearly scales binocular disparity (1-1, 1-2). Figure 1-2 illustrates the basic principle of binocular disparity. The eyes are turned inward to view the green fixation point, so that all points at the same depth fall on the same location in both retinas. The blue point behind the depth of fixation projects on different, but corresponding, locations on the retinas. The disparity between these locations, measured in degrees, is a consequence of the geometry between the points, the retinas, and the projected images (uncrossed disparity). Likewise, the orange point in front of fixation has a similar but opposite geometrical relationship (crossed disparity). The relationships lead to a vivid, unified stereoscopic percept of the points as being farther or closer than the depth of fixation (stereopsis), within certain limits. These limits, known as the diplopia threshold, refer to a fused percept of the stimulus when placed within the horopter, known as Panum's Fusional Area (Palmer 1999). Beyond the diplopia threshold, double images of a stimulus are seen. These images can still contribute to a strong sense of stereoscopic depth. In fact, human subjects perform well above chance in discriminating the depth of highly diplopic stimuli (Westheimer and Tanzman 1956; Ziegler and Hess 1997). Figure 1-4B is taken from (Westheimer and Tanzman 1956), and shows the average performance of subjects for discriminating the depth of highly diplopic stimuli. A depiction of the uncrossed

binocular disparity, θ, is shown in Figure 1-3, with reference to the green point of fixation at depth a, the blue point behind fixation at depth c, and the interocular distance I from Figure 1-2 . Conventionally, disparity is considered for both eyes, and the quantity is 2*θ. An approximation to disparity is simply:

$$\theta/2 \approx I*(c-a)/a^2 \qquad \textbf{1-1}$$

Note that θ is in radians, the approximation illustrates the scaling of disparity by the square of distance. This approximation works well for small disparities but the complete solution works for all values:

$$\theta = \tan^{-1}\left(\frac{2I(c-a)}{I^2+4ac}\right) \qquad \textbf{1-2}$$

The equation works for both uncrossed and crossed disparities, however the nonlinearities are amplified when considering large distances and large disparity values, a factor not present in the approximation commonly found in textbooks. In addition, an asymmetry is present when considering crossed versus uncrossed disparity; the distance from the fixation point to a point at a particular value of crossed disparity is smaller than the same value of uncrossed disparity, a factor also not present in the approximation. At large disparity values, these differences in distance become significant. This relationship is shown in Figure 1-4A, where the approximation is shown in red and the exact disparity value is shown as blue. Due to the scaling of disparity by distance, its usefulness as a fine scale depth cue decreases with fixation distance. For example, when fixating at 20

cm, an uncrossed (positive) disparity of 1° is 2.3 cm behind fixation, whereas when fixating at 1m the same disparity is ~1m, behind fixation. Binocular disparity uniquely identifies the depth of a visual stimulus given the viewing distance.

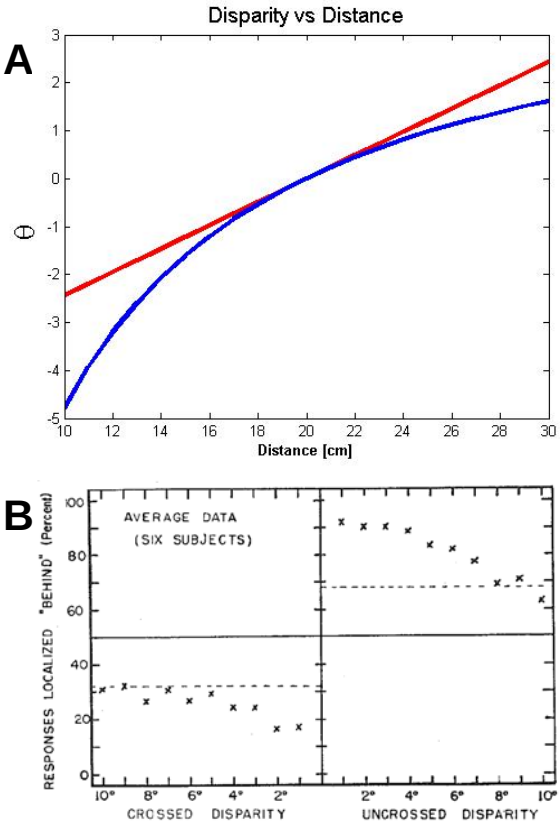

Figure 1-4– A: Disparity as a function of distance. Fixation Distance = 20 cm, I = 3.4 cm. The approximated disparity (red; 1-1) deviates from the actual disparity (blue; 1-2). B: The average performance of subjects reporting the depth of highly diplopic stimuli. The best subject performed nearly perfect for all disparities tested. (Westheimer and Tanzman 1956)

The above describes the disparity of individual points in the visual scene. One of the most interesting aspects of binocular disparity was discovered by Bela Julesz in 1971, when it was established that correspondence of points from random dot stereograms presented to each eye could be established to create a sense of stereoscopic depth. This amazing feature of the visual system launched studies on finding the neural substrate for such disparity detectors and inspired the formation of computational theories of stereo matching (Marr and Poggio 1979). In this thesis, binocular disparity specifically refers to the disparity of the reach target as an unambiguous well defined point in space. The stimuli used in this thesis work were isolated, individual light sources, and their perceived stereoscopic depth

relative to fixation depth was mainly a function of the retinal mechanisms described above.

1.4.1.1 Neural Substrates of Binocular Disparity Processes

A rich literature on disparity exists, and it has been studied using many types of stimuli: lines (van Ee and Schor 2000), gradients (McKee and Verghese 2002), image patches, random dot stereograms (Julesz, Papathomas et al. 2006), nonius lines. Binocular disparity also can include a temporal component when considering motion estimation, as well as playing a role in multimodal integration of motion (Kitagawa and Ichihara 2002). Functional magnetic resonance imaging (fMRI) has revealed the large network of brain structures involved in stereoscopic processing (Backus, Fleet et al. 2001; Shikata, Hamzei et al. 2001; Cumming 2002). In conjunction, the parietal cortex serves stereoscopic processing in close interplay with the occipital lobe (Nishida, Hayashi et al. 2001). The overlap of activation in stereoscopic processing and coordinating movements in the intraparietal sulcus (IPS) highlights the interrelated topology of the functions in the architecture of the neural processing, and possibly the flow of information. For example, the caudal intraparietal sulcus (area CIP) has single unit activity and significant BOLD activation during the perception and discrimination of surface orientation, defined by binocular disparity as well as other depth cues (Shikata, Hamzei et al. 2001; Orban, Janssen et al. 2006). Anterior regions of the IPS show sensitivity for the 3D shape of objects of manipulation, which is critical to the formation of grasp (Durand, Nelissen et

al. 2007). This thesis discusses disparity sensitivity in the medial IPS (mIPS) which has not been reported previously.

1.4.2 Vergence Angle

Three principal pairs of muscles rotate the eyes in the sockets, and their coordination enables 3 degrees of rotation to fixate objects in space. Conjunctive eye movements move the eyes together, rotating in the same direction to view objects at the same depth but different locations in azimuth. In order to view objects at different depths, both eyes must rotate horizontally in opposite directions, known as a disjunctive eye movement. The (horizontal) angle between the eyes – vergence angle – defines the depth of fixation, illustrated in Figure 1-5. The equation for vergence angle depends on the fixation distance D and interocular distance I:

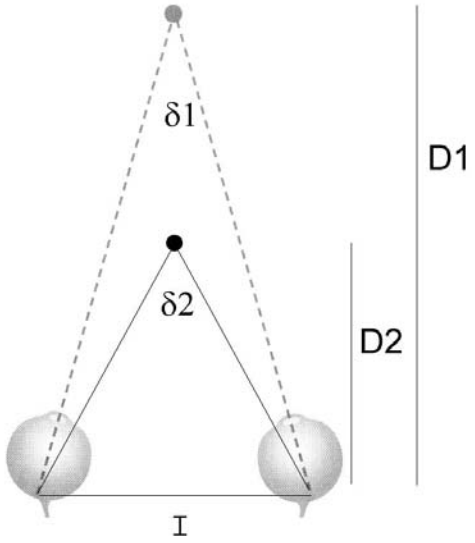

Figure 1-5 – Vergence Angle. I = Interocular Distance. D1 = Distance to far fixation point, δ1 is corresponding vergence angle.

$$\delta = 2 * \tan^{-1}\left(\frac{I}{2D}\right) \qquad \textbf{1-3}$$

Vergence angle expresses most power at close fixation, as shown in Figure 1-6. Again, due to the scaling by distance, vergence angle becomes a less reliable depth cue at far depths. In other words, the change in vergence angle in viewing far objects is small, and provides little information about their difference in depth. Vergence angle is considered a veridical depth cue because the feedback about tension from the extraocular muscles

uniquely determines the vergence angle, and hence viewing distance (Rogers and Bradshaw 1995; Wei, DeAngelis et al. 2003). Studies have shown the role of vergence angle in scaling information from other depth cues to produce both relative and absolute depth information (Peh, Panerai et al. 2002; Nefs and Harris 2008; Van Pelt and Medendorp 2008)

1.4.3 Accommodation

The lens of the eye is stretched or contracted by ciliary muscles that are concentrically placed around the pupil. The lens is adjusted in order to adjust the distance to the plane of focus. Under most natural viewing conditions, the plane of focus is determined by vergence angle. Accommodation, the control of the focal power of the lens, tracks vergence angle. As with the physiologically based depth cues discussed above, accommodation expresses most of its dynamic range in close range (~6 feet) (Fisher and Ciuffreda 1988; Palmer 1999). Analogous to vergence angle, the tension in the muscles that control accommodation provide information about the absolute distance to the plane of focus (Ebenholtz and Ebenholtz 2003). Accommodative demand

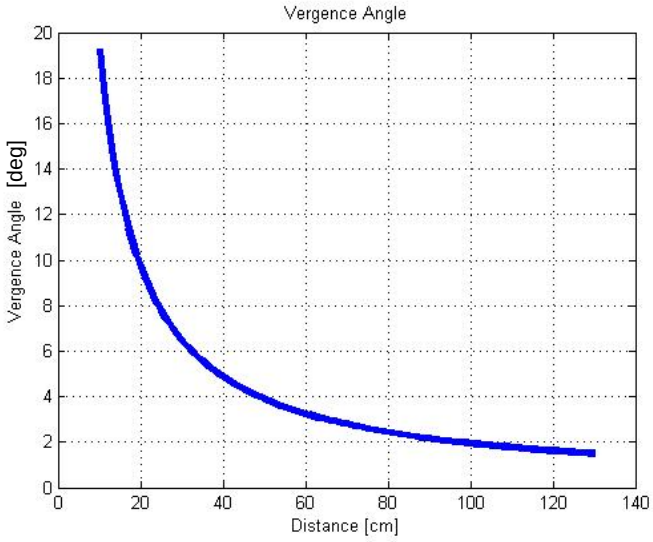

Figure 1-6- Vergence Angle VS Distance, I = 3.4 cm

matches the plane of fixation, and can provide the absolute distance of the surface that the eye is being focused on. Though accommodative demand maintains linearity with absolute distance, perceptual estimates of absolute distance based on monocular accommodation suffer from overestimation, compression, and a high dependence on stimulus characteristics (Fisher and Ciuffreda 1988). Another study has found that accommodation can provide ordinal information, where relative judgments of depth were made from one trial to the next, however accommodation is generally a poor depth cue when presented alone for the purposes of absolute depth estimation (Mon-Williams and Tresilian 2000).

An additional source of information that arises as a consequence of accommodation is the optical blur induced on elements in the visual scene that are not in the plane of fixation (Wilcox, Elder et al. 2000). Blur is an unsigned stimulus, that is, it cannot be determined from a single image whether the amount of spatial blurring is due to the object being in front of or behind the plane of fixation. This issue may be resolved in the visual system by the relatively frequent occurrence of eye movements which would allow the derivative of the blur signal to be compared to the direction of movement (convergence or divergence) to determine the sign through temporal integration.

1.4.4 Pictorial Depth Cues

A host of depth cues are present in natural visual scenes that are not the direct consequence of the differential projection of images on the retinas, the positioning of the

eyes, or optics; they can provide either absolute or relative depth information with monocular input. An excellent introduction to depth cues can be found in (Palmer 1999). Some pictorial cues require the operation of higher order processes to parse the visual scene to bind spatial properties to objects (*e.g.*, identifying and binding surfaces to objects), whereas others relate physical properties and constancies present in the scene itself. Linear perspective created by edges in a visual scene, and the occlusion of objects based on edges can create a sense of depth coined Da Vinci stereopsis (Nakayama and Shimojo 1990; Makino and Yano 2006). Perspective in the form of parallel and converging lines indicating a ground plane serve as depth cues as well (Wu, He et al. 2007), however perspective has also been shown to interact and constrain information from binocular disparity and occlusion to produce depth ordering of surfaces (Gillam and Cook 2001). Surface slant, presented by orthographic projection in monocular images, can provide substantial apparent depth and provide the ability to quantify depth comparable to stereoscopic judgments (Stevens and Brookes 1987).

Light sources, both ambient and directed, provide information about the distance of objects from the viewer because the intensity of reflected light decreases quickly (cubicly) with distance (Albert 2006). In addition, shadows cast by objects inform the viewer about the orientation, tilt, and slant of object surfaces in relation to the direction of the light source. Other depth cues, however, are required to create accurate percepts (Erens, Kappers et al. 1993). The texture of a surface, or the presence of regular high frequency components that are often present in solid natural surfaces, can allow both the determination of the orientation of that surface (slant and tilt), as well as comparisons of

other distances to that surface due to the increasing spatial frequency of elements in the surface with distance (He and Nakayama 1994; O'Brien and Johnston 2000). The rotational motion of rigid objects can create depth percepts that inform an observer of the 3D structure of an object, known as the kinetic depth effect (Sperling and Landy 1989; Wurger and Landy 1989). The size of objects (subtense) decreases with distance in a trigonometric relationship similar to that of vergence angle (Greene and Gentner 2001; DeLucia 2005). If the object has a familiar size, this information may be exploited to estimate its distance, as well as the distance of other objects in relation to it; if the object is novel and its size unfamiliar, the motion of the object in depth can give its changing depth if a stationary point of reference exists (whose angular subtense is unchanging).

Early studies have shown that motion parallax cues provide information for accurately estimating depth (Ferris 1972; Gogel and Tietz 1979; Rogers and Graham 1979; Koenderink and van Doorn 1981; Rogers and Graham 1982; Lappin and Fuqua 1983; Ono, Rivest et al. 1986). Motion parallax can induce the perception of surface depth similar to random dot stereograms (Rogers and Graham 1979; Rogers and Graham 1982). It has been shown in locusts that motion parallax information accurately guides predatory jumping movements, which rely on the extraretinal signal of head motion to calibrate and scale relative depth information from motion parallax (Sobel 1990). Motion parallax cues are scaled by absolute distance information at closer viewing distances (40-80 cm) in depth perception, likely from the extraretinal signal of vergence angle. At large viewing distances (160-320 cm), however, motion parallax cues produce the perception of motion instead of depth (Ono, Rivest et al. 1986). Self produced motion parallax, by

frontoparallel movements of the head, allow subjects to produce significantly better absolute distance estimates of objects compared to "artificial" parallax produced by object motion when the head remains stationary, indicating the importance of extraretinal signals for motion parallax based absolute depth perception (Panerai, Cornilleau-Peres et al. 2002). Other studies have compared the motion parallax produced by self produced movements and stimulus movements in the perception of depth and apparent motion (Ono and Ujike 2005; Ono and Wade 2005). Both binocular disparity and motion parallax rely on vergence angle to produce absolute depth/distance perception. In a reaching task, however, it has been shown that although motion parallax does produce normal scaling for transport (the amplitude or distance of the reach), it does not produce accurate scaling for grasp, whereas binocular disparity does for both (Watt and Bradshaw 2003), possibly indicating a depth cue specific specialization for grasp control.

Finally, the interaction of depth cues has been studied with the performance of human subjects in discrimination tasks to produce many models of cue combination in the literature (Landy, Maloney et al. 1995; Knill 2003; Hogervorst and Brenner 2004; Rauschecker, Solomon et al. 2006). The multiple levels of sensory processing interact with cognitive processes, such as attention, to create depth perception (Rose, Bradshaw et al. 2003).

1.4.5 Monocular Depth Cues in Reaching

Monocular depth estimates routinely suffer compression, such that the distance of near targets is overestimated and the distance of far targets is underestimated. Several studies have compared reach and grasp accuracy and dynamics under monocular and binocular viewing conditions. Estimates of absolute depth based on learned pictorial cues are accurate for reaching and grasping objects (Marotta and Goodale 1998). Without such learning, binocular information allows superior performance in prehension tasks (Bradshaw, Elliott et al. 2004), with a particular advantage for the terminal reach and grasp (Melmoth and Grant 2006). Monocular optic flow generated by head movement can provide depth information for reaching, and it has been shown that similar compression of perceived depth occurs (Bingham and Pagano 1998), and that verbal estimates and reaching errors in this task are uncorrelated (Pagano and Bingham 1998). This suggests that visuomotor control and perceptual estimates have separate underlying processing mechanisms leading to such a difference (a result that is further explored through studies examining visual agnosia patients, see (Carey, Dijkerman et al. 1998)). A recent study contends monocular compression of apparent depth during reaching tasks, and found that it is more consistent with general positional variance and increased perceptual uncertainty as compared to binocular vision (Loftus, Servos et al. 2004), and depends on the presence of other potential monocular cues in the environment.

Chapter 2 Reaching in Depth: Pilot Experiment

2.1 Summary

This pilot experiment was designed as a preliminary investigation of whether neural activity in the PPC is modulated by the depth of reach targets and vergence angle. A single juvenile macaque was trained to perform memory reaches with binocular fixation, and initial recordings to map the location of the medial bank of the IPS were performed. The data in this pilot experiment (90 neurons) subtended a large anterior-posterior extent of the mIPS in this pilot study (approximately 5mm), and includes recordings that fall at the anterior regions of PRR that transition into area 5. Studies indicate that area 5 contains a mixture of both hand and eye coordinate schemes for encoding target location, whereas PRR primarily encodes target location in eye centered coordinates (Lacquaniti, Guigon et al. 1995; Kalaska 1996; Batista 1999; Cohen and Andersen 2000; Buneo, Batista et al. 2008). As expected from the large span of recording sites, the results of this pilot experiment include neurons that encode in eye centered and limb centered coordinates. That is, the majority of neurons (42/90) encode target disparity and vergence angle, consistent with an eye centered reference frame, and a subpopulation of neurons (30/90) encode the absolute depth of the target directly in movement planning firing rates.

2.2 Motivation for Experimental Design

Neurophysiology in other areas in the IPS show the widespread affect depth cues have when viewing a stimulus (Sakata, Shibutani et al. 1985; Sakata, Shibutani et al. 1994; Taira, Tsutsui et al. 2000; Tsutsui, Jiang et al. 2001; Tsutsui, Sakata et al. 2002; Sakata, Tsutsui et al. 2005; Durand, Nelissen et al. 2007), as well as the influence of depth cues for visuomotor control (Sakata, Taira et al. 1995; Murata, Gallese et al. 1996; Sakata, Taira et al. 1997; Sakata, Taira et al. 1998; Sakata, Taira et al. 1999). Oculomotor control involves the coordination of multiple cortical areas and brainstem nuclei. In order to purposefully view an object outside the plane of fixation, a movement plan to the target object must be formed prior to execution. It is apparent that the planning of eye movements requires an estimate of the depth of saccadic targets, and the studies in area LIP indicate that this computation is occurring there (Gnadt and Mays 1995; Genovesio and Ferraina 2004), among other possible places. The movement vector must take into account initial and final eye position, and in the case of a target placed at a different depth than that of fixation, the movement plan for that disjunctive eye movement is done in reference to the initial vergence angle. The natural frame of reference for an eye movement plan is a retinal one.

Reach planning has been studied for reaches to targets in azimuth and elevation at a fixed egocentric distance. Figure 2-1A illustrates such a target configuration, where one reach and fixation target configuration is shown in dark colors, alternate target locations shown in light colors, and all targets are in a single frontoparallel plane. Previous work in the lab has shown that reaches to peripheral targets are encoded in a retinal reference frame

by PRR neurons (Batista 1999). The planning activity for reaches to the same target changed when the fixation target changed, however remained constant if the spatial relationship between the two remained constant. Reach targets were always at the same depth as fixation, and on corresponding locations on the 2 retinas in planning these reaches. In other words, the previous studies in PRR that examined target encoding in an eye centered reference frame considered the cyclopean eye. This experiment examined whether the same cortical area would respond if different areas of the retinas were stimulated with a cue for a reach target. Figure 2-1B illustrates a reach and fixation target configuration to examine this response. For example, one reach and fixation target configuration, shown in dark colors, places the targets at the same egocentric distance, as in Figure 2-1A. However, other configurations, where any combination of light colored reach and fixation targets is possible, place the targets at different egocentric distances, or different frontoparallel planes.

The introductory material presented thus far suggests that area MIP, and the population of PRR neurons, is well positioned in terms of anatomical connectivity to be visually stimulated by a reach target in disparity. Apart from the visual response of the neurons, which is ostensibly a direct consequence of the input from earlier visual areas, we examined whether the neuron encoded target depth in working memory. In order to examine working memory activity the visual stimulus, which is the cue to the reach target, is turned off and neural activity during this memory period is examined 200ms after the removal of the stimulus to allow for the decay of any reverberant activity of feedback visual processes due to pure visual stimulation.

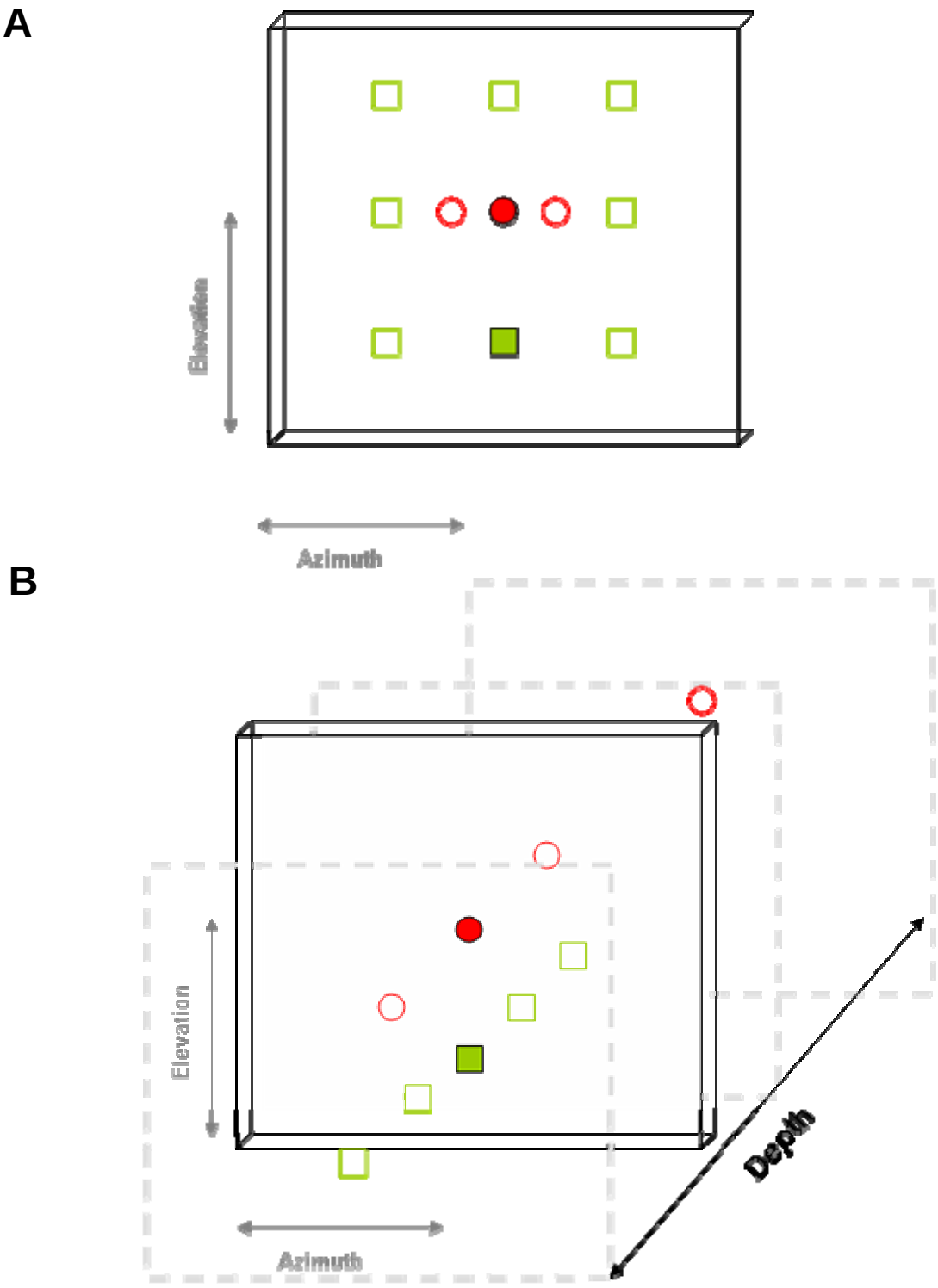

Figure 2-1 Fixation (red) and reach (green) target configurations. A: Target configuration used in previous experiments to study reach planning in 2D (azimuth and elevation) at a single egocentric distance. One target configuration is shown in dark colors, the lighter reach and fixation targets show other possible locations of targets. B: Target configuration used to study reach planning in 3D (depth), where fixation and reach targets were placed at different egocentric distances. One target configuration is shown where both reach and fixation targets are at the same depth (filled). Alternate targets are shown in light color outside the frontoparallel plane (outline).

2.3 Experimental Design Considerations

Binocular fixation is maintained to remove the any contamination of movement planning for the reach by eye movements. Eye movements can modulate neural activity in PRR, and it is important to eliminate any motor effects during visual stimulation or movement planning. Since vergence angle is a reliable and veridical depth cue, it is important to ensure that it does not have dynamics during movement planning that could provide information outside that from the visual presentation of the stimulus. For instance, it would be possible for the subject to not only maintain a memory of the depth of the stimulus, but enhance it with vergence eye movements made from the fixation target to the remembered location of the reach cue. In the view that most reaching is done under visual guidance of the hand to the target, such eye movements comprise a rehearsal of the future movement and enhance the estimate from this aspect. Additionally, such rehearsals using eye movements can enhance the perception of the estimated location by averaging from the dynamics of the vergence angle. If such eye movements occurred in the presence of the fixation stimulus, the additional cue of the disparity of the fixation stimulus, and the dynamics of the disparity during changing vergence, provide a salient cue for depth estimation. Likewise, the blur induced by the changing accommodative demand induced by vergence provides another form of information. As discussed in Trotter et al. (Trotter, Celebrini et al. 1992), vergence eye movements, and indeed the other cues that would be patently present due to the fixation stimulus, would provide

important information that would ambiguate the neural activity associated with the encoding of target depth for planning a reach movement.

Moving the stimulus in azimuth would incur an additional information depth cue, vertical disparity, which is the differential size of the retinal projection of the stimulus in each eye (Ogle 1954; Banks, Backus et al. 2002; O'Kane and Hibbard 2007). This depth cue may be useful, however does not provide veridical information about the depth of the stimulus since this would require prior knowledge of the size of the object. From the viewpoint of experimental design, if the stimulus was placed in different azimuthal locations, it is unclear how to disambiguate the effects of vertical disparity and horizontal disparity without using a virtual environment where the images projected on each retina could be explicitly controlled. In keeping with a more natural reaching context, and reducing the necessary control experiments necessary to disambiguate the influence of these different depth cues, the target location was kept central to eliminate the possible effect of vertical disparity. It is likely that most depth cues contribute synergistically in visual processes that provide input to the PPC in order to perform the visuomotor transformations necessary for goal directed reach movements.

The reference frame studies discussed in the last chapter explicitly tested the encoding of reach targets when initial limb position was changing, and in fact found that this encoding was more correlated when targets were referenced to eye position rather than limb position (Batista, Buneo et al. 1999). Though most neurons were less sensitive to changes in initial hand position eye position during movement planning, limb position

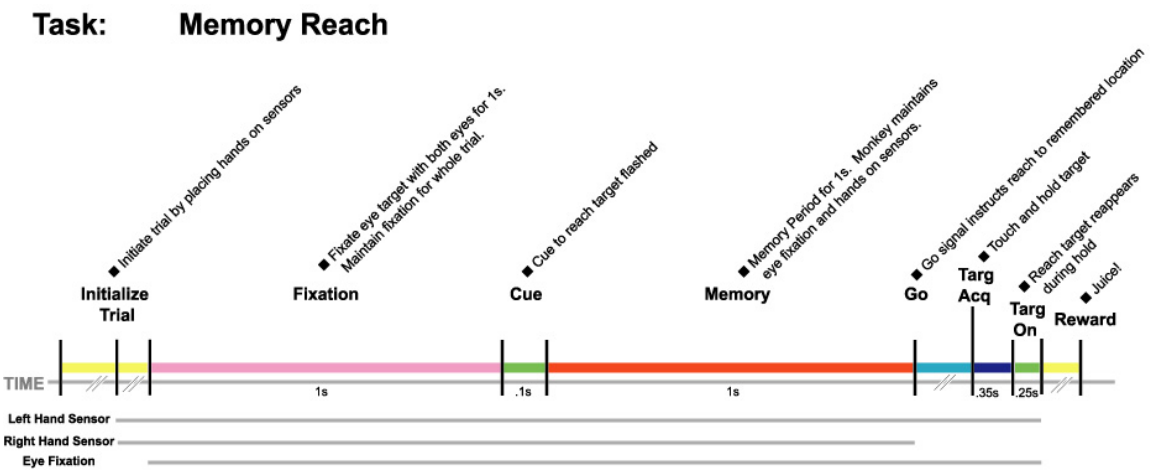

Figure 2-2- Timeline for Memeory Reach Task. Horizontal Line segments at bottom indicated the duration required for fixation of each hand and eyes. Diagonal lines in colored time line indicate variable length of duration. See

can have an effect on neural activity in PRR. In particular, initial hand position can gain modulate tuning for target location in eye centered coordinates in PRR, and is a method for encoding the initial hand location in this reference frame (Buneo, Jarvis et al. 2002). This is a convenient representation which can be used directly to form a movement plan in eye centered coordinates. Considering these findings, we chose to keep the position of the hands constant until the movement was to be made. This ensured that neural activity was not contaminated by hand movements unrelated to the instructed one, and ensured that neural activity did not reflect changes from trial to trial for an instructed reach to a target at a given depth. The fixation of the hands allowed the direct comparison of movement plans for different target depths.

This preliminary investigation explored the basic existence of a representation for reach target depth and vergence angle using reach targets that were fixed in space for each level of vergence. We examined the tuning for reach target depth to see if it changed with vergence angle. A constant reach target tuning curve across vergence angle suggests that

neurons are encoding the absolute depth of reach targets, and uses a reference frame that is insensitive to the position of the eyes. Reach target tuning that changes with fixation depth suggests that neural activity is related to both target depth and the vergence angle.

2.4 Methods

A rhesus macaque (juvenile male, ~5kg) was initially trained to perform memory reaches in the dark. This period of training required the hands to be fixated on 2 capacitive sensors before the movement. The stimuli were presented in a dark chamber, and were physically isolated from each other to prevent cross contamination of luminance. The reach stimulus was a green square (1.5 cm length) presented on an LCD screen mounted to a 3 axis Cartesian robot (Samsung FARA RCM-4M, with SRC+ controller). The screen was fixed in azimuth and elevation, and modulated solely in depth (distance from the subject). A touchscreen was mounted in front of the LED screen in order to record the position of touches, calibrated to be in register to the position of the reach stimulus. Fixation stimuli were red LEDs placed inside a tube for isolation, also placed in depth at 15, 25, 35, and 105 cm from the subject's face. The interocular distance was 34mm, thus the fixation stimuli corresponded to 13°, 7.7°, 5.5°, and 1.9° of vergence angle. Stimulus presentation was computer controlled, and behavior signals were monitored in real time using custom software in Labview (National Instruments) and C++. The position of the reach stimulus was changed during intertrial intervals only. The speed was adjusted to make the time that the motors were on identical for each movement of the stimulus to offset possible auditory cues from the manipulation of the depth of the screen.

Capacitive sensors which sensed touch were used to monitor the hands for fixation throughout the trial, and were placed at hip level 15 cm apart in width, and 15 cm in front of the animal's face.

Each trial had a fixation, cue presentation, memory, and movement period. A cartoon of trial epochs, stimuli presentation, and the state of the monkey is shown in Figure 2-5. Trials were initiated by placing both hands on sensors, after which the fixation stimulus appeared. Before implantation, we could not monitor the animal's eye position, and he was trained to make memory reaches with the use of the dimmed fixation stimulus as a go signal, with hand fixation on sensors. After implantation, a fixation period of ~1sec required binocular fixation within a 2° diameter spherical window (2° diameter window for horizontal, vertical, and vergence eye position). After successful fixation, the cue to the reach was briefly flashed (100-200 ms), and a go signal was given to indicate the reach movement should be performed by dimming the fixation stimulus to half the previous illumination. Precise illumination values were calibrated electronically, computer controlled, and kept constant throughout all experiments. A timeline for the events in a trial is shown in Figure 2-2. After the go signal was presented, a continuous touch for 350ms within 2.5 cm radius window in the absence of the reach cue was required. If this condition was met, the reach cue was presented, and a continuous touch for 250ms in the presence of the cue was required. A juice reward and auditory feedback (high pitched tone) were presented after the successful completion of a trial. A low tone was presented immediately after a trial was aborted at any stage to facilitate the learning of erroneous actions.

Upon successful training of the memory reach task without eye fixation, the animal was implanted with an acrylic head cap, head holder, scleral search coils, and a recording chamber in sterile surgical procedures under anesthesia. The head cap implantation consisted of bone screws and a titanium post embedded in dental acrylic used to fixate the head in the experimental setup. Scleral search coils were implanted between the sclera and conjunctiva of each eye (Judge, Richmond et al. 1980). These coils were soldered to coaxial connecters embedded in the acrylic of the head cap. Changes of the phase of currents induced by magnetic fields in quadrature allowed the horizontal and vertical angle/position of the eyes to be monitored in real time. Eye position was calibrated before each experimental session. This fixation was binocular, and required the measurement of the position of both eyes in order to monitor vergence angle, which was subject to the same window. A surface normal chronic recording chamber was implanted above a craniotomy to access the posterior section of the IPS, at a location based on magnetic resonance images registered to the orbits of the eyes used for stereotaxic placement (Figure 2-4). The Caltech Institutional Animal Care and Use Committee approved all protocols.

Neural recordings were made with a single electrode FHC Microdrive (hydraulic) using Platinum/Iridium electrodes in the range of 1-3MΩ. Signals were amplified by a headstage (10), a preamp (50x), and an amplifier (10x) in the Plexon system. Spikes waveforms were further amplified in software if necessary and sorted online (Offline Sorter, Plexon). Spike times, spike waveforms, and analog behavioral signals (eye

positions, hand sensor signals, touch position from touchscreen) were recorded to hard disk by a Plexon system.

Initial recordings were made to locate the mIPS, however not included for analysis. The average location of all recordings included for analysis (90 neurons) were located at approximately 4P, 5.25L (Horsley-Clarke coordinates), and extended approximately 5mm in the anterior-posterior extent, and 2 mm medial-lateral extent. The recordings likely span multiple areas in the mIPS; primarily the anterior regions of PRR (MIP), and the transition region to area 5.

The animal made reaches to all the targets placed in fixed positions in space while fixating each separate red fixation stimulus at different depths. Fixation depth was randomized from trial to trial, while reach target depth was randomized between blocks of 5 trials. These fixed locations were placed 25 cm to 35 cm from the animal, spaced by 2.5 cm in space and resulted in different disparities of the reach target being tested at each vergence angle, see Table 2-1.

	Reach Target Depth					
Vergence Angle		25	27.5	30	32.5	35 cm
	13°	-5.15	-5.86	-6.44	-6.94	-7.37
	7.7°	0	-0.70	-1.29	-1.79	-2.22
	5.5°	2.22	1.51	0.93	0.43	0
	1.9°	5.93	5.22	4.63	4.13	3.71

Table 2-1– Binocular Disparity of reach stimuli classified by vergence angle and reach depth

2.4.1 Disparity Values of Reach Targets

The disparities associated with each reach depth from the different vergence angles are different, and shown in Table 2-1.

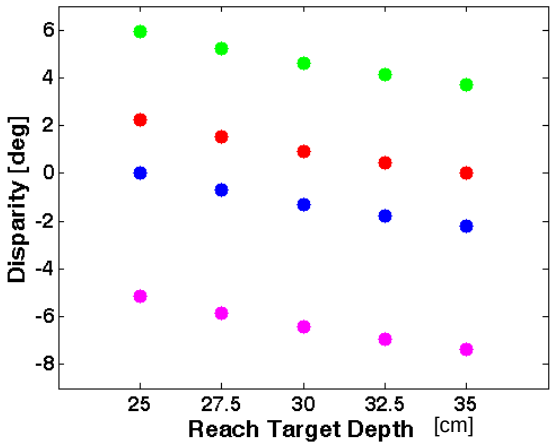

Figure 2-3 Disparity of reach targets at each vergence angle. Nonlinear change in disparity occurs for a fixed vergence angle when reach targets vary in depth from 25 to 35 cm in 2.5 cm increments. Different ranges of disparity are tested at each vergence angle. Disparity change between reach targets is the same at each vergence angle.

As seen from the disparity values in the table, the sampling of disparity is non-uniform. The disparity ranges sampled at each vergence angle is different as a result of the targets being fixed in space, and the difference between disparities within a vergence angle can vary as well. Note that the range and values of disparities tested at each reach target depth (absolute depth) is also different, however changes the same amount of disparity for reach target depth since absolute depth is uniformly sampled[1]. The difference in disparities between columns remains constant for different vergence angles; that is, the difference in disparity between a target at 27.5 cm and 25 cm is ~0.7° for all vergence angles. The fact that disparity sampling is different for each vergence angle has implications that are discussed in the next section and addressed in the subsequent experiment.

[1] Note also that the range of disparity tested at a reach target depth (~11°) is much larger than the change in disparity values and the range at each target depth (~0.7°).

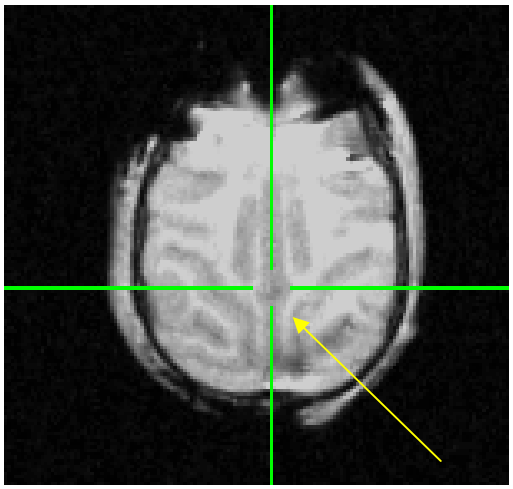

Figure 2-4- Axial slice from Monkey G MRI, with location of recording chamber origin center indicated by yellow arrow.

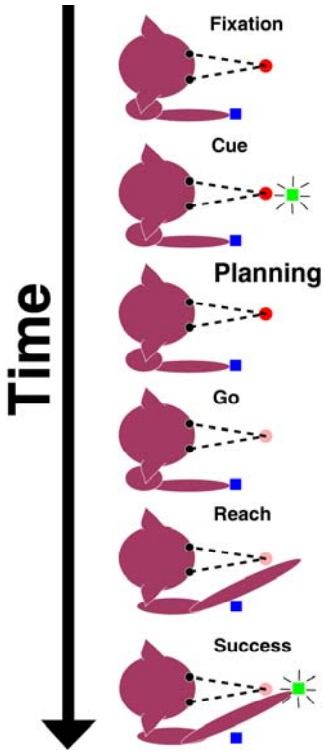

Figure 2-5– Memory reach task outline of basic epochs.

A

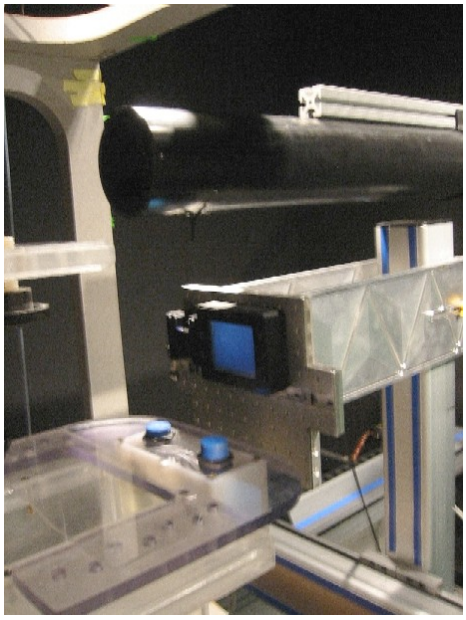

B

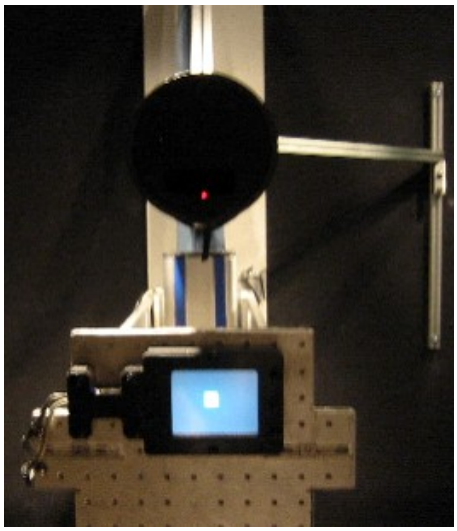

Figure 2-6– A -Side view of experimental setup under illumination. Monkey chair made of clear acrylic is visible at left. Blue round cylinders are touch sensors. Metal structures with blue stripes is the Cartesian robot. Black tube attached to metal strut houses red LED fixation stimuli. B - Frontal view of experimental stimuli under illumination.

2.5 Results

The firing rate responses of 90 isolated single units were recorded over several months. Significant modulation by the depth of the reach target and vergence angle could occur in multiple combinations, and have different implications about the disparity of the reach target (see Table 2-1).

These are categorized into the classes below:

A. Main effect of Reach Target Depth/Disparity across Vergence Angle
B. Individual effect of Reach Target Depth/Disparity at a Vergence Angle(s)
C. Individual effect of Disparity for a reach target(s) fixed in depth + Effect of Vergence Angle
D. Main effect of Vergence Angle across Reach Target Depth
E. Effect of Reach Target DEPTH Without Effect of Vergence = (A+B) – C – D

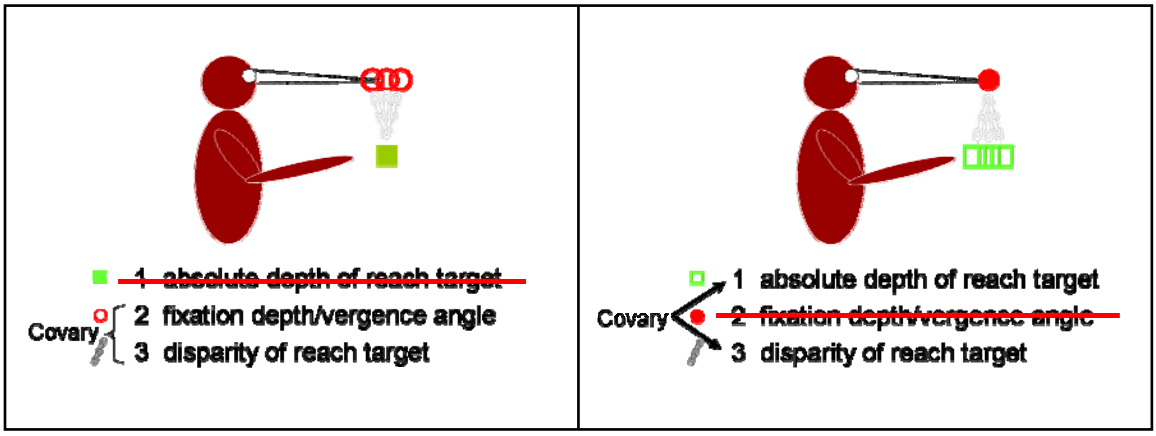

Figure 2-7 – Co-variation of reach target depth, fixation depth, and disparity of reach target.

At a single level of vergence, a change in the depth of the reach target corresponds to a change in disparity of the reach target (Class B). Likewise, for a single fixed depth of the reach target (absolute depth), a change in vergence angle corresponds to a change in disparity (Class C). Consequently, the disparity values for all reach targets change when vergence angle changes (Class A). This means that the modulation in tuning for reach targets at different fixation depths may be due to the different target disparities, the different vergence angle, or a combination. A main effect of vergence angle can occur across all target depths tested (class D); note that different disparities occur for the reach targets at each level of vergence. This means that a main effect of vergence angle may be a manifestation of changing reach target disparity, and is related to Class A.

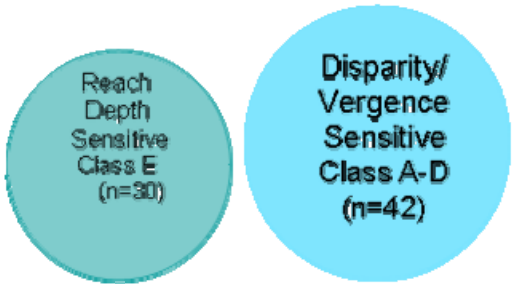

Figure 2-8 Diagram of responses in mIPS population. 80% (72/90) of all neurons were modulated by reach target depth, vergence angle, or both. The majority of neurons were sensitive to both reach target disparity and vergence angle (42/90). This population expressed changes in firing rate due to both reach target depth and vergence angle (which indicates sensitivity to disparity), or reach target disparity for a reach target fixed in depth but with changing vergence angle.

A neuron encoding the absolute depth of a reach target should be sensitive to only the absolute depth of the target, not to changes in reach target disparity by different fixation depths when the absolute depth remains the same (not a member of Class C). An absolute depth encoding neuron should be insensitive to changes in vergence angle and the corresponding disparities of reach targets across target depths (not a member of Class

D). This means that the tuning to reach target depth should remain invariant under changing vergence. This is denoted as Class E.

In contrast, a neuron encoding the disparity of the reach target would be modulated by changes in disparity that are incurred by a fixed target with changing fixation depth (Class C), constant fixation depth and changing reach target depth (Class A and B), or effect of vergence angle (Class D). The neural population can thus be broadly classified into 2 categories: reach depth sensitive (Class E; absolute depth encoding), and disparity/vergence sensitive (Class A-D). The number of neurons in these categories is shown in Figure 2-8.

This section begins with examining a neuron from a minority class of cells which have significant planning period responses to reach depth, but seemingly an insignificant response to vergence angle (reach depth sensitive, Class E). These neurons may be encoding the absolute depth of a reach target, in a manner which is independent of the retinal location of the target and vergence angle. Next, the majority class of task modulated neurons that express significant modulation by both reach depth and vergence is presented, with several examples of tuning (disparity/vergence sensitive, ClassesA-D).

2.5.1 Vergence Insensitive Neurons

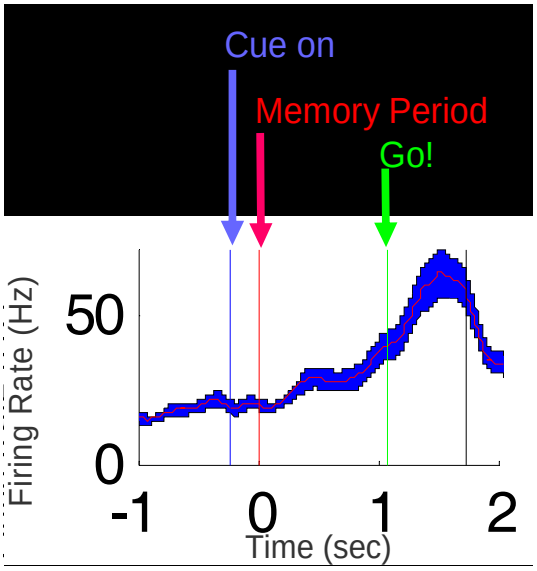

Figure 2-9- Response of a PRR neuron to a memory reach in depth. Fixation was at 13° of vergence, stimulus depth was 25 cm (from eyes). Vertical lines indicate beginning of trial epochs. Black vertical line at right indicates average time feedback was presented. Red trace is trial average, blue indicates standard error.

Figure 2-9 shows the peristimulus time histogram of the firing rate of a neuron for a memory reach in depth to a target at 25 cm depth when fixating at 13° vergence angle. The dynamics of this response is typical for PRR neurons, where an elevation of activity occurs during the memory period, and a motor response is seen during the movement. The preferred gaze angle may illicit a firing rate higher than the baseline rate observed in the inter-trial intervals where "random" visuomotor behavior is occurring. When the cue to the reach stimulus is presented, a rise in the firing rate is observed if the stimulus is preferred. Figure 2-11 shows the PSTHs for all reach depths and vergence conditions recorded. What is immediately evident is the suppression of activity in the 3rd row, which corresponds to reaching to a stimulus at a depth of 27.5 cm. This suppression is present for all vergence angles. Looking at the difference in firing dynamics, we can see that for preferred depths, the firing rate rises during the memory period continually through the movement, whereas at the non-preferred depth, the firing rate does not rise, and the associated motor response is much lower. A tuning curve for the average firing rate during the memory and movement periods is shown in Figure 2-10. The line thickness portrays the data from a single vergence angle, where the thickest line if for 13°

vergence and the thinnest for 1.9°. Little difference is seen during the memory period, and the tuning curves are indistinguishable for the motor response (green).

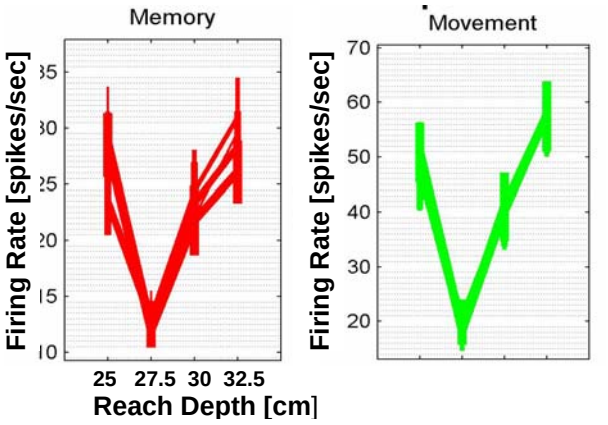

Figure 2-10–Reach depth tuning curves for neuron in Figure 4-6 during memory period and reach movement period. Tuning curves from different vergence angles shown by different line thickness (closest vergence is thickest).

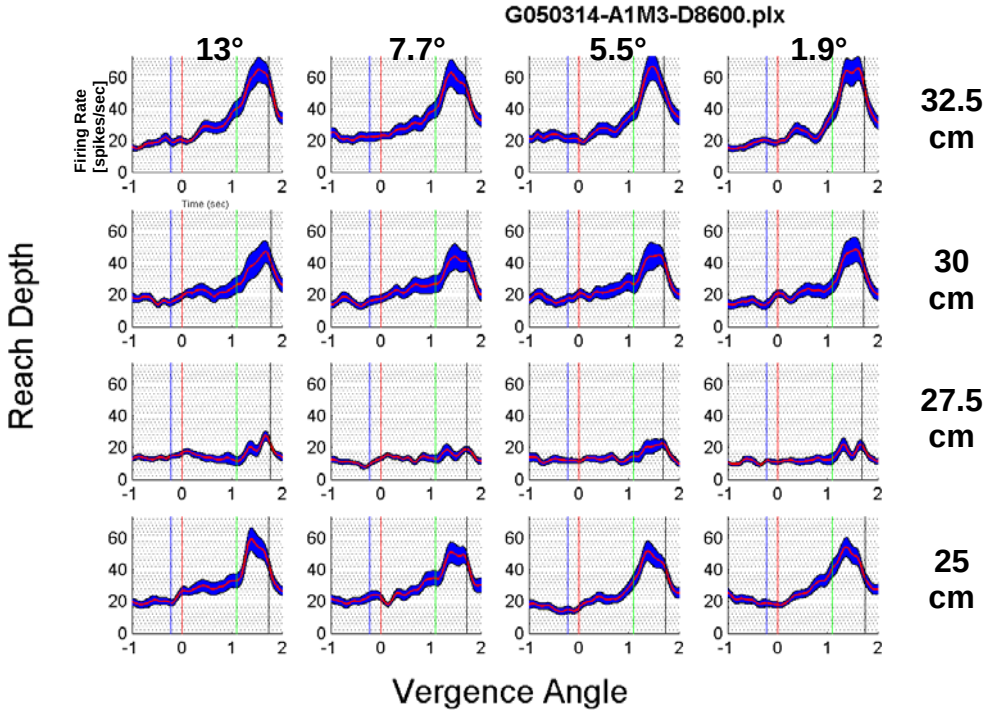

Figure 2-11-Example PSTHs from an mIPS neurons for all reach depth/vergence angle conditions.

This cell exhibits clear and robust tuning for the depth of the stimulus, with an approximately 50% change in firing rate due to a 2.5 cm change in depth of the stimulus from 25 cm to 27.5 cm. The encoding of reach depth by this cell appears unaffected by vergence angle (ANOVA main or individual effect for a single reach target, $P > 0.05$; ANOVA reach depth main or individual effect at a single vergence angle $P < 0.05$). The suppression of activity in the neuron at 27.5 cm happens at very different values of disparity (ranging >10°, from -5.86° to +5.22°), and together with the insensitivity to vergence angle this suggests that this cell may be encoding the absolute depth of the reach target rather than target disparity.

33% (n = 30) of the population in this data set followed this statistical trend, and fall into Class E. Several samples of these profiles are shown in Figure 2-11. A variety of reach depth tuning profiles were observed, ranging from linear (A), polynomial (D), Gaussian-like or modal (B), saturating/sigmoidal (C), and inhibitory (E).

Neurons in Class E indicate tuning to the absolute depth of the reach target, however many neurons in this population exhibit subthreshold (statistically insignificant)

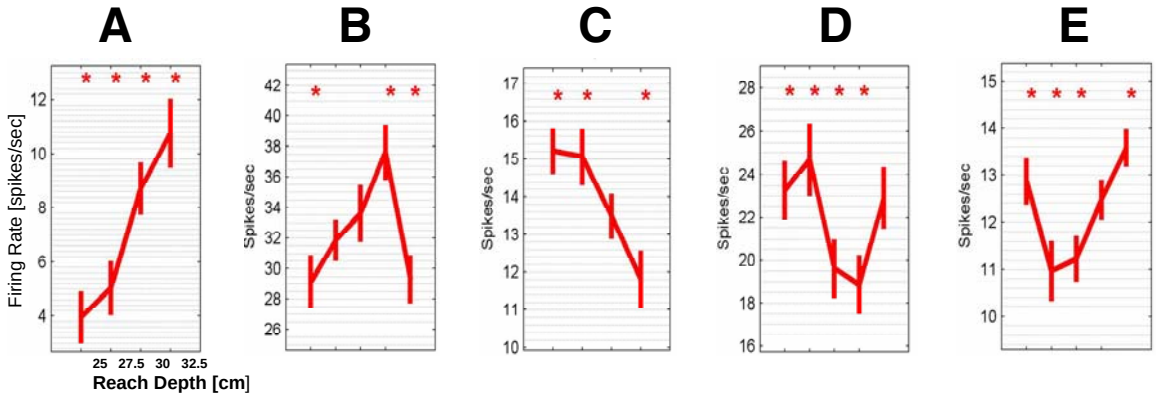

Figure 2-12- Memory period reach depth tuning for vergence insensitive neurons. These reach depth tuning curves are averaged across fixation depth.

modulation by changing target disparity while absolute target depth is held constant. This may indicate a mixture of reference frames, or the undersampling of the disparity sensitivity of the neurons. As discussed in 0, the range of disparity tested at each reach target depth is ~11°, and the change in disparity at a constant vergence angle between reach target depths ~0.7°. The change in disparities tested across reach target depths at constant vergence angle is small when compared to the range tested at a single reach target depth. Neurons may be sensitive to particular ranges of disparity, however with the sparse sampling of target disparity at each reach target depth, it is possible that the disparity sensitive range is not probed. The smaller changes in disparity tested at a constant vergence angle may elicit modulation, which may occur at each level of vergence depending on the disparity sensitive range for the neuron. Neurons in Class E ("vergence insensitive") may thus appear to encode absolute target depth because the disparity sensitive range was only tested across reach target depth, and not at a constant absolute depth. Examining the reach tuning from different vergence angles in such a "vergence insensitive" cell illustrates the fact that reach depth tuning can indeed change even though vergence may not have a main effect by ANOVA. The reach depth tuning for each vergence angle from the neuron in Figure 2-12B is shown in Figure 2-13A. Not only is the tuning depth (or range) changing by vergence (the range @ 7.7° is ~27-34Hz, @ 13° it is 27-41Hz), but the shape of the profile is changing by vergence. Similar "vergence insensitive" cells are shown in Figure 2-12B-D, where the top row is the reach depth tuning curve averaged from the different vergence angles, and the bottom row shows the tuning curves from each vergence angle. The statistic measures a change in the means of each reach tuning curve from different vergence angles, and although it

indicates that the means are statistically the same, clearly the shape of reach tuning profiles are changing with vergence. Testing the effect of vergence angle for individual reach targets fixed in depth (Class C) results in a significant difference in planning activity for 22% (13/59) of neurons that did not have a main effect of vergence (averaging across reach target depths). This difference in firing rate for a fixed reach target contains 2 changing factors: vergence angle and reach target disparity, which is explored further in Chapters 3-5 in the subsequent experiment. The majority of neurons that are vergence insensitive do exhibit changes in profile shape, and may be using a reference frame that is a mixture between eye centered and limb centered. Neurons that robustly maintain tuning to target depth across different vergence angles, as shown in Figure 2-10 at the beginning of this section, encode the absolute depth of the target, however are rare (~10% of reach tuned cells) in the population.

2.5.2 Reach Depth and Vergence Sensitive Neurons

80% of the population showed significant modulation of planning period responses that were due to a combination of vergence angle, reach target depth, and the disparity of the reach target. 43% of all neurons had a significant change in firing rate for a reach target fixed in depth but at different levels of disparity due to changing vergence angle. These neurons do not encode the absolute depth of the reach target since their firing rate changes even when absolute depth does not.

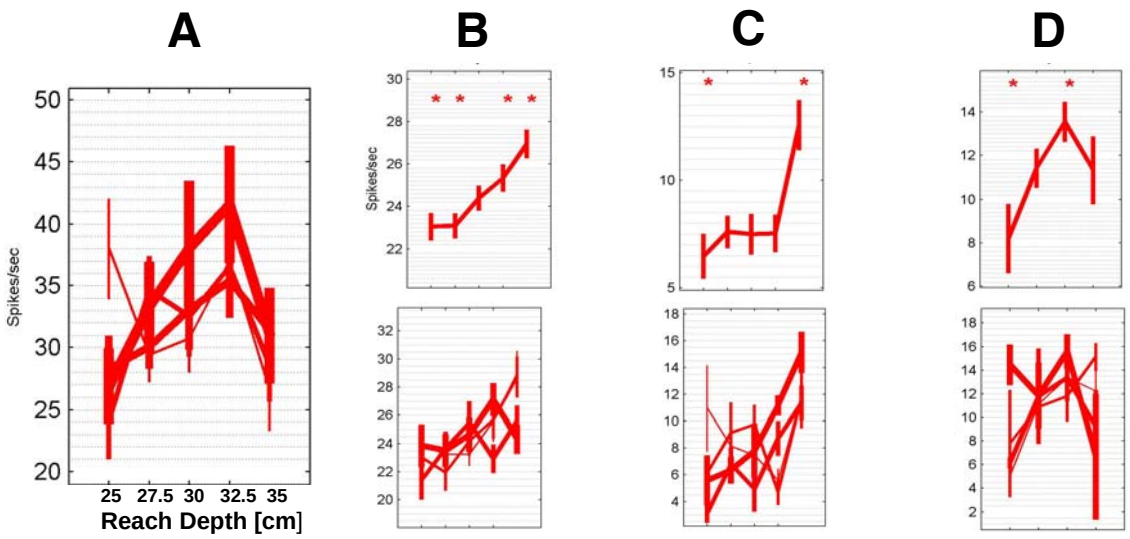

Figure 2-13- Reach depth tuning curves for different "vergence insensitive" cells. These cells had significant modulation due to reach depth, no effect from vergence angle. A: Reach depth tuning curves at each vergence angle for neuron in Figure 2-12B. B-D: The reach depth tuning curve is averaged across fixation depth in the top rows for the neurons in B-D. The reach depth tuning curves at different vergence levels are plotted in different line thicknesses in the bottom row in B-D. Marked changes in reach depth tuning can be seen at different levels of vergence.

A tabulation of the population responses is in Figure 2-15A. 67% of mIPS neurons were sensitive to reach target depth during movement planning, which attests to the strength of reach depth as a modulator of neural activity in PRR. The results in the table include multiple classes described at the beginning of this section; cells in Class E (absolute depth encoding cells) are sensitive to the depth of the reach target as are disparity sensitive cells in Class A. The 2D response field was not probed for each neuron, and reach depth was only tested in a single location in azimuth and elevation; it is reasonable to assume most cells do not have their frontoparallel response fields in this location, and that the large proportion of cells responding to reach depth are being strongly modulated in their non-preferred 2D location. The tuned motor response is a significant feature in this data set, and most cells had similar tuning for cue, memory and motor epochs. As

seen in the table, there were more cells with tuned memory period activity than tuned visual responses due to the depth of the reach target, a feature also true for vergence. The results from linear regressions on reach target depth and vergence angle are shown in Figure 2-15A. We found a larger number of neurons had significant linear regressions ($P< 0.05$) for reach tuning than vergence during movement planning. Figure 2-15B shows the distribution of significant reach target depth tuning across vergence angle for all cells in the population. Overall it can be seen that reach target depth tuning occurs with similar frequency across the population for the different fixation depths.

47% of neurons had significant modulation by the disparity of the reach target when reach target depth changed or when it remained constant and vergence angle varied (ANOVA $p < 0.05$) during movement planning (Class A-D). Most neurons exhibit the feature that vergence and disparity modulates the shape of reach tuning profiles at

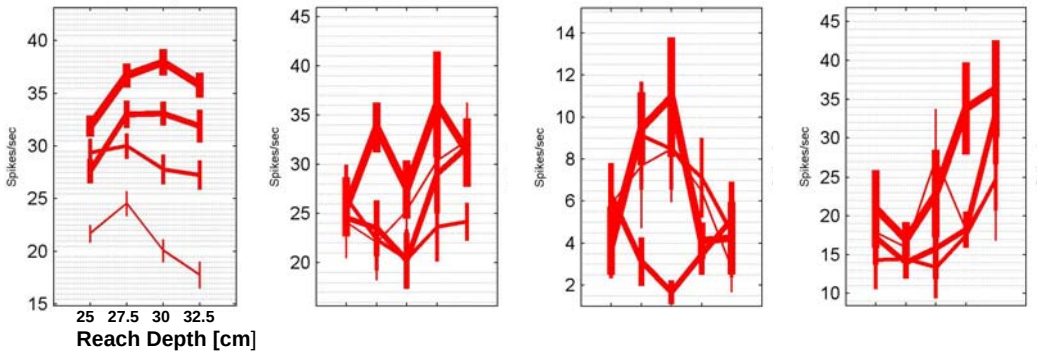

Figure 2-14 – Neurons sensitive to target disparity at different vergence angles.

different fixation depths during movement planning, as seen in 2.5.1 and Figure 2-13. Several disparity and vergence sensitive neurons (Class A-D) are shown in Figure 2-14. These changes in tuning shape can range from a change in multiplicative gain, where a reach depth tuning curve may "flatten out" at one vergence angle and be highly peaked at another, to changes that result in very different peak characteristics.

We sought to examine how often reach target depth tuning changes due to fixation depth (and different values of target disparity) by employing an additive gain model. An additive gain model on reach depth tuning would describe only a constant magnitude change in firing rate across all reach target depths due to vergence. Additive gains by vergence angle were tested using planar regressions. Planning period firing rate was regressed on reach target depth and vergence angle for disparity/vergence sensitive neurons in Class A-D (note that absolute depth encoding neurons, Class E, do not have significant vergence regressions). A well fit additive gain model by vergence angle on reach depth would indicate that neural activity is encoding reach target disparity the same way at different vergence angles, despite the fact that the disparity values are very different at each fixation depth. If such a model fit well, these neurons may accomplish this by large shifts in disparity tuning. 32% (14/44) disparity/vergence sensitive neurons had significant planar regressions for reach depth and vergence angle. These planar regressions are poor fits to the data, and the R^2 values are shown in the histogram in Figure 2-15C. This indicates that disparity/vergence sensitive neurons do not have an additive gain by vergence angle on reach target depth, as expected for planning period responses that encode reach target disparity.

A

P <= 0.05	Reach ANOVA	Vergence ANOVA	Reach Regression	Vergence Regression
Cue	38	16	32	13
Memory	61	31	49	22
Movement	64/90	34/90	51/90	22/90

B

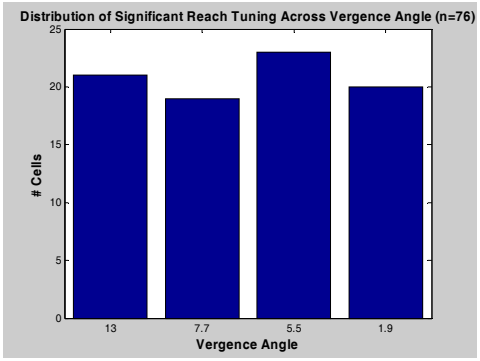

C

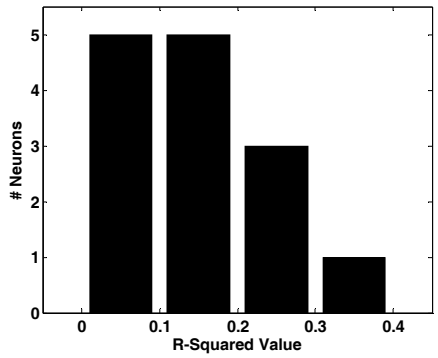

Figure 2-15 – A: Tabulation of ANOVA and Linear regression for reach target depth and vergence angle for different trial epochs. B: Histogram of the number of neurons with significant tuning to reach target depth at each level of vergence. C: Histogram of R^2 values from significant planar regressions on disparity/vergence sensitive cells. This additive model is valid for 14 cells, however is a poor fit to the data. Mean R^2=0.15.

2.6 Discussion

The above data support the hypothesis that neurons in the mIPS show sensitivity to the depth of a reach target. 58% of reach depth sensitive neurons encoded target disparity (Class A-D), represent the reach target location in an eye centered reference frame. A subpopulation of neurons (42%; Class E) of reach depth sensitive neurons encode the absolute depth of the reach target, and exhibits spatial tuning that is invariant to changes in vergence angle. Many of the neurons in Class E exhibit some changes in reach depth tuning at different vergence angles that indicate a mixture reference frames. These changes in reach depth tuning may be due to solely the change in vergence angle, or may be due to the different values of target disparity tested at each vergence angle. The data and experimental design do not permit distinguishing between the two possibilities or the most likely scenario that both vergence and disparity are the cause of the change in reach

depth tuning observed. In order to test this, it is necessary to sample the same values of disparity at different levels of vergence, and compare the disparity tuning curves. In addition, the disparity values should be sampled in an even manner, that is, the difference between disparity values that are sampled in the neural response should be constant to better characterize tuning. These factors are considered in the experimental design presented in the next chapter.

71% of the mIPS population is modulated by reach target depth during the execution of the reach movement. The origin of the tuning during the motor response may be due to an efferent copy of motor commands coming into PRR, proprioceptive feedback, or the direct participation of the neurons in driving circuits in the motor and premotor cortices to which they project. The magnitude of a purely motor response would increase with a larger reach movement, and in this case, reach targets at increasing depth would elicit a larger response. Tuning during the movement often resembles the tuning during movement planning or cue presentation, and as seen above, occurs in many profile shapes and is not always monotonic with target depth. A high correlation of firing rate with increasing reach depth would indicate a pure motor response during the movement, however this data set indicates a mean correlation of $R^2 = 0.05$ (very similar to the memory period correlation $R^2=0.04$). In fact, 78% of cells that have a tuned motor response also have a tuned movement planning response, a proportion that is larger than expected if motor responses and movement planning responses were unrelated. Lastly, a purely motor response would not be modulated by fixation depth since it has no bearing on the magnitude of the reach movement; however 41% of reach depth tuned neurons

were significantly tuned to vergence angle. This suggests that the neural activity during the motor response has a strong visual component rather than purely motor one.

Neural activity in many areas in the mIPS, and in particular PRR, is known to have visual responses to stimuli presented as targets for reaches and saccades. These responses are often robustly elicited by the presentation of visual stimuli (visual burst) and are modulated by spatial parameters, such as their location on the retina. The population of neurons from the mIPS recorded in this study shows that tuning to the depth of the visual stimulus during presentation is not a direct predictor of the tuning of a neuron during movement planning. 84% of cells that have tuning during cue presentation have tuning for the depth of the reach target during the memory period, however almost half of the neurons (48%) that have tuning for the depth of the reach target during movement planning lack tuning for the cue presentation. This converse relationship indicates that tuning during movement planning is an emergent property that is not predicated on the neuron being responsive to the direct visual stimulation from the reach target, and is consistent with the encoding of movement intention rather than purely stimulus location associated with spatial attention (Gail and Andersen 2006; Quian Quiroga, Snyder et al. 2006). When considering the neuronal population, this means that downstream cortical areas receive more information about the goal of the upcoming reach during movement planning rather than during the direct presentation of that goal. It appears that just as the integration of neural activity during planning can reflect the direction of an intended reach movement and comprises a sensorimotor transformation, the depth of the impending movement is encoded for that purpose as well.

The results from this experiment establish that neurons in the mIPS are widely sensitive to reach target disparity. The targets used in this experiment were fixed in space and were sometimes fused, slightly diplopic (when they were within the region of patent stereopsis), or were highly diplopic at the different levels of vergence tested. (All targets were highly diplopic at 1.9° of vergence.) Disparity sensitive responses to stimulus presentation may be a direct consequence of processes extending from earlier visual areas known to be sensitive to large disparities, however the diverse and robust tuning to diplopic targets during *movement planning* establishes the participation of this neural population in a visuomotor role that is apart from pure visual responses. Significant reach depth tuning in the population is distributed evenly across the vergence angles tested. Two of the fixation depths tested in this experiment lie outside the region of reach targets tested; at 13° = 15 cm, and 1.9° = 105 cm. The approximate uniform distribution of reach tuning across vergence (Figure 2-15B) suggests that encoding is spread throughout the joint hand-eye space in depth without a bias for closer or farther targets for the hand or the eye. Additionally, there is not an increased incidence of tuning in the population when the fixation target lies "within range" of the reach targets (7.7° and 5.5°), which suggests that the encoding in PRR is flexible in encoding targets both close and far from fixation. This is exemplified by the frequency of reach target tuning in the population at 1.9° of vergence. The neural activity from the population demonstrates that PRR operates in a general context of reaching where neural activity can encode the depth

of fused targets that are close to fixation depth and targets that are highly diplopic, far from the depth of fixation.

Chapter 3 Encoding of Egocentric Distance in PRR: Experimental Design and Methods

3.1 Motivation from Pilot Experiment

The neural activity in the mIPS shown from the previous experiment was modulated by the depth of the reach target and fixation target. The disparities created by the modulation of both targets in depth were non-uniform, and spanned different ranges for each vergence angle. The previous target configuration confirmed the hypothesis that neurons in the mIPS encode the depth of targets. In the following experiment, recording locations were located approximately 5mm posterior to the locations in the pilot experiment in an effort to record at the center of the putative PRR. It was hypothesized that the change in recording location would sample the classical population of PRR neurons that encode in retinal coordinates, and hence yield a much smaller proportion of neurons encoding the absolute depth of the target (as seen in the anterior transition areas recorded in the pilot experiment). The pilot experimental design contained different disparity values for the reach targets at each vergence angle, which did not allow the attribution of response modulation to either disparity or vergence angle. This experiment

is designed to explicitly examine how egocentric distance is encoded by the firing rates during movement planning by separating the two factors.

It is possible to represent egocentric distance by encoding the absolute depth of the target directly. This method of encoding target depth is independent of fixation depth, and requires that neural activity is not modulated by vergence angle. Alternatively, the egocentric distance of the target can be represented by a relative depth that is referenced to fixation depth, such as the disparity of the target. To fully specify egocentric distance in neural activity based on disparity, a representation of fixation depth, which is determined by vergence angle, is also required. Previous studies have shown that disparity tuning is gain modulated by vergence angle as early as V1 during stimulus presentation (Trotter, Celebrini et al. 1992), and during the planning activity for eye movements in depth in LIP (Gnadt and Mays 1995; Genovesio and Ferraina 2004).

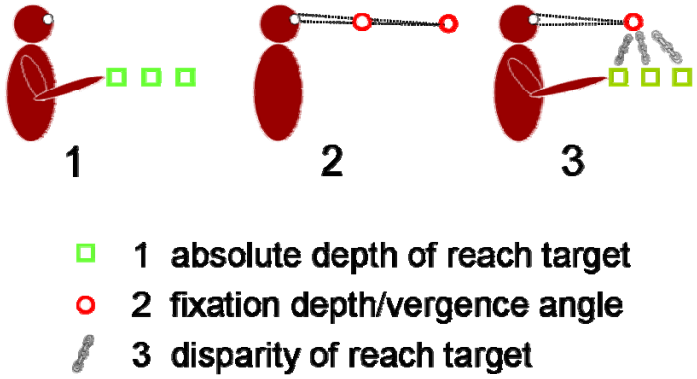

Figure 3-1 – Variables under study in experiment. Co-variation relationships shown in Figure 3-2.

Figure 3-1 shows the symbols used to illustrate the 3 variables under study in the experiment: 1) absolute depth of the reach target, 2) fixation depth/vergence angle, and 3) disparity of the reach target. Figure 3-2 illustrates the covarying relationships between the variables. The disparity of the reach target, vergence angle, and the absolute depth of the reach target are related in 3 ways: A) disparity and vergence angle covary for a reach target at a constant absolute depth, B) absolute depth of the reach target and vergence angle covary for a target at a constant disparity, and C) disparity and absolute depth covary when vergence angle remains constant.

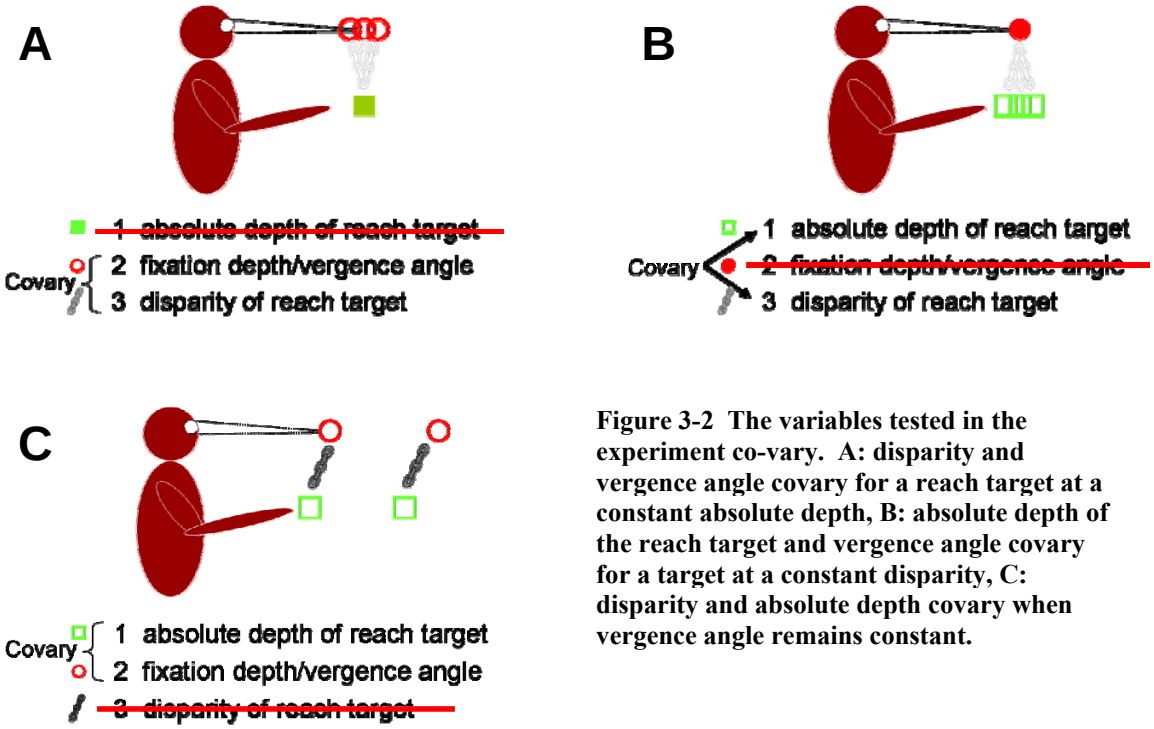

Figure 3-2 The variables tested in the experiment co-vary. A: disparity and vergence angle covary for a reach target at a constant absolute depth, B: absolute depth of the reach target and vergence angle covary for a target at a constant disparity, C: disparity and absolute depth covary when vergence angle remains constant.

3.2 Experimental Design Considerations

We examined whether PRR neurons encode the disparity of the reach target and vergence angle, or instead encode the absolute depth of the reach target during movement

planning. Each neuron was tested with a memory reach task that required binocular fixation using reach and fixation targets that were separate and modulated solely in depth in two experimental configurations. In Experiment 1, reach targets were coupled with fixation targets such that the same target disparities were sampled at different vergence angles (Figure 3-3A-Coupled Reach Targets;). The disparity tuning of PRR neurons, the effect of vergence angle, and the interaction between disparity and vergence angle by gain modulation and disparity tuning shifts were explored with coupled reach targets. Reach targets in Experiment 2 were fixed in space and were decoupled from fixation targets, so that all reach targets were tested with each fixation target (Figure 3-3B-Decoupled Reach Targets). Decoupled reach targets tested different ranges of disparity at each vergence angle, and many targets appeared highly diplopic due to their large disparity values. This configuration allowed us to examine the encoding of reach targets with constant absolute depth, but with different disparities due to changes in vergence angle (Figure 3-4B, Figure 3-5). All reaches were initiated from the same location and the position of both hands remained constant until the cue to execute the reach was presented. This ensured that neural activity was not modulated by the distance of the hands from the body but reflected changes in egocentric target distance only.

There is a tradeoff in designing the target configuration between the sampling range of disparity and the different fixation depths used. A large positive/uncrossed disparity at far fixation quickly falls outside the reachable distance, and limits the testable range of disparity at smaller vergence angles. It is evident from the pilot experiment that population reach tuning is distributed across vergence space, and the chance of observing

target depth tuning is maximized when a wide span of vergence is probed in each experimental session.

These considerations led to a redesign of fixation depth stimuli from the previous experiment to sample vergence at 13°, 9.7°, and 6.5° for a disparity range of [-1.5° : +1.5°] in 0.5° increments in Experiment 1. The choice of disparity range is based on the findings of Ogle presented in Chapter 1, which found that stereoscopic depth is reliably perceived in this range, dubbed "patent stereopsis". The perception of the depth of targets does indeed occur well outside this range, however the increased diplopia does not produce the percept of stereoscopic depth. It has been hypothesized that 2 neural systems process the small range of "fine stereopsis" and large, diplopic range of "coarse stereopsis" separately (Shimono 1984). Previous work has shown that the perception of highly diplopic targets is direct and not precedent on proprioception from the extraocular muscles or an efference copy of the vergence angle (Ziegler and Hess 1997). The results from the pilot experiment found PRR neurons have a large range of disparity sensitivity that corresponds to targets in the region of coarse stereopsis.

The premise of this experimental design is to explore the neural response of PRR to reach targets placed in both fine and coarse regions of stereopsis. No subdivision in neural encoding is implied by the 2 experimental target configurations, however they correspond to two distinct scenarios in hand eye coordination. Coupled reach target disparities in the range of patent stereopsis place their depth "close" to the depth of fixation. This design will allow the examination of disparity sampled at small intervals at 3 levels of vergence

to explore changes in disparity encoding due to fixation depth. Conversely, large disparities that induce the diplopic coarse percept of depth place decoupled reach targets "far" from fixation depth. We can consider the two hand-eye coordination scenarios where 1) we are fixating the target we are to reach to, or 2) fixating elsewhere. The first situation couples fixation and target depth, whereas in the second situation fixation and target depth are decoupled. The disparity ranges tested from both experiments from each level of vergence are shown in Figure 3-4B. The colored bars indicate the regions of disparity sampled at each vergence angle, and the gray shaded range of disparity indicates the disparity region tested for coupled reach targets specifically.

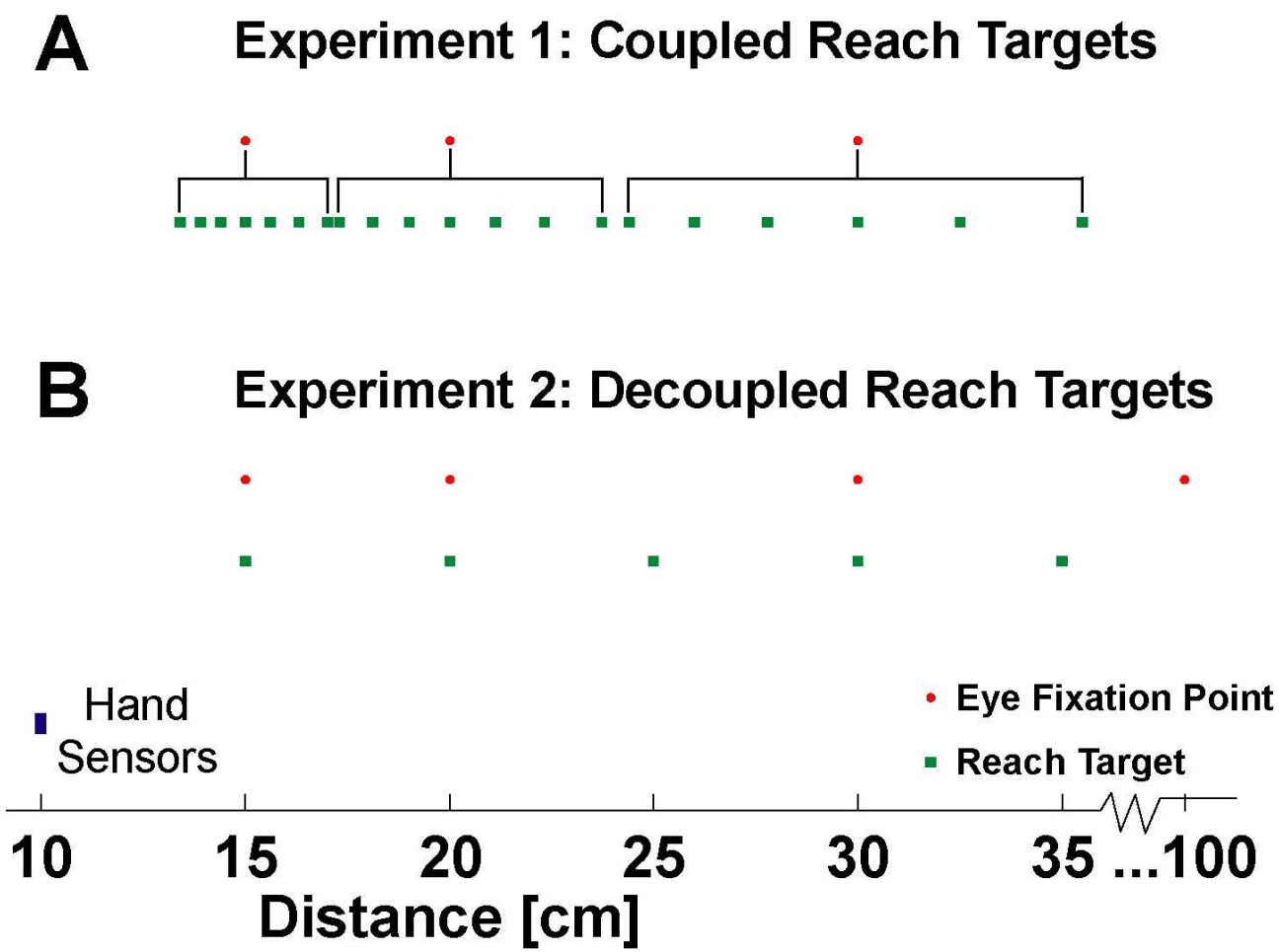

Figure 3-3 – Fixation and reach target configurations tested for each neuron. Fixation targets are shown as red circles, reach targets are shown as green squares. Reaches are initiated from the hand sensor, shown as a blue rectangle. A: Coupled reach targets are placed at symmetric disparities from the fixation target in Experiment 1. B: Decoupled reach targets are tested with each fixation target in Experiment 2.

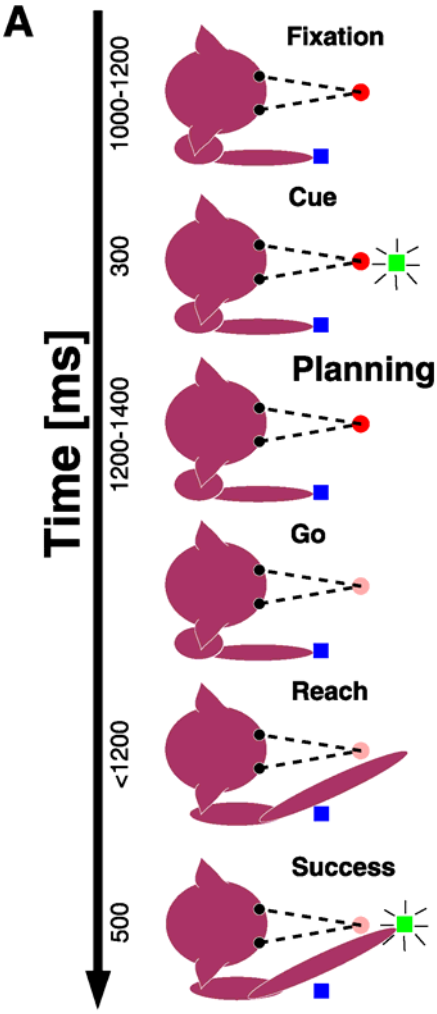

Figure 3-4 A: Trial time line of epochs and stimulus presentation. The length of the epochs are indicated on the time axis. The stimuli colors and shapes are the same as shown in Figure 5-1. B: Disparity and Vergence Sampling for both Experiment 1 and 2 combined. The colored bars indicate the region of disparity tested at each vergence angle. The gray shaded region indicates the disparity region for coupled reach targets in Experiment 1. This region overlaps for 13°, 9.7°, and 6.5° of vergence. The colored regions that do not overlap with the shaded gray region are those tested with decoupled reach targets in Experiment 2. C: Structural magnetic resonance images showing the estimated center of recording sites (cross) in the PRR in the medial IPS in the left hemisphere (radiological convention - images are reflected about the horizontal axis) of monkey T.

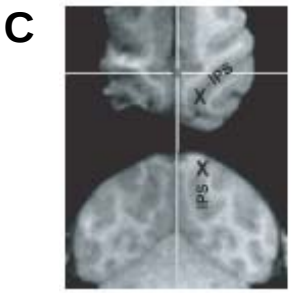

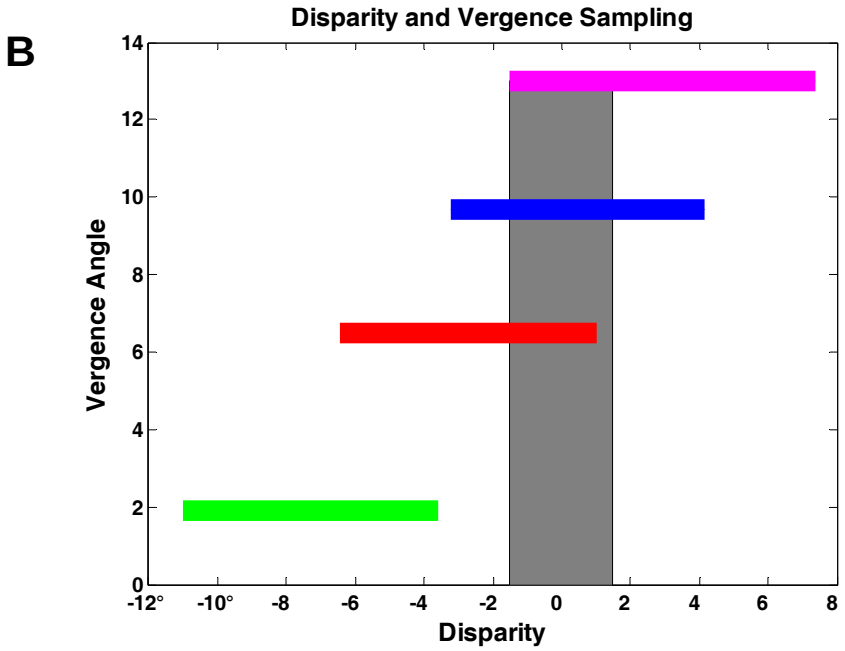

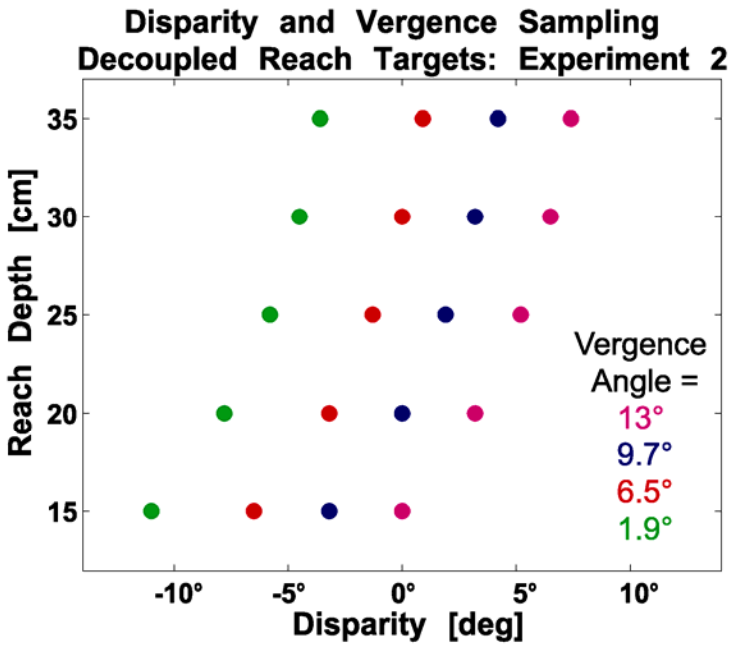

Figure 3-5 Disparity and Vergence Angle Sampling for Decoupled Reach Targets in Experiment 2. The distance of decoupled reach targets is shown on the y-axis (Reach Depth). Different reach target disparities were tested at each vergence angle, however the absolute depth of reach targets was at 5 constant values [15:5:35 cm]. Decoupled reach targets at 13° vergence angle are shown in magenta, for 9.7° in blue, 6.5° in red, 1.9° in green.

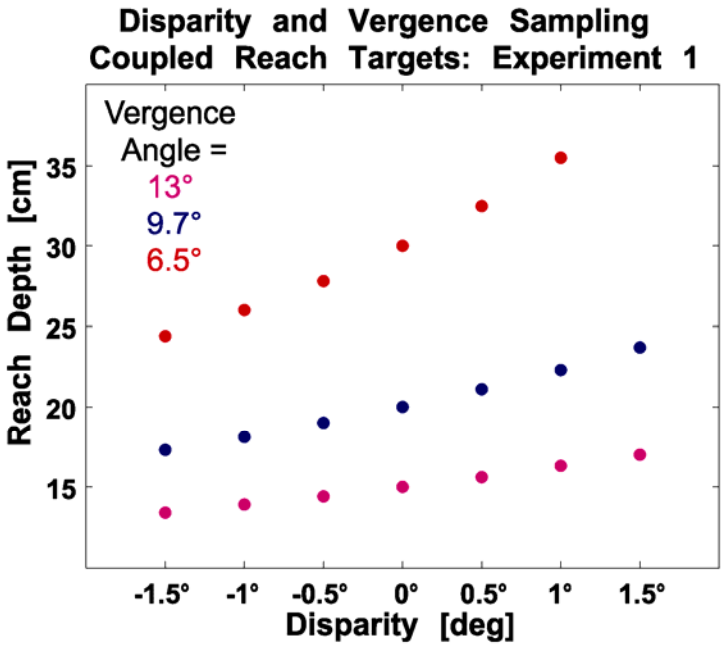

Figure 3-6 – Disparity and Vergence Angle Sampling for Coupled Reach Targets in Experiment 1. The distance of coupled reach targets is depicted on the y-axis (Reach Depth). The same reach target disparities were tested at each vergence angle. Coupled reach targets at 13° vergence angle are shown in magenta, for 9.7° in blue, and 6.5° in red. The 1.5° disparity target at 6.5° vergence angle was outside the reach span of both monkeys (not shown).

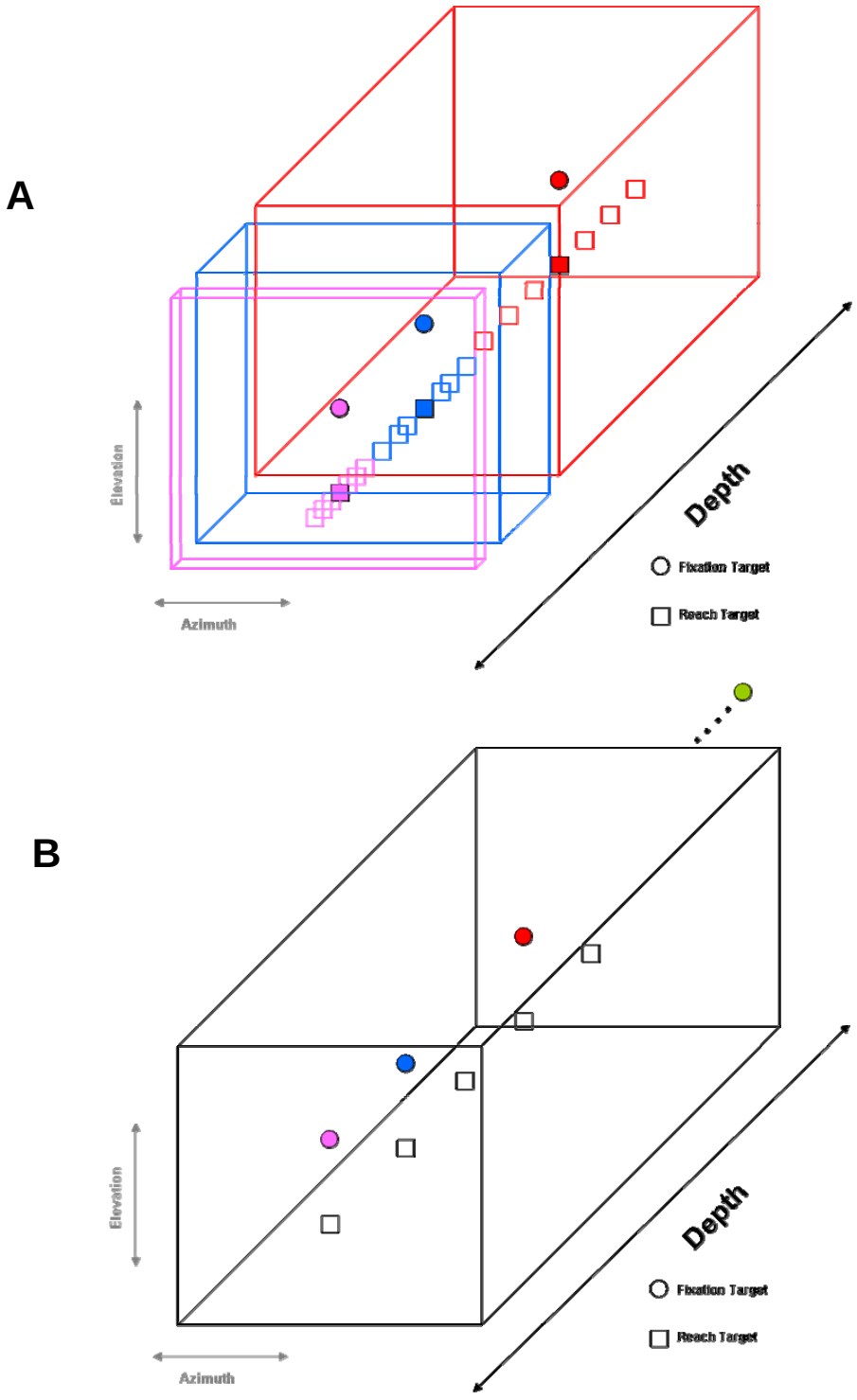

Figure 3-7 – Depiction of reach and fixation targets in 3D space. Fixation targets are shown as circles, reach targets are shown as squares. A: Coupled depth in Experiment 1, colors of fixation targets, reach targets, and extent of absolute depth tested with each fixation target correspond to each other. B: Decoupled depth in Experiment 2, all reach targets are tested with each fixation target, so extent of absolute depth tested is the same with each fixation target.

3.3 Methods

Memory Reach Task

Two rhesus macaques were trained to perform memory reaches with binocular fixation. The stimuli were presented in a dark chamber, and reach target and fixation stimuli were physically isolated from each other to prevent cross contamination of luminance. Trials were initiated when the hands were placed on 2 capacitive touch sensors located at hip level 10 cm in front of the face. Both hands were required to remain stationary until the cue to perform the reach movement was given. A fixation stimulus appeared after trial initiation, and the monkey was required to fixate this stimulus within a spherical window with 1° radius for the entire trial. The monkey maintained fixation on the fixation stimulus for all epochs, including during the reach movement and presentation of feedback after a successful reach. Trial epochs are shown in Figure 3-4A. After 1000-1200 ms of fixation (Fixation), the reach stimulus flashed for 300 ms (Cue), and a memory period of 1200-1400 ms followed during which the monkey maintained hand position and gaze (Planning). The cue to perform the reach movement was signaled by the dimming of the fixation stimulus to half its previous luminance (Go). The monkey had 1200ms to perform a reach with the right hand to a clear touchscreen centered on and in front of the reach stimulus (Reach). If the touch position occurred within a 2.5 cm radius around the target for 250ms, the reach stimulus reappeared for 250ms, during which the touch position had to be maintained (Success). Upon success a juice reward and auditory tone was delivered. Reach and fixation targets were arranged in 2

experimental configurations. In Experiment 1, reach targets were coupled with fixation targets such that the same target disparities were sampled at different vergence angles (Figure 3-3A-Coupled Reach Targets; Figure 3-4B; Figure 3-6; Figure 3-7A). Because coupled reach targets with crossed disparities had to be placed within the monkey's reach span, the distances of fixation stimuli were constrained. The disparity tuning of PRR neurons, the effect of vergence angle, and the interaction between disparity and vergence angle by gain modulation and disparity tuning shifts were explored with coupled reach targets. Reach targets in Experiment 2 were fixed in space and were decoupled from fixation targets, so that all reach targets were tested with each fixation target (Figure 3-3B-Decoupled Reach Targets; Figure 3-4B; Figure 3-5; Figure 3-7B). Decoupled reach targets tested different ranges of disparity at each vergence angle, and hence did not constrain the depth of the fixation stimulus to be within the monkey's reach span. A fixation stimulus was placed at a "far" depth (1m) in addition to the fixation stimuli in Experiment 1, and many targets appeared highly diplopic due to their large disparity values at the different vergence angles. This configuration allowed us to examine the encoding of reach targets with constant absolute depth, but with different disparities due to changes in vergence angle.

Stimuli

Fixation stimuli were red circular LEDs (2mm diameter), centered in azimuth and placed in elevation at eye level at 15, 20, 30, and 100 cm from the monkey's face (see Figure 3-3). The interocular distance for both monkeys was 34mm, thus the fixation stimuli

corresponded to 13°, 9.7°, 6.5°, and 1.9° of vergence angle. The reach stimulus was a square green LED (5mm side). The reach stimulus and touch screen were mounted to a 3 axis Cartesian robot (Samsung FARA RCM-4M, with SRC+ controller; Suwon City, Kyungki-Do, Korea). They were centered in azimuth, fixed in both azimuth and elevation, and modulated solely in depth at the distances designated in Figure 1B and C. Stimulus presentation was computer controlled, and touch sensor (Omron Electronics LLC, Schaumburg, IL), touchscreen (Microtouch; 3M Touch Systems, Methuen, MA), and eye position signals (CNC Engineering, Seattle, WA) were monitored in real time using custom software written in Labview (National Instruments) and C++. The position of the reach stimulus was changed during intertrial intervals only. The time duration that the motors of the Cartesian robot were powered to change the position of the reach stimulus was kept constant in order to offset possible auditory cues from the manipulation of the depth of the reach stimulus. Reach and fixation stimuli were randomized in blocks of 5 trials. The experiments were performed in the dark except for the intertrial interval between block when the lighting in the chamber was briefly flashed to prevent dark adaptation.

Animal Preparation and Recording Procedure

Monkeys were implanted with head posts for reach training. Both monkeys performed reaches with the right limb. MRIs were performed to determine the stereotaxic location of the intraparietal sulcus. After initial training, the monkeys were implanted with scleral search coils (Baer Wire) in each eye to monitor the position of both eyes (Judge,

Richmond et al. 1980). Structural MRIs were performed to determine the stereotaxic location of the intraparietal sulcus for subsequent recording chamber placement (Figure 3-4C, Figure 2-4). Surface normal recording chambers were implanted above the posterior parietal cortex to allow access to the medial wall of the intraparietal sulcus in the left hemispheres of both monkeys. Following the implant surgeries the monkeys were trained to perform the memory reach task with binocular fixation. All surgical procedures were done under general anesthesia and in accordance with National Institutes of Health guidelines. The Caltech Institutional Animal Care and Use Committee approved all protocols.

Recording

Extracellular neural signals were recorded using a three channel microdrive with quartz insulated platinum-tungsten electrodes with impedances of 1.0-2.5 mΩ (Thomas Recording, Giessen, Germany). Signals were preamplified in the microdrive by 20x, an 8 pole low pass filter (<20kHz) by 7x, and then bandpassed and amplified 50x to isolate spiking neural activity (Plexon; Dallas, TX). Spike waveforms were viewed and sorted online (Sort Client; Plexon) and subsequently digitized and recorded to hard disk. Spike waveforms were inspected offline and further sorted to isolate single units and assess stationarity (Offline Sorter; Plexon). The signals from the capacitive touch sensors, the touchscreen, and horizontal and vertical positions of both eyes were recorded via the Plexon system onto hard disk. Preliminary single unit recordings were conducted using a memory reach task to locate reach related, planning period activity in the recording

chambers. Recording chambers were mapped to identify a region of interest based on the functional definition of PRR (Snyder, Batista et al. 1997), with the center located at approximately 9P, 5.25L (Horsley-Clarke coordinates). The data from the recording chamber mapping procedure was not included for analysis in this study. All subsequent single unit recordings made after chamber mapping were included in the analysis regardless of activation for the task or planning period, or the presence of tuning in any epoch. In addition, neurons with any level of responsiveness were recorded in an effort to eliminate the general bias toward recording neurons with generally high firing rates.

Analysis

The spike rates of 137 single units (90 from monkey G; 47 from monkey T) were analyzed from successful reach trials. Results were qualitatively the same from both monkeys and are presented jointly. Spike rates for the planning period were considered 200ms after the reach stimulus cue offset to ensure that activity from visual processes related to the cue presentation, onset, and offset did not contaminate the planning period spike rate. Data collected for all units that were analyzed (n = 137) included all fixation and reach target configurations in both Experiment 1 (n = 20 total configurations) and Experiment 2 (n = 20 total configurations), with a minimum of 5 trials per condition. The disparities of coupled reach target in Experiment 1 ranged from -1.5° to +1.5° in 0.5° steps with respect to the fixation stimuli at 15 and 20 cm, and disparities ranged from -1.5° to +1.0° in 0.5° steps with respect to the fixation stimulus at 30 cm (n = 20 total

configurations; see Figure 3-6). For all analyses comparing disparity responses at 2 vergence angles, only disparity values that were sampled at both vergence angles were used in the calculations. The disparities of decoupled reach targets in Experiment 2 had different values and ranges with respect to the fixation stimuli (n = 20 total configurations, see Figure 3-5). Coupled and decoupled reach target disparities were considered separately in all but the following analyses: 1) to assess whether cells were disparity sensitive overall; and 2) for the population disparity tuning shown in Figure 4-12 (red bars), where disparities from both experiments were grouped by vergence angle and tested for significant modulation. Modulation by disparity or vergence angle was considered significant by ANOVA ($P < 0.05$), and yielded very similar results using Kruskal-Wallis in all tests ($P < 0.05$).

Disparity Classification

The disparity tuning classification procedure was based on the classes previously described in V1 (Poggio and Fischer 1977; Poggio 1995). Disparity tuning was classified subjectively by inspecting significantly tuned planning period disparity response profiles and designating them to “Zero Tuning”, “Near + Tuned-Near”, or “Far + Tuned-Far” categories if the response profile exhibited the features described for one of those classes, and was otherwise designated as “Complex”. Neurons with peak features for zero disparity were classified in the “Zero Tuning” category, and included both excitatory and inhibitory tuning. Neurons with excitation for a large range of crossed disparities (-1.5°: -0.5°) or a peaked response (excitatory or inhibitory) for crossed disparity where

classified as “Near + Tuned-Near”. Neurons with excitation for a large range of uncrossed disparities (+0.5°:1.5°) or a peaked response for uncrossed disparity were classified as “Far + Tuned Far”. Neurons with multimodal, or broad tuning that included both crossed and uncrossed disparity were classified as “Complex”. A principal components analysis (PCA) was performed on zero-tuned, near + tuned-near, and far + tuned-far disparity tuning curves. The firing rates in the disparity tuning curves were mean subtracted and normalized to [0, 1] (in order remove magnitude information and examine tuning shape) prior to PCA.

Disparity Tuning Cross Correlation

Disparity tuning curves from Experiment 1 at each vergence angle from the cue, planning, and movement periods were cross correlated. The disparity tuning curves from all vergence angles only included disparity values from -1.5° to +1.0° in 0.5° steps. The cross correlation value at zero lag is considered a correlation coefficient, ranging from $-1 \leqslant \rho \leqslant 1$.

$$\rho = \frac{\sum_i (X_i - \mu_x)(Y_i - \mu_y)}{\sqrt{\sum_i (X_i - \mu_x)^2 (Y_i - \mu_y)^2}}$$

3-1

The zero lag cross correlations were compiled for 1) cue and planning periods, and 2) planning and movement periods. A permutation test was employed to determine the significance of cross correlations. Trials were shuffled, and disparity tuning curves at each level of vergence and each period were calculated from the shuffled data (preserving

the number of trials for each condition obtained in the experimental session) and cross correlated at zero lag. The cross correlations at zero lag between disparity tuning curves from different periods were considered significant if they exceeded the magnitude of 95% of shuffled cross correlation values at zero lag ($P < 0.05$).

DTI

Disparity Tuning Index was a measure of modulation by disparity at a single level of vergence.

$$DTI = \frac{(\max - \min)}{(\max + \min)} \quad \textbf{3-2}$$

DTI was calculated for planning and cue period responses without subtraction of baseline firing rates (Uka, Tanaka 2000) to allow a direct comparison with results published on the DTI observed in other cortical areas. DTI was computed using the average firing rates at each disparity level during movement planning or cue period. The Pearson correlation coefficients were calculated for the DTI at different pairings of vergence angle from individual neurons across the population and were all significant ($p < 1e\text{-}5$). We performed several nonparametric tests to detect differences in DTI across the population at different vergence angles.

Vergence Tuning Index

Vergence Tuning Index (VTI) is a measure of modulation by vergence at a single level of target disparity:

$$VTI = \frac{(\max - \min)}{(\max + \min)} \quad \textbf{3-3}$$

VTI was calculated for planning and cue period responses without subtracting baseline firing rates. The VTI was measured using coupled reach targets in Experiment 1 and compared at different disparities across the population of neurons. VTI contains 3 samples at each level of target disparity (13°, 9.7°, and 6.5° vergence angle), and only target disparities commonly sampled at all vergence angles were considered (-1.5° to +1.0° in 0.5° steps).

DDI

Previous studies have used the Disparity Discrimination Index (DDI) (Prince, Pointon et al. 2002; Uka and DeAngelis 2003) to measure the effect of disparity with reference to neuronal firing rate variance:

$$DDI = \frac{\max - \min}{\max - \min + 2 * \sqrt{SSE/(N - M)}} \quad \textbf{3-4}$$

where max is the maximum mean firing rate (averaged across trials) observed for disparity at one level of vergence, min is the minimum at the same level of vergence (same convention used in DTI above), SSE is the sum of squared errors about the mean

responses, N is the total number of trials, and M is the number of disparities tested. The term $\sqrt{SSE/(N-M)}$ is a measure of the firing rate variance. It was calculated at each level of vergence and analyzed similar to DTI.

Vergence Gain Model

A gain model was employed to determine whether vergence acted upon disparity as a linear operator. This was done at two levels of vergence, and one disparity tuning curve was regressed onto the other using linear least squares:

$$Y = b * X + c \qquad \textbf{3-5}$$

where Y and X are disparity tuning curves at different fixation depths, b is the multiplicative gain and c is the additive gain by vergence angle. We performed a bootstrap analysis (Efron and Tibshirani 1993) where trials were selected with replacement to form resampled disparity tuning curves. We used 500 resamples in the bootstrap analysis. Vergence gain was considered significant for a given pair of disparity tuning functions if the bootstrap yielded a significant correlation coefficient (r-value) from the regression (95% confidence interval using percentiles did not contain 0).

Absolute Target Depth and Disparity Modulation

Index A was a measure of the modulation of planning period firing in individual neurons neuron which varied vergence angle and disparity for targets at constant absolute depth:

$$\text{Index A} = \frac{(\max - \min)}{(\max + \min)} \quad \textbf{3-6}$$

Index A was measured at 3 absolute target depths (15, 20, and 30 cm) and vergence angles (13°, 9.7°, and 6.5°). These 3 vergence angles created 3 different disparities for each reach target at a constant absolute depth. Figure 4-29 shows the vergence angle and reach target sampling for Index A, where 3 groups of targets with constant absolute depths but varying disparity and vergence angle are circled. Index A from the reach targets at the different depths were subsequently averaged for each neuron to obtain a single index for comparison to Index B. Index B was a measure of the modulation of planning period firing rate in individual neurons which varied vergence angle and the absolute depth of reach targets while maintaining constant disparity:

$$\text{Index B} = \frac{(\max - \min)}{(\max + \min)} \quad \textbf{3-7}$$

Index B was measured using at the same targets and vergence angles as Index A. The target and vergence angle configurations created 3 different reach target disparities (0°, -3.2°, and +3.2°), and the responses were averaged across disparity for each neuron. Figure 4-30 shows the vergence angle and reach target sampling for Index B, where 3 target groups with constant disparity are circled. The modulation was computed for each disparity group and then averaged across disparity groups to obtain a single value for each neuron. 3 reach targets had 0° disparity at 15,20, and 30 cm (13°, 9.7, 6.5° vergence angle); 2 reach targets had -3.2° disparity at 20 and 30 cm (13° and 9.7° vergence); and 2 reach targets had +3.2° disparity at 15 and 20 cm (9.7° and 6.5° vergence).

Shifting Responses

Shifting responses were measured by cross correlating pairs of disparity tuning curves from coupled reach targets in Experiment 1 for individual neurons. This method has been used previously on spline interpolated tuning curves (Shenoy, Bradley et al. 1999). We opted to not interpolate and instead use the raw data to calculate shifts in disparity, using a bootstrap permutation test to determine the significance of a shift from cross correlation. The tuning curves were mean subtracted before computing the cross correlation:

$$CC(j) = \sum_{n} X[n]Y[n+j] \qquad \textbf{3-8}$$

where *CC(j)* is the cross correlation value at lag *j*, and $X[n]$ and $Y[n]$ are disparity tuning curves from two different fixation depths. The maximum lag in the cross correlation was 3 (±1.5°) to ensure that all cross correlations included at least 3 points. A permutation test was employed to determine the significance of cross correlations. Trials were shuffled, and disparity tuning curves at each level of vergence were calculated from the shuffled data (preserving the number of trials for each condition obtained in the experimental session) and cross correlated. Shifting responses between disparity tuning curves at different vergence angles were considered significant if they exceeded 95% of shuffled cross correlation values ($P < 0.05$). A histogram of significant shift values from all pairs of disparity tuning curves was calculated. An alternate criterion for selecting the

optimal shift value was to normalize the cross correlations by the square root of the product of the power of the 2 signals:

$$\frac{CC(j)}{\sqrt{P(X)P(Y)}}$$

This criterion yielded qualitatively similar results in the distribution of optimal shifts, with an overall reduction in the number of significant shifts observed. This criterion was evaluated with simulated receptive fields (see below) and was extremely sensitive, and was not used for comparison.

Simulated Receptive Fields

Spatial receptive fields were simulated using gaussian functions:

$$f(d) = ae^{-(d-\mu)^2/(2\sigma^2)} \quad \textbf{3-9}$$

where d is depth (cm), a is the height of the Gaussian peak, μ is the location of the peak in depth (cm), and σ is the width of the Gaussian function. The peak location and width for the functions were randomly selected from uniform distributions where the μ ranged from 15 to 35 cm in 1 cm increments, and σ ranged from 1 to 5 cm in 0.1 cm increments. The choice of a (peak height) did not effect the computation. Samples of these Gaussian tuning functions were taken at the spatial locations corresponding to the disparity and vergence samples taken in Experiment 1 for coupled reach targets. For example, Gaussian tuning functions were evaluated at the spatial locations of disparity samples [-1.5°:0.5°:1.5°] for coupled reach targets for 13° fixation at d = 13.4, 13.9, 14.4, 15, 15.6,

16.3, and 17 cm. These samples formed a set of simulated disparity tuning curves from a neuron with a Gaussian tuned spatial receptive field. These simulated disparity tuning curves were then cross correlated to measure shifting responses in an identical manner as described above. Similarly, significant shifts were obtained by permutation tests, and compiled in a histogram. Power normalized cross correlations were extremely sensitive; alignment of very small features from the tuning curves yielded large normalized cross correlations (>0.95), and were not appropriate for comparison. Instead, the significance criterion from permutation tests used the cross correlation value $CC(j)$ as in the prior section.

Mutual Information

The mutual information between planning period firing rates and stimuli were calculated. The stimuli used were the coupled reach target disparities, and the vergence angles from Experiment 1. Information theoretic measures have been used previously with dynamic firing rates compiled across trials (Paninski, Fellows et al. 2004). Mutual information is the overlap of the entropy of 2 signals. The entropy of a signal is based on the probability distribution of its values. The entropy calculations for the neural signal use the binned mean firing rates across the planning period for each trial. Firing rates were binned in 1Hz bins from 0Hz to the maximum firing rate observed. The entropy of a neural response, $H(N)$ is:

$$H(N) = -\sum_{i=1}^{m} P(N_i) \log P(N_i)$$

3-10

Where *m* is the number of bins, and $P(N_i)$ is the probability of observing the firing rate in bin i. The mutual information, *MI*, can be expressed in terms of the neural and conditional entropies:

$$MI(N,S) = H(N) - H(N|S)$$

3-11

where

$$H(N|S) = -\sum_{j=1}^{n}\sum_{i=1}^{m} P(N_i)P(S_j|N_i)\log\frac{P(S_j|N_i)P(N_i)}{P(S_j)}$$

The neural entropy can be rewritten:

$$H(N) = -\sum_{i=1}^{m} P(N_i) \log P(N_i) = -\sum_{i=1}^{m}\sum_{j=1}^{n} P(N_i)P(S_j|N_i)\log(P(N_i))$$

$$\text{since } \sum_{i=1}^{m}\sum_{j=1}^{n} P(S_j|N_i) = 1$$

Now we can re-express *MI*(*N*, *S*):

$$MI(N,S) = -\sum_{i=1}^{m} P(N_i) \log P(N_i) + \sum_{i=1}^{m}\sum_{j=1}^{n} P(N_i)P(S_j|N_i)\log\frac{P(S_j|N_i)P(N_i)}{P(S_j)}$$

$$= \sum_{i=1}^{m} P(N_i)\left(\sum_{j=1}^{n} P(S_j|N_i)\log\frac{P(S_j|N_i)P(N_i)}{P(S_j)} - \sum_{j=1}^{n} P(S_j|N_i)\log P(N_i)\right)$$

resulting in

$$MI(N,S) = \sum_{i=1}^{m} P[N=i] \sum_{j=1}^{n} P[S=j|N=i] \log \frac{P[S=j|N=i]}{P[S=j]}$$

3-12

The equation above thus describes the mutual information in terms of the probabilities of the stimuli (disparity or vergence values, usually near uniform due to experimental design), the probabilities of firing rates during movement planning, and the probability of observing a firing rate given a stimulus value. These values are directly computed from the data.

Normalizations of mutual information by the entropies of the quantities have been used in order to compare mutual information measures. We used the following normalization to compare the mutual information of firing rate with disparity versus vergence for individual cells:

$$NI(N,S) = \frac{2 * MI(N,S)}{H(N) + H(S)}$$

3-13

Where NI is normalized mutual information, *MI* is the mutual information between 2 quantities, *N* is the firing rate data, *S* is the stimulus data (*e.g.*, disparity levels or vergence levels), and *H* is the entropy of a given quantity. It is also referred to as symmetric uncertainty in the literature (Press, Teukolsky et al. 1992; Ping-Sung Liao 2006).

A measure of significance for *NI* was calculated using bootstrap permutation tests. Firing rate data was shuffled to randomize the association of firing rates with disparity and vergence levels, and the *MI* and *NI* were recalculated to from the shuffled data. *NI* was considered significant if the actual value was greater than the average *NI* from the randomized data.

Chapter 4 Encoding of Egocentric Distance in PRR: Experimental Results

To investigate how a reach target is represented in three dimensions, we recorded the spiking activity of PRR neurons from two rhesus macaques trained to fixate and perform memory reaches to targets at different depths. Reach and fixation targets were configured to explore whether neural activity directly reflects egocentric distance as the amplitude of the required motor command, which is the absolute depth of the target, or rather the relative depth of the target with reference to fixation depth. The results show that PRR reflects egocentric distance in visual coordinates, which is integral to the early stages of reach planning and supports hand-eye coordination in depth.

This chapter begins with behavioral data, and is followed by a brief summary of the overall responses to reach target disparity and vergence angle. The sections that follow examine the classification of disparity responses, the strength of disparity tuning, gain modulation and shifts of disparity tuning by vergence angle, and a comparison of the influence of vergence angle and disparity on planning period responses using different measures.

4.1 Behavior

We sought to investigate the representation of reach depth, disparity of the reach target, and vergence angle in the neural activity of PRR neurons. We examined the behavioral data, mainly eye position and reaction times, to determine whether it contained modulation that could affect the outcome of planning period responses to disparity and vergence. For example, it is possible that the monkey could make rapid saccades to the target during or just after target presentation. Since targets are placed in depth (at disparity from fixation depth), the difference would be reflected in vergence eye position from before, during, and after the cue (during planning). Likewise, we looked to see if there was a systematic change in vergence eye position during movement planning with the disparity of the reach target that could affect memory period neural activity. These changes in vergence eye position would be directly related to target disparity; so a disparity of -1.0° (crossed) would yield a vergence eye position that is 1.0° greater (closer fixation) than when the target was at 0° disparity. Lastly, we examined that the possibility that the changes in vergence eye position were smaller in magnitude than the target disparities tested, but were still systematically changing with target disparity. A similar approach was taken examining reaction times, where we investigated whether changes is reaction time due to reach target disparity could be modulating the neural response during movement planning.

Figure 4-1 shows vergence eye position in a session from Experiment 1 for the three fixation targets and all coupled reach target disparities. Vergence angle did not vary with

the disparity of the reach target (ANOVA; $P > 0.33$) or change due to presentation of the stimulus (ANOVA; $P > 0.31$). Vergence eye position across sessions had a median difference of 0.09° before and after the presentation of the stimulus, with 99% of all vergence eye positions with <0.33° difference. We compared vergence eye position during movement planning for reach targets placed at zero and nonzero disparities to determine whether fixation depth changes were similar in magnitude to changes in reach target disparity. The smallest reach target disparity tested in all experiments was 0.5°, whereas the median of the difference in vergence eye position between zero and non-zero target disparities across sessions was 0.13°. Ninety-two percent of vergence eye positions during movement planning had a <0.33° difference due to nonzero target disparity, which did not change for fixation targets (ANOVA; $P > 0.67$). Though changes in vergence angle were much less than the smallest reach target disparity tested, we examined the possibility that they systematically varied with disparity and found a very low correlation (mean $r^2 = 0.02$ across sessions). Figure 4-2 shows the vergence eye position for both animals for a session from Experiment 2, decoupled reach targets. The vergence eye position behavior for both animals was very similar, with identical experimental constraints on the behavior used in all sessions.

The peak hand velocity varies linearly with target distance. We did not measure the dynamics of the hand, but were able to determine average reach velocity by dividing target distance by the time taken to reach (time from reach onset when leaving the hand sensor to target acquisition on the touchscreen). An example of average reach velocity to coupled reach targets is shown in Figure 4-3A, where a large regression slope is

observed, indicating that average reach velocity increases with target distance. This was true across all experimental sessions (regression slope > 1, P<<0.05). Figure 4-3B, C shows the average reach velocity to decoupled reach targets for both animals for comparison. Average reach velocity of both animals were very similar.

We examined whether changes in reaction time could have a role in modulating planning period responses. Figure 4-4A shows reaction times for reaches to coupled reach targets, with a regression slope very close to 0 and a low correlation coefficient, indicating that reaction time doesn't vary with reach target depth (mean $r^2 = 0.02$ across sessions). Figure 4-4B, C shows reaction times for both animals when reaching to decoupled reach targets for comparison, both with insignificant regression slopes. We looked for a systematic change in reaction time due to reach target disparity. The reaction times to coupled reach targets as a function of reach target disparity is shown in Figure 4-5B. The near zero slope from linear regression and low correlation (see figure) indicate that there is disparity overall, from crossed to uncrossed, does not effect reaction times for reach targets This could occur as a linear function of disparity, however it could also increase linearly from zero to non-zero disparity (either crossed or uncrossed), depicted in Figure 4-5A. To examine this, we computed the correlation coefficient for separately for 0°:+1.5° and -1.5°:0° target disparity, and averaged them. We found a median reaction time difference from zero to nonzero target disparity of 30ms, which did not systematically vary with disparity (mean $r^2 = 0.02$ across sessions). .These behavioral data show that vergence angle and reaction times did not vary with the presentation of the reach target or its disparity to modulate the neural response.

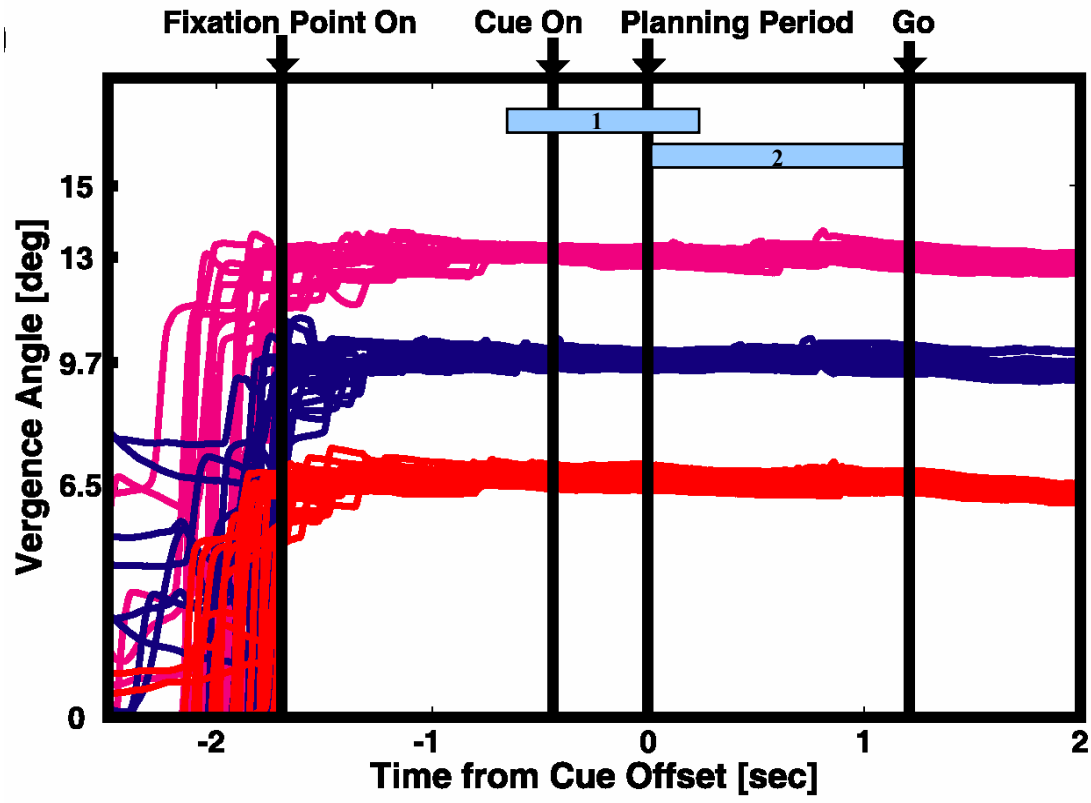

Figure 4-1 Vergence eye position for an experimental session shown for all coupled reach target disparities tested at each fixation distance, from trial initiation through reward. Vergence angle is maintained from the onset of the fixation stimulus (magenta vertical line), through the disparity cue presentation (blue), planning period (red), reach movement onset (green), and target acquisition (black). Vergence did not change with the presentation of the cue (P > 0.31, see blue horizontal bar 1) or vary with the disparity of the reach target (P > 0.33, see blue horizontal bar 2). The average deviation of vergence after cue presentation was 0.08°, and the average deviation from zero to non-zero disparity was 0.13°. $R^2 = 0.0173$.

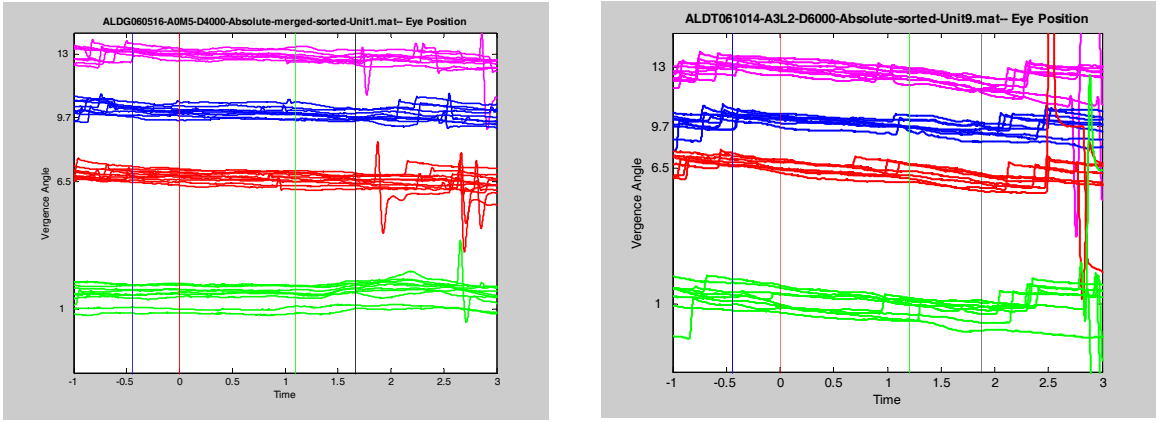

Figure 4-2 Vergence eye position for monkey G (left) and monkey T (right) from a session for Experiment 2 (decoupled reach targets), with vergence eye position for all reach targets. Blue vertical line = cue on, red = cue off/memory being, green = go signal, black=target acquisition.

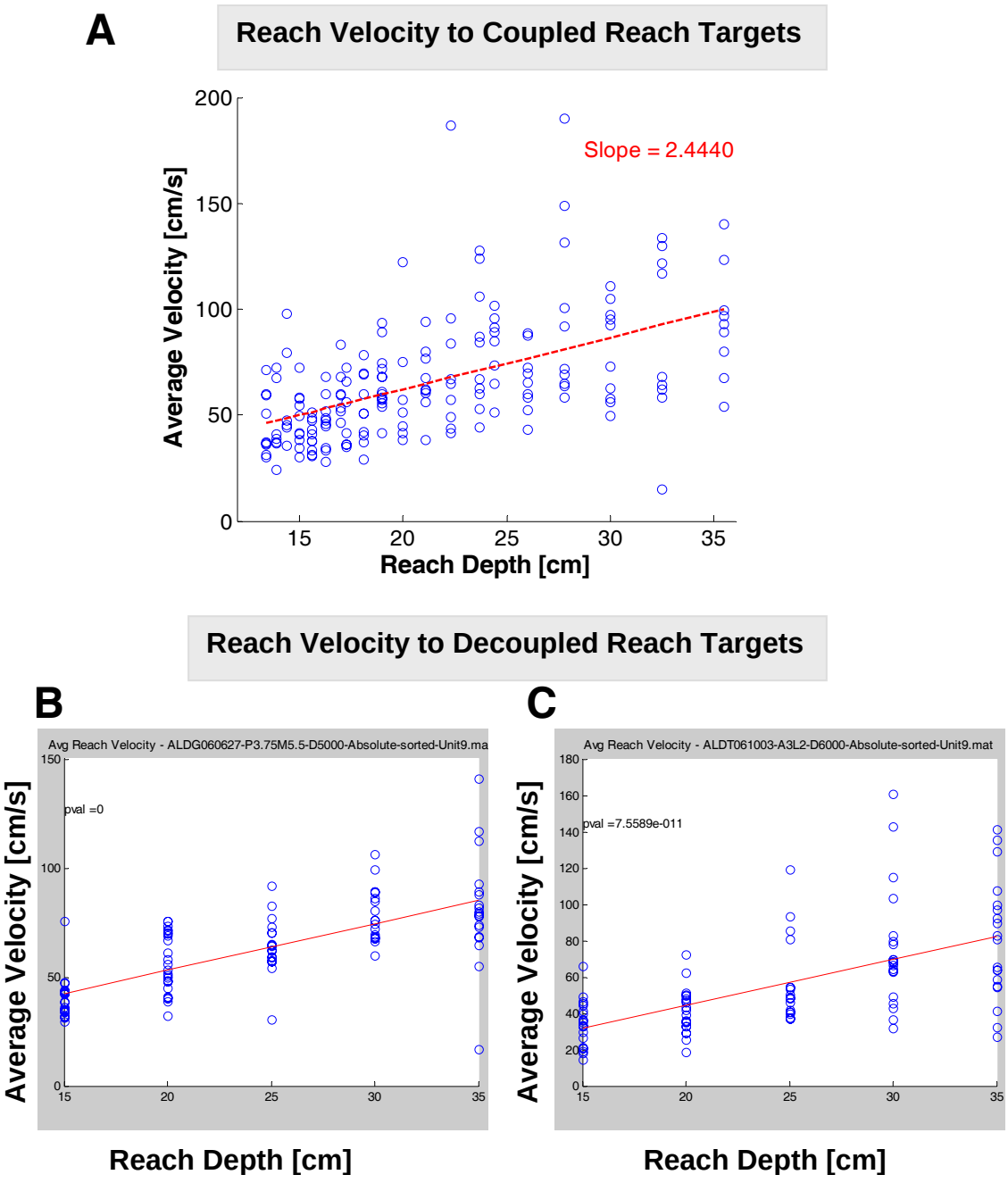

Figure 4-3 A - Average velocity of reaches as a function of coupled reach target depth. The regression slope was highly significant (P < 1e-9). B and C – Average velocity of reaches to decoupled reach targets for monkey G (left) and monkey T (right). Both regressions yielded highly significant regression, with the p values shown on the plots.

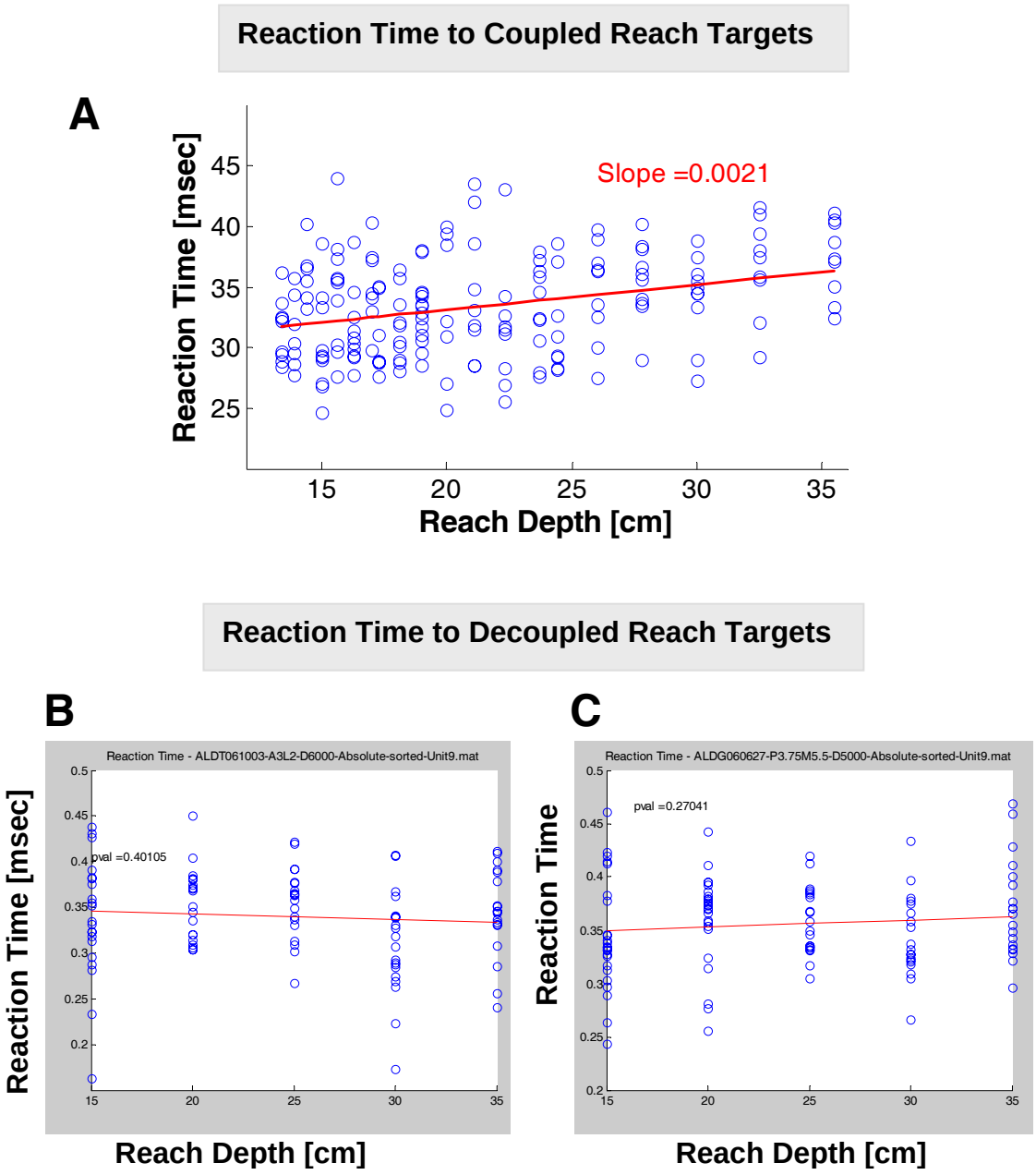

Figure 4-4 A - Reaction time as a function of coupled reach target depth. Slope of regression is, near 0, indicated on graph. Correlation of reach depth and reaction time was low as well (r^2<0.05). B and C – Reaction times as a function of decoupled reach target depth for monkey T (left) and monkey G (right) from a session from Experiment 2, with all vergence angles for all reach targets shown. P values from regressions indicates no significant slope (or correlation) exists between reach target depth and reaction time.

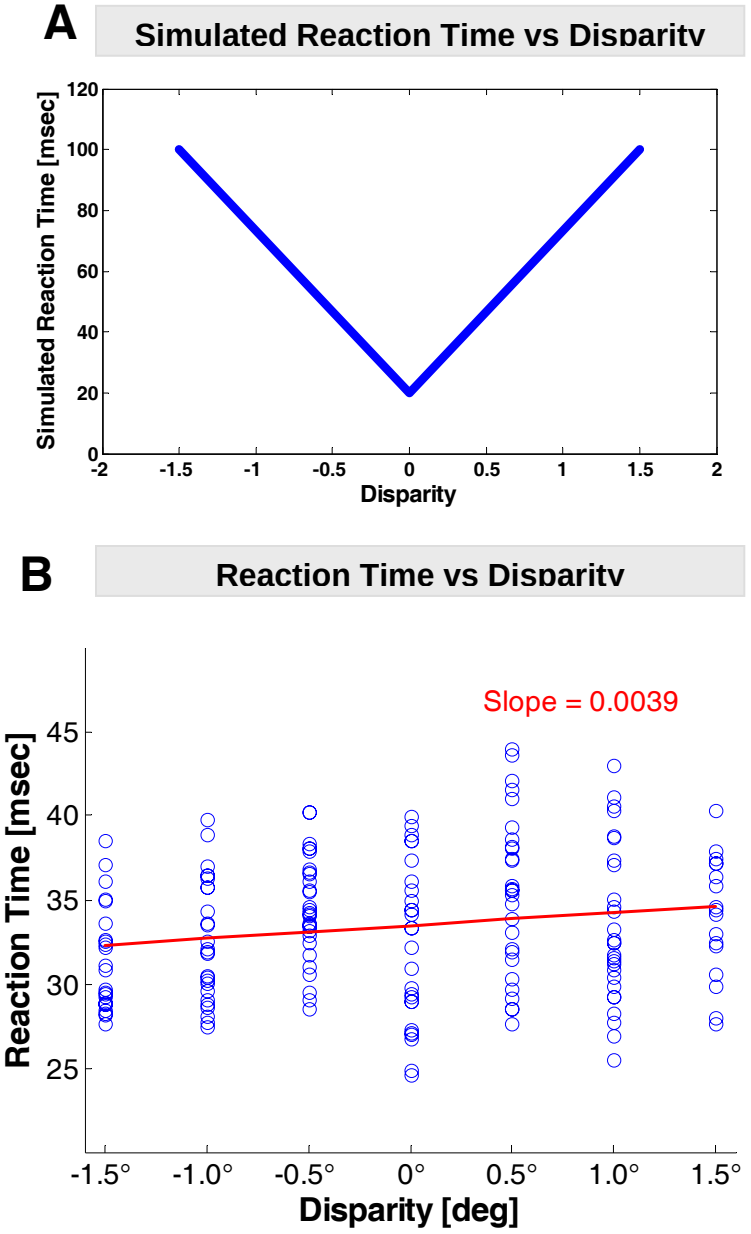

Figure 4-5 A- Simulated reaction time as a function of coupled reach target disparity. We hypothesized that reaction time might increase from zeroto nonzero target disparity. B – Reaction time as a function of coupled reach target disparity from an actual experimental session (monkey G). A pure linear relationship did not exist (regression slope shown in panel), and the relationship depicted in the top panel did not exist, as measure by averaging the correlation coefficients for reaction time from 0°:+1.5° and -1.5°:0° (r^2 = 0.0997).

4.2 Disparity and Vergence in PRR - Overview

One hundred thirty seven PRR neurons were recorded from 2 animals. These neurons were recorded in a blind fashion (see Methods). 82% (112/137) of recorded neurons had a significant effect from reach target disparity during movement planning.[2] The large proportion of responsive neurons signifies the strength of modulation by disparity since reach targets were in a fixed location in azimuth and elevation. It can be assumed that most of the neurons do not have a preference for reach targets in this location in the frontoparallel plane, and means that the modulation of target disparity often occurred in a neuron's nonpreferred 2D receptive field. Additionally, since eye fixation targets were also fixed in azimuth and elevation, the configuration also constrains the direction/ 2D location of the reach target relative to fixation (targets directly below fixation). Taken together, it is evident that despite the constraints of frontoparallel location, target disparity is a strong modulator of planning period activity in PRR.

Disparity sensitivity emerged in a larger proportion of the PRR population in Experiment 1 for movement planning (56%, 76/137) than for the cue period during the presentation of the reach target (34%, 46/137; ANOVA $P < 0.05$). 67% (92/137) of PRR neurons had significant modulation during movement execution at a constant vergence angle, however this modulation may also reflect motor related signals such as motor efference or proprioceptive feedback. The shape of disparity tuning from the cue period was reflected in the planning and movement period responses in PRR neurons, and suggests that

[2] Several classes of responses to disparity and vergence were described in 2.5, and this result (82%) includes Class A and B (effect of reach target disparity across all vergence angles or at a single level of vergence).

information from visual responses during stimulus presentation influences neural activity during planning and executing the reach movement (Section 4.4.1).

The modulation of planning period activity by both target disparity and vergence angle at the population level is important. An estimate of the egocentric distance or absolute distance to the target in an eye centered reference frame requires a representation of disparity and viewing distance. The fact that both signals are present at the population level suggests that PRR uses an eye centered reference frame to encode the location of a reach target. In fact, if there was a lack of vergence modulation in PRR neural activity, a complete representation of target location would not be present in PRR, and the usefulness of a pure disparity signal in downstream cortical processing would patently depend on the presence of a vergence signal in the subsequent stages of processing. Downstream cortical areas can obtain an estimate of the egocentric distance of a reach target if a representation of vergence angle can be recovered in conjunction with disparity from PRR neurons. Vergence angle significantly modulated planning period activity in 74% (101/137) of the population for coupled reach targets with constant disparity (ANOVA; $P < 0.05$).[3]

[3] This is a new class of response not previously described in Chapter 2 because it is a feature that could only be tested with the new experimental design discussed in Chapter 3.

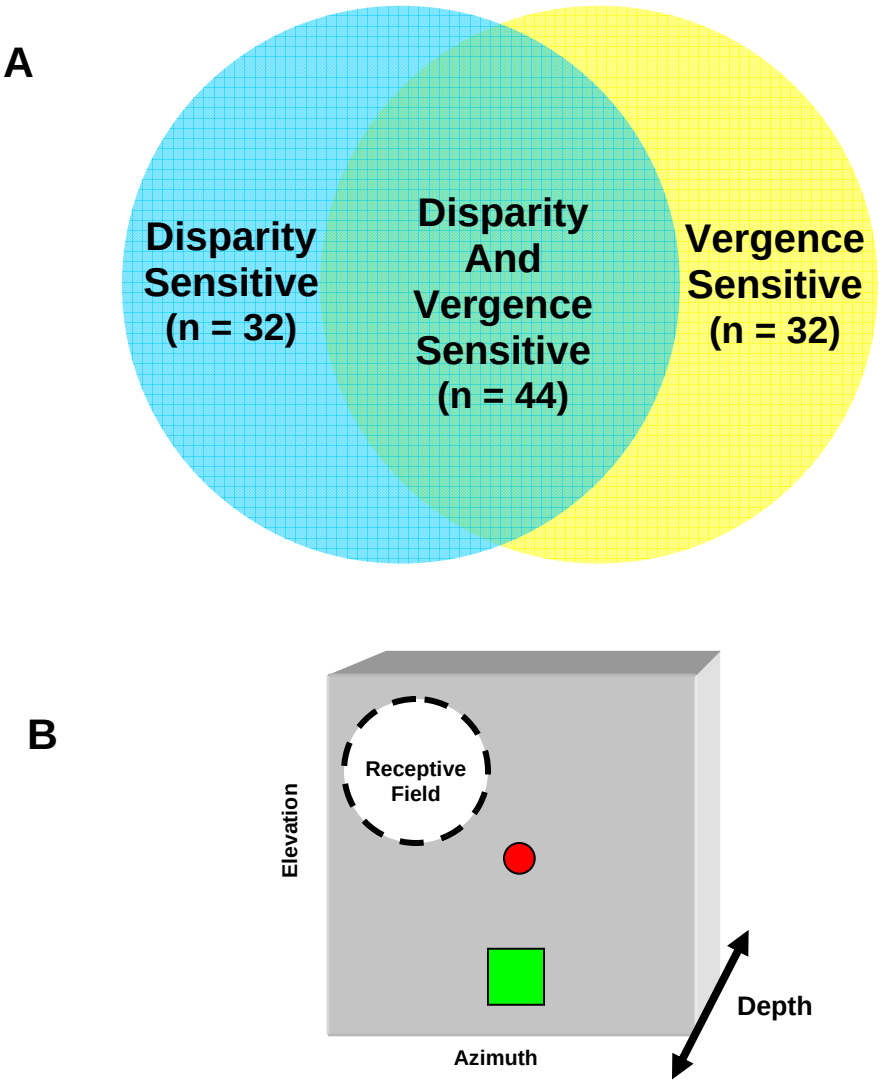

Figure 4-6 - A: Illustration of population sensitivity to coupled reach target disparity and vergence angle. A population of neurons (n = 76 total) expressed modulation by disparity for at least one level of vergence, with a subpopulation with modulation exclusively due to disparity, labeled "Disparity Sensitive". A population of neurons (n = 76 total) expressed modulation by vergence angle (across all disparity), with a subpopulation due to vergence exclusively, labeled "Vergence Sensitive". The majority of neurons from both overall populations (60% of each group) expressed modulation by both, labeled "Disparity and Vergence Sensitive". B: Diagram illustrating a hypothetical receptive field in 3D. The red circle is the fixation point, and the green square is the reach target. The frontoparallel receptive field of the neuron is shown by the dashed circle; it does not encompass the reach target.

4.3 Vergence Angle in PRR

Vergence angle significantly modulated planning period activity in 74% (101/137) of the population for coupled reach targets with constant disparity (ANOVA; $P < 0.05$). 58% (44/76) of neurons that were sensitive to coupled reach target disparity (n = 76) had a main effect of vergence angle (ANOVA; $P < 0.05$). A large proportion (52%, 32/61) of disparity insensitive neurons (61/137) was also significantly modulated by vergence angle (ANOVA; $P < 0.05$); these neurons directly represent fixation depth during planning. (See Figure 4-6A.) It remains possible that this disparity insensitive population of neurons is sensitive to disparity as well as vergence in other frontoparallel locations (Figure 4-6B). In addition, it has been shown that neurons in area 7a are sensitive to fixation position in 3D (Sakata, Shibutani et al. 1980); the use of a single of frontoparallel location for fixation targets in depth likely underestimates the degree of vergence angle sensitivity in the PRR population.

A Vergence Tuning Index (VTI; see 3-3), similar to DTI, was based on response modulation by vergence angle for reach targets at a constant disparity and computed for PRR neurons. The mean of the maximum planning period VTI from each neuron in the population (n = 137) is 0.4326 (±0.2348) with a median VTI of 0.3612, and is nearly identical to and correlated with the DTI (see Figure 4-7). VTI is likely underestimated due to the fact that only 3 samples (13°, 9.7°, 6.5° vergence angle) were obtained at each disparity.

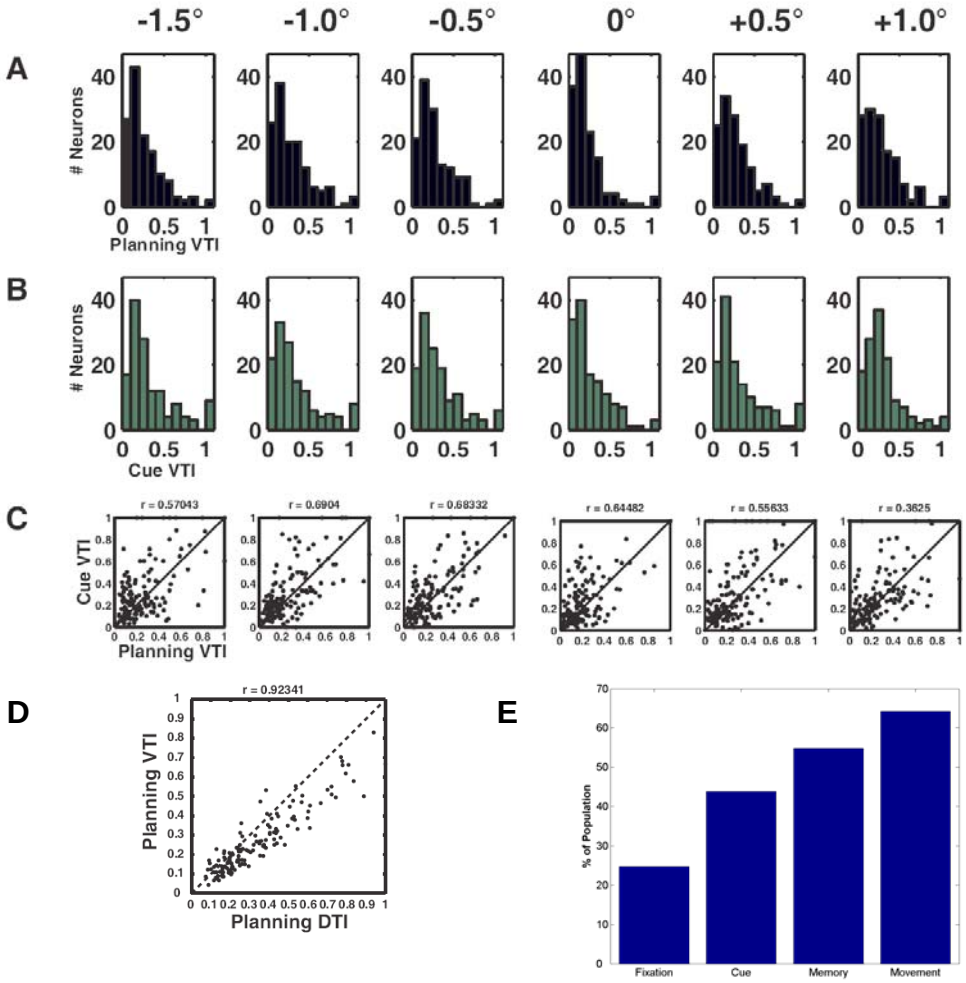

Figure 4-7 VTI from Experiment 1. A: Histograms of planning period VTI for all neurons (n = 137). The average VTI was similar across disparity, however there was a significant difference with a lower VTI for targets at 0° disparity (Kruskal-Wallis; P = 0.0277), which was found to be only between targets at 0° and -1.0° disparity (Kruskal-Wallis with Bonferroni correction for multiple comparisons, P < 0.05). B: Histograms for cue period VTI for all neurons (n = 137). There is no difference in VTI due to target disparity (Kruskal-Wallis; P > 0.17). C: VTI is paired for planning and cue periods for all neurons. The VTI averaged across disparity is similar for cue and planning periods (μ_{cue} = 0.3103±0.1896, $\mu_{planning}$ = 0.2678±0.1606; Kruskal-Wallis; P > 0.07), and no significant differences exist between cue and planning VTI at each level of disparity (Kruskal-Wallis, all P > 0.06). The average difference between cue and planning VTI across neurons and disparity is -0.0425, which is a 13.69% reduction of the cue VTI during planning, and the difference does not vary with disparity (Kruskal-Wallis; P > 0.90). The correlation of the average VTI across disparity between the cue period and planning period is r = 0.84 (P < 1e-5) and correlations between VTI during the cue period and movement planning at each level of disparity are shown (P < 1e-5 for all r). D: The planning period DTI and VTI, averaged across vergence angle and disparity respectively, is paired and shown for all neurons (n = 137), with a correlation of r = 0.92 (P < 1e-5). E: Proportion of vergence sensitive cells by epoch.

Fixation period activity was least modulated by vergence angle in this study. Figure 4-7E shows the percentage of cells in the population significantly modulated by vergence angle during coupled reaches. In this case, activity during an epoch was averaged across disparities within a vergence angle, and differences in firing rates between vergence levels were examined. The visual stimulation of the cue had a greater effect due to vergence; however the modulation by vergence during the memory period effected over half the population. An even larger proportion was modulated during the reaching movement. This illustrates the visuomotor nature of the neurons, where the neural firing rate during the visual guidance of the hand critically depends on the position of the eyes that determines the viewing distance. The firing during the reach could be a result of pure feedback from the motor areas that are coordinating the muscle movements required to make the reach, however the modulation by vergence angle shows this is not the case. The modulation by vergence during this motor action instead suggests that the firing is related to the visual guidance of the hand, however since vergence angle and reach depth covary in the coupled design (Figure 3-2C), different regions of space or sampled with each vergence angle as seen in Figure 3-7A. Comparisons on vergence angle modulation when reach depth is constant (Figure 3-2A) are performed with decoupled targets, and can be found in 4.10 as Index A.

The fact that vergence angle modulates the planning period neural activity of many disparity tuned neurons in PRR suggests that target depth is directly encoded by these cells. A population of neurons sensitive to only vergence angle (pure vergence) supports the functionality of an eye centered encoding scheme by explicitly representing the depth

of fixation (Figure 4-6A; yellow). Pure vergence encoding cells may be the source of the vergence modulation observed in disparity sensitive cells though lateral connections. In addition, vergence encoding cells serve as a relay for the vergence signal to downstream cortical areas. These downstream cortical areas could in turn use a pure disparity signal (not modulated by vergence) and combine the information from a pure vergence encoder to infer the egocentric depth of a target. Again, it remains possible that pure vergence encoding cells for one frontoparallel target configuration may additionally encode the disparity of a reach target in another frontoparallel configuration. Figure 4-6B shows a hypothetical 3D receptive field for a neuron. The reach target does not fall in the frontoparallel receptive field, and thus the neuron does not show sensitivity to the disparity of the reach target, however the neuron may still encode the vergence angle when fixating the fixation stimulus. Several examples of neuronal tuning during movement planning for pure vergence encoders are shown for all experimental conditions of disparity and vergence in Figure 4-10 to Figure 4-9. A robust, statistically significant change in planning period firing rates is observed for vergence only.

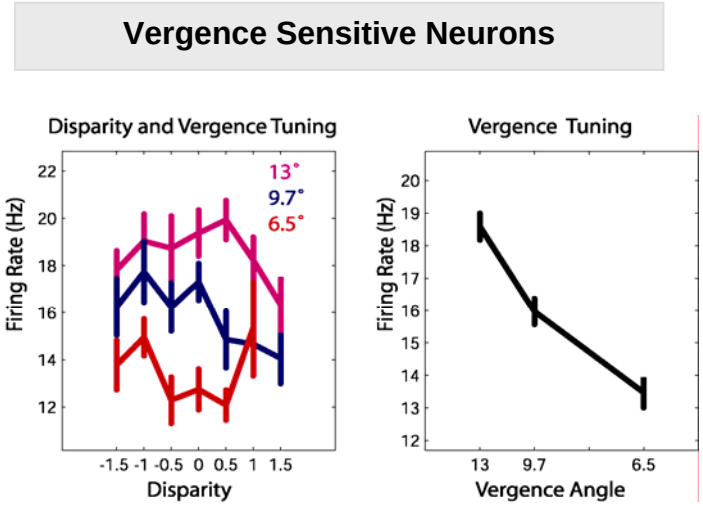

Figure 4-10 - Vergence Encoding cell with near fixation preference. No significant response to disparity; Vergence ANOVA P = 6.2172e-015

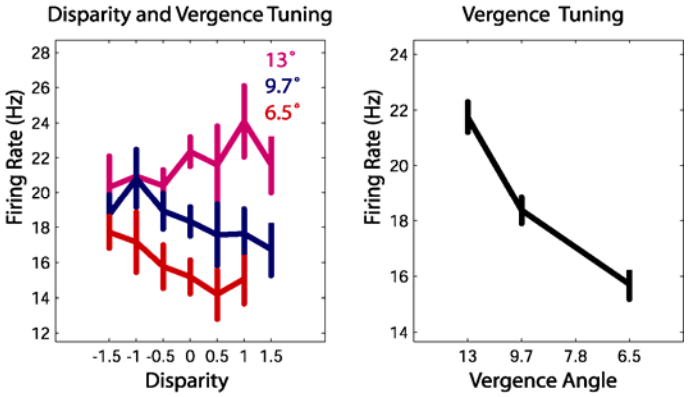

Figure 4-8 - Vergence Encoding Cell. Preference for "near" fixation Vergence ANOVA P = 1.4688e-013.

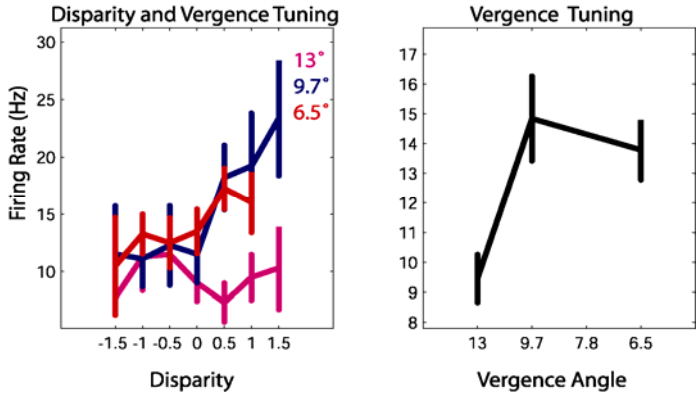

Figure 4-9 - Vergence Enocding Cell. This cell encodes vergence for only positive disparities. Vergence ANOVA P = 0.00071504. Preference for "far" fixation.

4.4 Disparity Response in PRR

Figure 4-11A shows the firing rate response of a neuron at 13° of vergence angle for two coupled reach target disparities in Experiment 1. There is a significant increase in firing during movement planning for a crossed disparity of -1.5° which is not present when the reach target is at zero disparity. The neuron exhibits significant modulation and nonlinear tuning for the disparity of the reach target (ANOVA, main effect; P = 9.7e-6; P = 5.0e-3, for 13° vergence; P = 1.3e-2 for 9.7° vergence; Figure 4-11B) during the planning period, which is a typical feature of disparity tuning in this neural population and in other cortical areas. Disparity is similarly encoded at two vergence angles and demonstrates a preference for near targets (crossed disparity).

Coupled reach target disparities in Experiment 1 significantly modulated planning period activity in 56% of the neural population (76/137)[4], whereas the wide range of disparities included from both experiments significantly modulated 82% of the population. The large number of sensitive neurons signifies the strength of modulation by disparity since reach targets were in a fixed location in azimuth and elevation, and not necessarily probed in the preferred 2D response field of each neuron. Figure 4-12 shows the distribution of significant disparity tuning responses across vergence angle for coupled

[4] Significant modulation is considered if $P < 0.05$ using n-way ANOVA (linear model) for at least one level of vergence. Using non-parametric Kruskal-Wallis ANOVA, it is 49% of the population. A main effect of disparity across all vergence is seen in 32% of the entire population using Kruskal-Wallis. A square root transformation was applied to all firing rates to determine if the mean-variance relationship due to Poisson like firing affected ANOVA calculations, which showed 57% of cells were significantly modulated by coupled reach target disparity. This transformation does not effect non-parametric statistics since the assumption of homogeneity of variance is not present.

reach targets (purple), decoupled reach targets (black), and both coupled and decoupled target disparities at the vergence angles in common (red). The proportion of disparity tuning in the population does not vary with fixation distance for coupled reach targets (X^2; $P > 0.8$), or for the different ranges of disparity at each vergence angle for decoupled reach targets (X^2; $P > 0.6$) or when including both (X^2; $P > 0.9$). Taken together, the population response suggests that the network level planning activity in PRR encodes reach target disparity evenly across fixation depth. The number of neurons with significant modulation for the small disparities tested in Experiment 1 and for the large disparities in Experiment 2 at the same vergence angle (independent of significant differences between small and large disparities tested between both experiments) was similar across vergence angle (n = 15/137 for 13° vergence, n = 17 for 9.7°, and n = 16 for 6.5°). Many neurons that were tuned to the large crossed disparities (-3.6° to -11°) of reach targets when viewing the farthest fixation stimulus (vergence angle = 1.9°; n = 45; ANOVA; $P < 0.05$) were also tuned to the small disparities tested in Experiment 1 (30/45; ANOVA; $P < 0.05$). The sensitivity to both small and large disparities may indicate that PRR plays a general role in planning movements to targets that may require either fine or coarse depth discrimination.

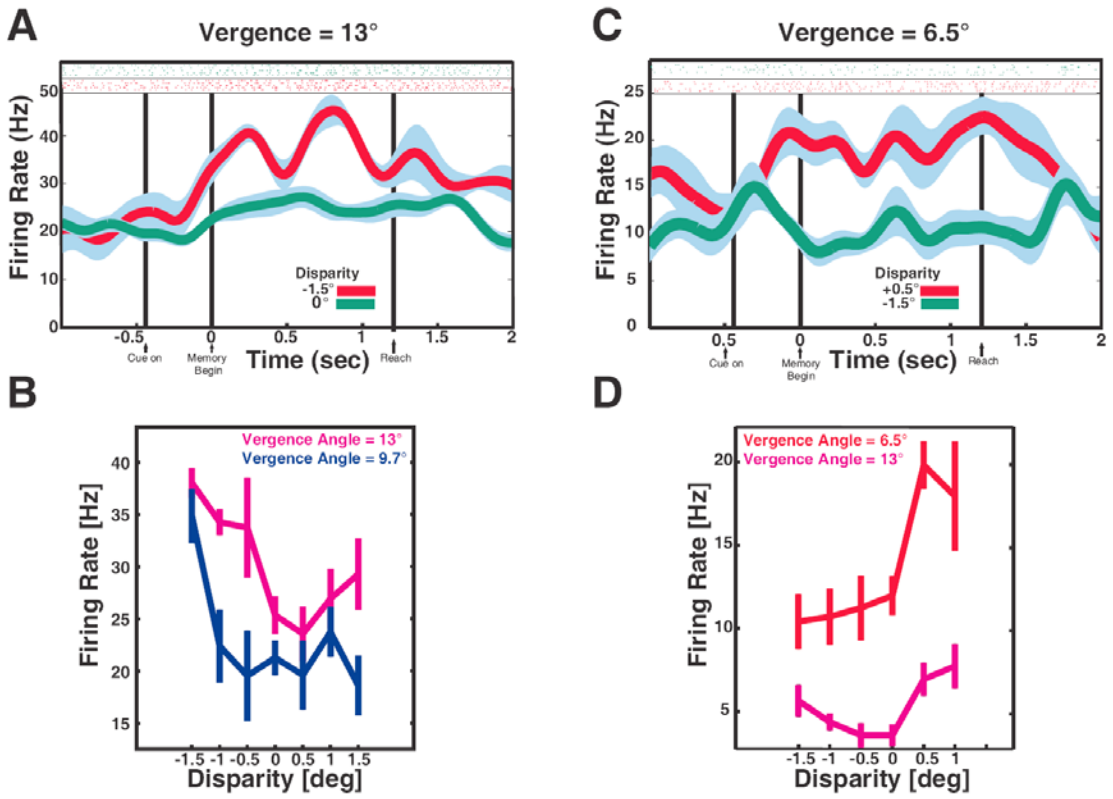

Figure 4-11- Example neurons. A: Neuron response to reach targets at -1.5° disparity (red) and 0° disparity (green) while fixating at 13° of vergence angle. Light blue represents standard error of firing rate. B: Reach target disparity tuning curves during movement planning for 13° (magenta) and 9.7° (blue) vergence for the neuron in (A). Vertical lines indicate standard error of firing rate for each condition. C: Neuron response to reach targets at +0.5° disparity (red) and -1.5° disparity (green) while fixating at 6.5° of vergence angle. D: Reach target disparity tuning curves during movement planning for 13° (magenta) and 6.5° (red) vergence for the neuron in (C). The neuron exhibits gain modulation of disparity tuning by vergence angle.

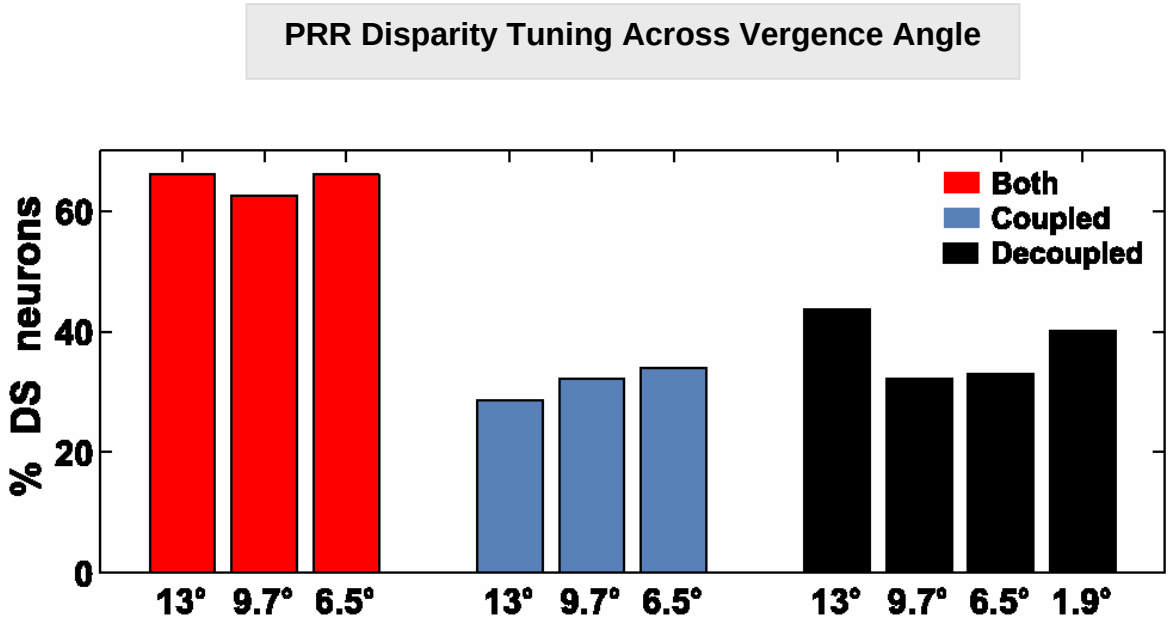

Figure 4-12- Proportion of disparity tuning at each vergence angle from the disparity sensitive population of cells (n= 112/137). The proportions are shown separately for each experimental configuration due to the different disparity ranges tested. Coupled target disparities in Experiment 1(blue), decoupled target disparities in Experiment 2 (black), and for both (red).

4.4.1 Disparity Tuning Responses During Cue, Planning and Movement Periods

Although fixation behavior is constant throughout these periods, other factors differ: 1) visual stimulation by the presentation of the reach target occurs only in the cue period, 2) the reach occurs in the movement period, and disparity tuning responses may also reflect motor related signals such as motor efference or proprioceptive feedback. The shape of disparity tuning from the cue period was reflected in the planning and movement period responses in PRR neurons (Figure 4-13A, B). Cross correlating the disparity tuning curves for the cue, planning, and movement periods for each neuron yields correlation coefficients that measure the similarity of disparity tuning between different periods.

These data suggest that a representation of target disparity formed during stimulus presentation carries into the formation of movement plans, and that spiking activity during the guidance of the hand to the target also reflects aspects of target disparity that were encoded in movement plans, in conjunction with other movement related signals.

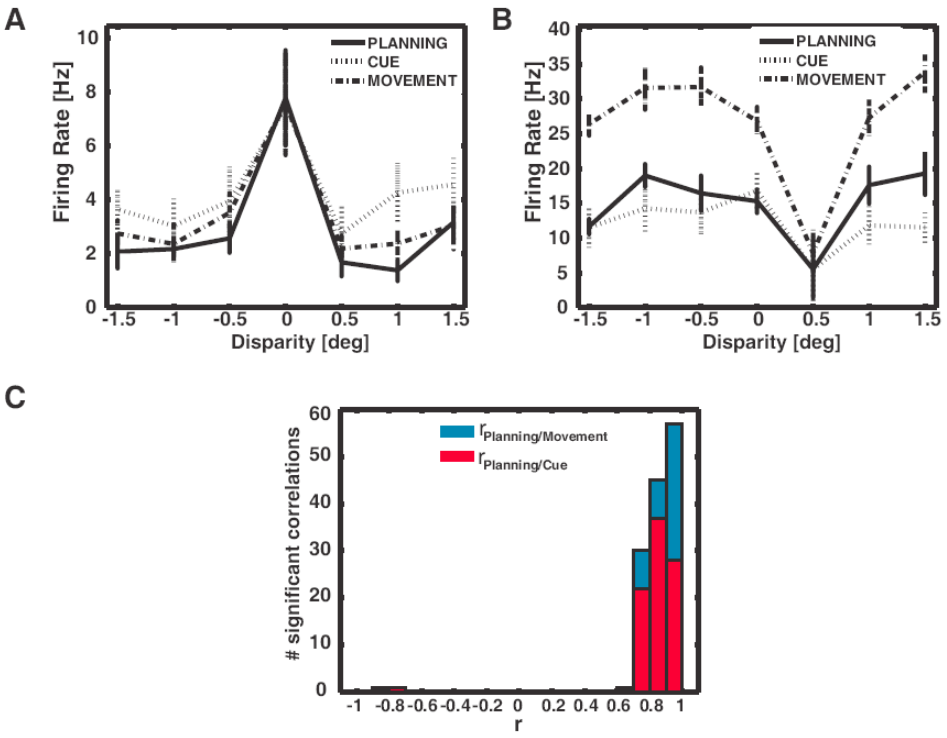

Figure 4-13 – Disparity tuning during different trial epochs. A: Neuron response at 13° vergence angle for different trial periods with significant correlation (P < 0.05) for tuning between periods. The cross correlation at zero lag between the cue and planning period was 0.9273, and between the planning and movement period was 0.9897. B: Neuron response at 13° vergence angle for different trial periods with significant correlation (P < 0.05) for tuning between periods. The cross correlation at zero lag between the cue and planning period for this neuron was 0.7732. The cross correlation at zero lag between the planning and movement period for this neuron was 0.7819. C: Histogram of significant cross correlation values at zero lag (P < 0.05) between cue and planning periods (red, n = 88), and planning and movement periods (blue, n = 136). The average magnitude of significant correlations are very similar (μ = 0.84 for cue and planning, μ=0.86 for planning and movement) and not significantly different (Kruskal-Wallis; P > 0.08).

4.4.2 Disparity Tuning in Other Cortical Areas

An example of disparity tuning from several V1 neurons is shown in Figure 4-14 (top) (Trotter, Celebrini et al. 1992). Note the diversity of tuning profile shapes, disparity preferences, gain modulation by fixation depth, and the presence of disparity sensitivity across different ranges when sampled at different vergence angles, an issue that will be explored in a subsequent section of this thesis. Figure 4-14 (bottom) shows the disparity tuning of IT neurons during the viewing of 3D objects (Uka, Tanaka et al. 2000). Figure 4-15 shows responses from disparity tuning obtained both from oriented bars and dynamic random dot stereograms (where correspondence is not uniquely established) in area V4 neurons. Disparity is finely sampled in this experiment, and reveals complex profiles that are both excitatory and inhibitory in different disparity ranges. Figure 4-16 shows disparity tuning profiles in LIP obtained during movement planning for saccadic eye movements in depth. Two studies examined disparity tuning in LIP and chose to use cubic functions of disparity as a model to fit the tuning (Gnadt and Mays 1995; Genovesio and Ferraina 2004). Cubic models are flexible because they can approximate linear, and modal, Gaussian like tuning with the quadratic term. However, they cannot approximate saturating responses, such as a sigmoidal one, or more than one region of excitation or inhibition (multimodal) well. The biological relevance of a cubic model of tuning is unclear. Complex models of tuning, such as cubic functions, have been used to describe tuning features in neurons for subsequent analysis, for example, to explore shifting and gain interactions due to vergence angle, however do not lend any further insight to the encoding mechanism behind the tuning; the reasons for the expression of

cubic tuning in a disparity tuned neuron is not proposed or examined. Though cubic functions of tuning did fit well to some neuronal responses in PRR, it did not describe significant complex disparity tuning and was not a useful model for subsequent analysis. Methods that do not require functional approximation were used to examine disparity tuning and its interactions with vergence angle.

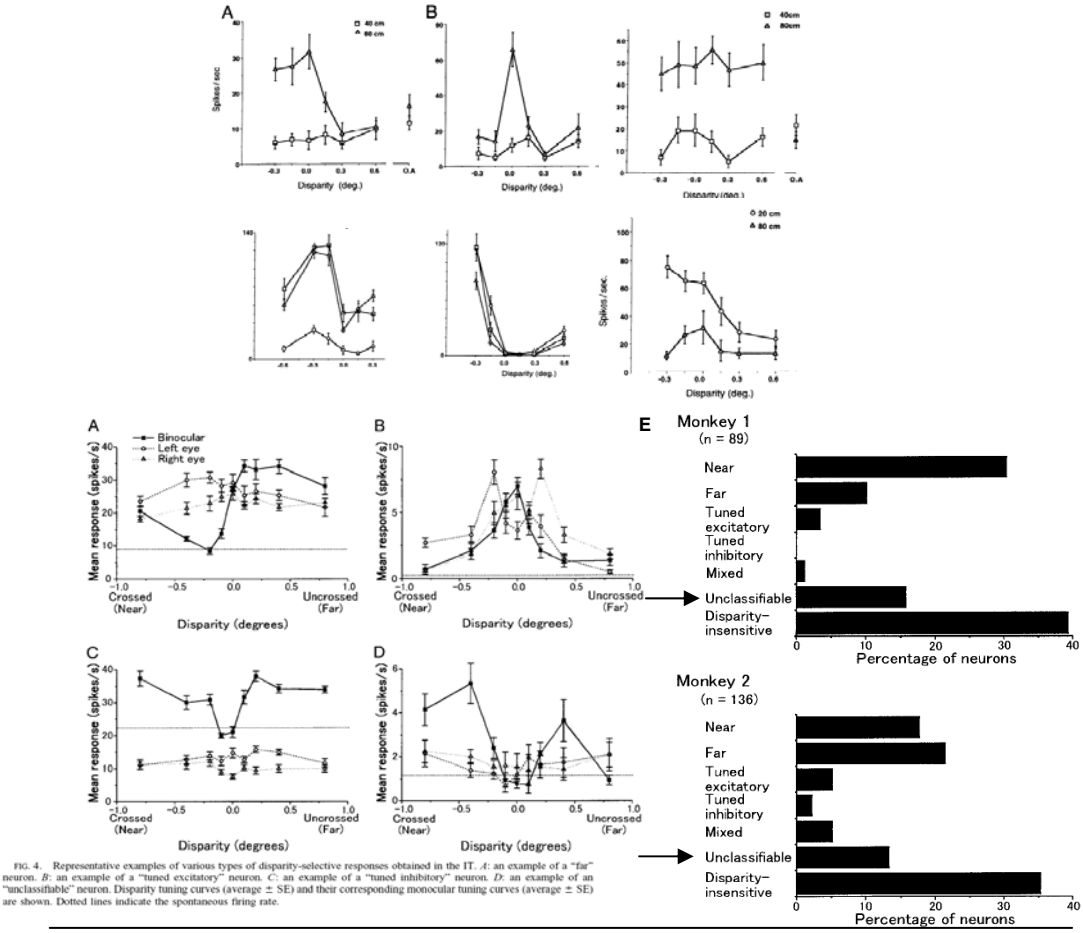

FIG. 4. Representative examples of various types of disparity-selective responses obtained in the IT. *A*: an example of a "far" neuron. *B*: an example of a "tuned excitatory" neuron. *C*: an example of a "tuned inhibitory" neuron. *D*: an example of an "unclassifiable" neuron. Disparity tuning curves (average ± SE) and their corresponding monocular tuning curves (average ± SE) are shown. Dotted lines indicate the spontaneous firing rate.

Figure 4-14- TOP Disparity tuning profiles in V1. Disparity tuning is shown for each neuron at various fixation distances. Note the gain modulation effect of vergence angle on disparity tuning. (Trotter, Celebrini et al. 1992)

BOTTOM Disparity tuning curves in area IT, where the solid black traces are the binocular disparity tuning curves of interest. (A) shows a "far" neuron, (B) shows a zero disparity selective neuron, also known as tuned excitatory. (C) shows a zero tuned inhibitory neuron. (D) shows an unclassifiable/complex neuron. (E) – Classification of disparity tuning in the population. Arrows highlight the Complex category for both monkeys. (Uka, Tanaka et al. 2000)

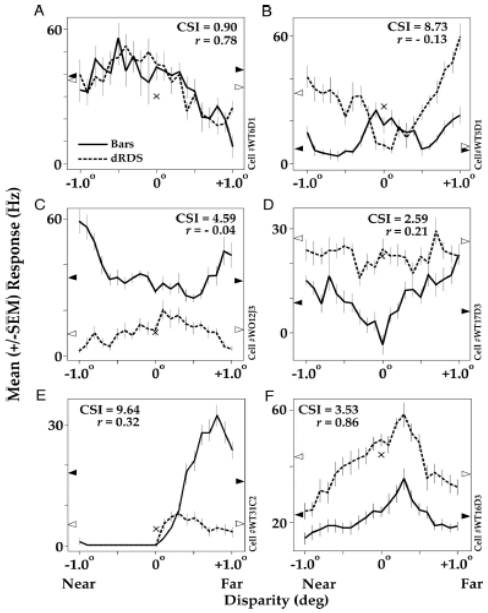

Figure 4-15 - Disparity tuning to bars and dynamic RDS in area V4 neurons. (A) Far neuron. (B) Zero tuned neuron. (C) Complex (D) Zero tuned. (E) Far neuron (Hinkle and Connor 2005)(F) Far tuned neuron. Note that (B) and (C) may express multimodal tuning outside the disparity region tested.

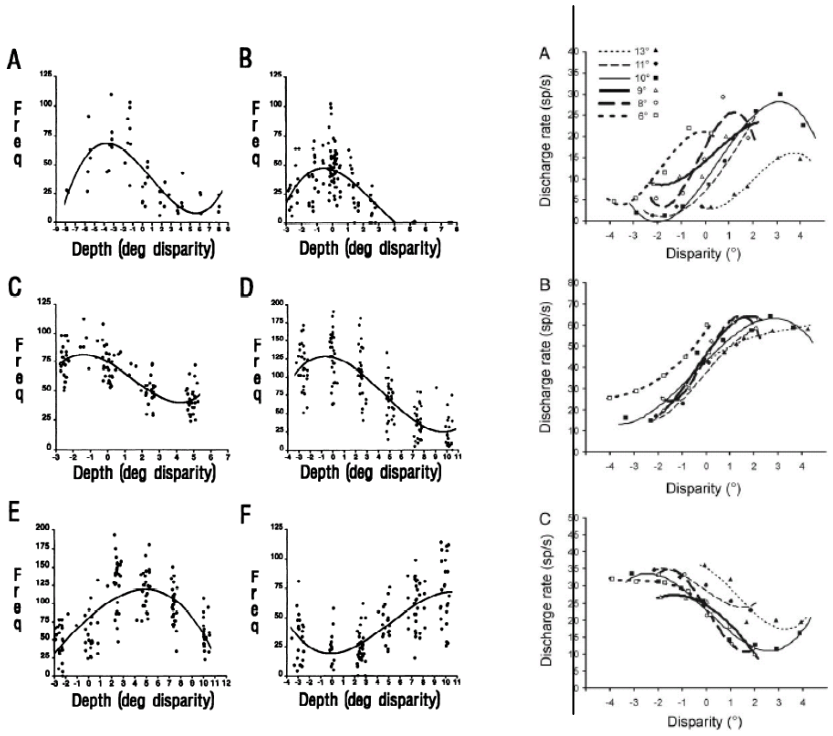

Figure 4-16 Planning period responses from LIP neurons to disparity of the target for saccades. LEFT – These responses are from a single level of vergence, and where firing rates are modeled by a cubic function of disparity. (Gnadt and Mays 1995) RIGHT – Responses to disparity from multiple levels of vergence, where disparity tuning is modeled by a cubic function of disparity and shift (also in the cubic) by vergence angle.(Genovesio and Ferraina 2004)

4.4.3 Disparity Tuning Classification in PRR

Disparity tuning has been studied in other cortical areas, and it is frequently found that the shape of the tuning is complex. A common form for disparity tuning does not exist, because it can range from nearly linear, Gaussian like, sigmoidal, cosine-like, and finally multimodal, which is perhaps the most common form. Poggio and Fisher described subjective categories of tuning for disparity as near, near-tuned, far, far-tuned, and zero-disparity selective, which can be used to describe modal or monotonic responses (Poggio and Fischer 1977; Poggio 1995). A category amended to the above in many studies is Unclassifiable/Complex, which includes multimodal disparity tuning and can often express excitatory preference for disparity ranges that are both near and far. Figure 4-14 (bottom) details the categorical breakdown of the disparity sensitive neurons in IT, and shows that a large percentage are unclassifiable/complex (Uka, Tanaka et al. 2000).

As with other visual cortical areas, the disparity tuning observed in PRR neurons covers a variety of profile shapes, as well as excitation and inhibition in single and multiple regions of disparity. Significantly tuned coupled reach target disparity responses were classified into zero-tuned, near and tuned-near, far and tuned-far classes (see Methods) and occurred with the same frequency (X^2; $P > 0.5$). Neurons with multimodal or broad tuning that span the above categories were classified as complex. Figure 4-17A shows the distribution of classification, with a similar proportion of tunings across all categories (X^2; $P > 0.15$). A principal components analysis was performed on the disparity tuning curves for zero-tuned, near and tuned-near, far and tuned-far classes.

The first 3 principal components capture 79% of the variance in the data (differences in tuning profile shapes). Projections of the disparity tuning curves using the 1st and 2nd principal components are shown in Figure 4-17B, and account for ~64% of the variance. Zero-tuned neurons are unimodal, and the 1st principal component produces a separation between excitatory and inhibitory zero-tuned neurons. The 2nd principal component produces a separation between near and tuned-near and far and tuned-far classes ($\mu_{PC2}^{near} \pm\sigma = -0.23\pm0.27$; $\mu_{PC2}^{far} \pm\sigma = +0.15\pm0.15$). The "tighter" clustering of tuning in the far and tuned-far class indicates a greater similarity in tuning profile shape in this group classification. The addition of the 3rd principal component also produces a separation between near and tuned-near and far and tuned-far classes, and accounts for ~15% of the variance in tuning profile shape ($\mu_{PC3}^{near} \pm\sigma = +0.10\pm0.28$; $\mu_{PC3}^{far} \pm\sigma = -0.14\pm0.23$). Projections of disparity tuning on the first 3 principal components is shown in Figure 4-17C. The results show that a linear orthonormal basis set can account for the differences in tuning shapes that have been described using subjective classification, however the distribution of shape features varies continuously, and does not form tight, widely separated clusters. The large number of complex tuned neurons shows that there exists a substantial non-classical component in encoding disparity. This suggests that disparity tuning in PRR does not form discrete classes, which is a feature shared in other extrastriate cortical areas such as the middle temporal cortex and inferior temporal cortex (Uka, Tanaka et al. 2000; DeAngelis and Uka 2003).

Several disparity tuning curves are shown in Figure 4-20 to Figure 4-18, which exemplify the disparity classes discussed above and the diversity of profile shapes observed in the population. Zero tuned responses are shown in Figure 4-18. These disparity tuning profiles exhibit either an excitatory or inhibitory peak for a target disparity of 0°, and are typically Gaussian like. In particular, Figure 4-18A shows a neuron with the same tuning and preferred disparity of 0° at 2 vergence angles. Near disparity responses show excitation for a large range of crossed disparities, whereas near tuned responses may show excitation or inhibition for one disparity or a limited range of disparities. Examples of near + near tuned disparity responses from movement planning are shown in Figure 4-19. The neuron in Figure 4-19A exhibits a robust Gaussian-like excitatory response for -0.5° of target disparity at 6.5° of vergence. The tuning depth for this neuron is nearly 35Hz; zero and positive disparities elicit only 13% of the firing rate response observed at -0.5° of disparity. Several neurons exhibited tuning that was an approximately linear, such as in Figure 4-19 B and D which show planning period responses from 2 cells at different vergence angles. Linear disparity tuning was generally rare in this population, and a discussion of the quantitative aspect of the disparity response is discussed in the next section.

Preference for a large range of uncrossed disparity is classified as far, and excitatory or inhibitory preference for a limited range of uncrossed disparities is considered far tuned; both categories are considered together in this work. A sigmoidal like far response is seen in the neuron in Figure 4-20A, and an example of inhibition to produce a far tuned response is seen in Figure 4-20C. Complex and often multimodal tuning for disparity

was most often observed in the population of PRR neurons. Figure 4-21 documents some of the complex tuning curves observed during movement planning. The complex tuning profiles had the feature of different regions of excitation and inhibition for disparity.

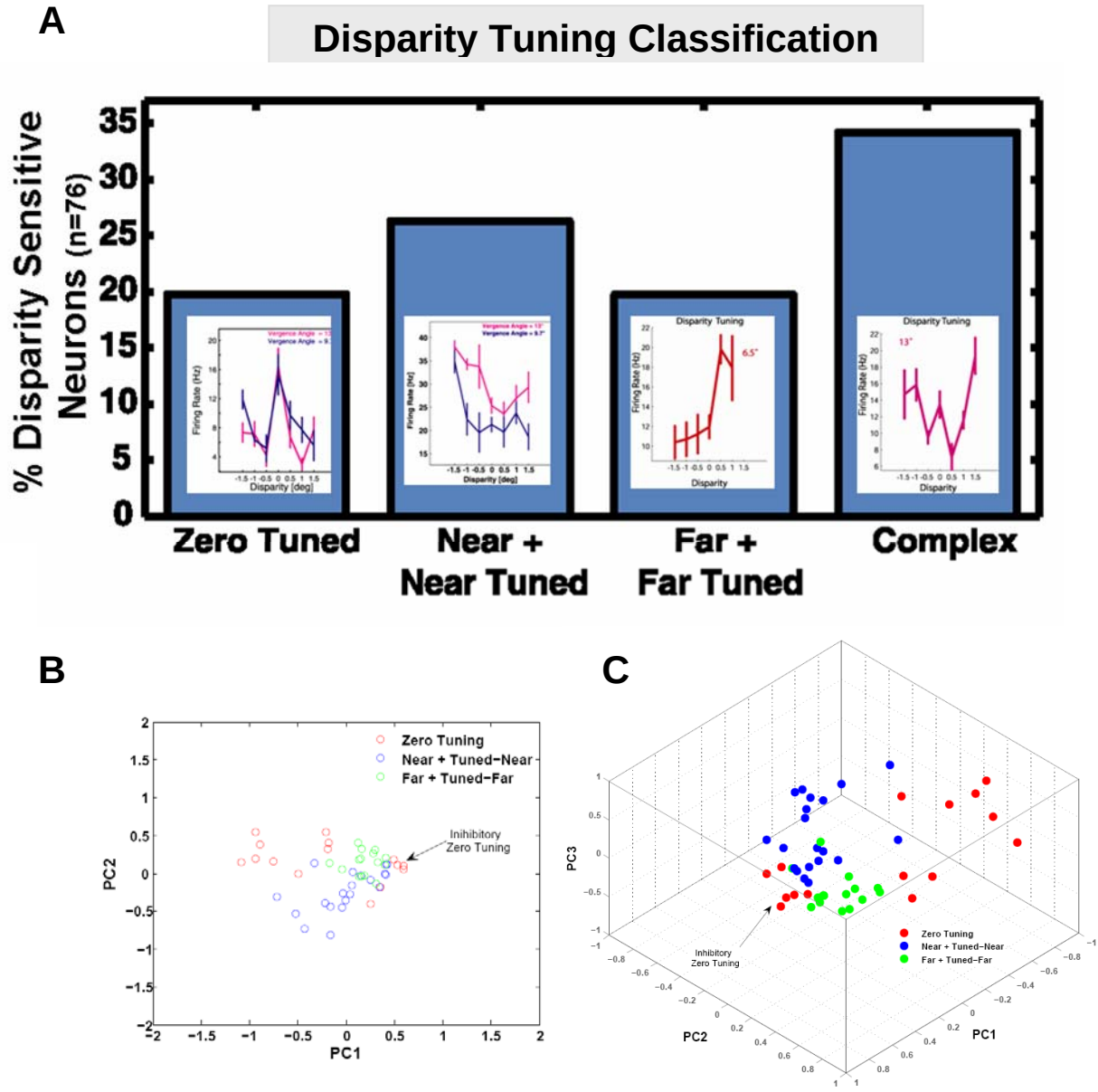

Figure 4-17- A: Classification of disparity sensitive cells from coupled target disparity tuning in Experiment 1, embedded with representative samples from the PRR population. B: Projection of the 1st and 2nd principal components of disparity tuning curves; colors indicate original classification (Complex tuned group not included). C: Projection of the 1st, 2nd, and 3rd principal components of disparity tuning curves (Complex tuned group not included).

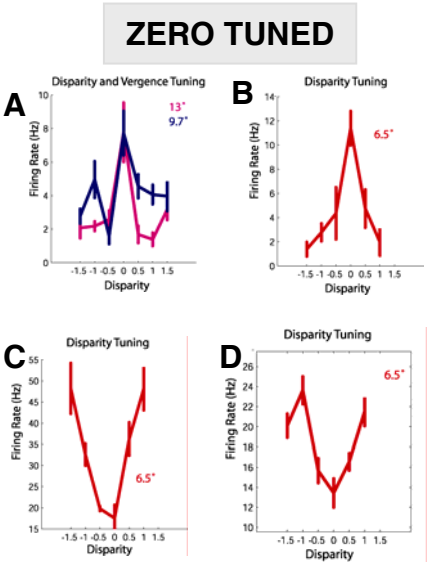

Figure 4-18 - A – Zero tuned disparity response at two levels of vergence (13° and 9.7°). B: Zero tuned excitatory disparity response for one vergence angle. C and D: Zero tuned inhibitory response for one vergence angle.

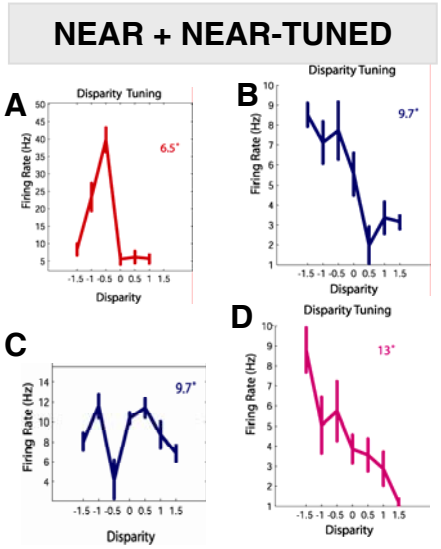

Figure 4-19 - Near+ Near tuned disparity tuning from different neurons. A: Excitatory Gaussian like tuining profile. at 6.5° vergence angle during movement planning. B: Near linear disparity tuning. C: Inhibitory near tuned response. D: Near linear disparity tuning.

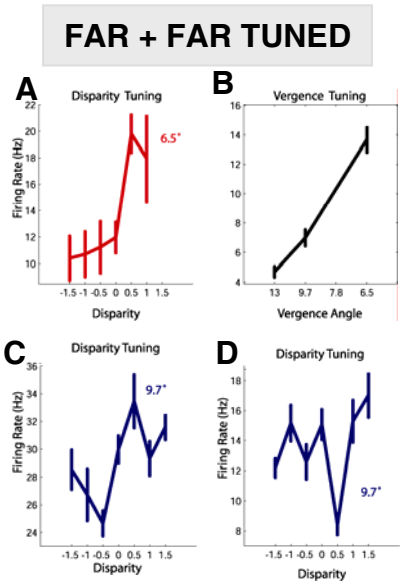

Figure 4-20 Far + Far Tuned disparity responses. A: Far excitatory disparity response at 6.5° vergence. B: Vergence tuning for neuron in A, where disparity response gain by vergence is near linear. C: Far excitatory disparity response. D: Far tuned inhibitory disparity response.

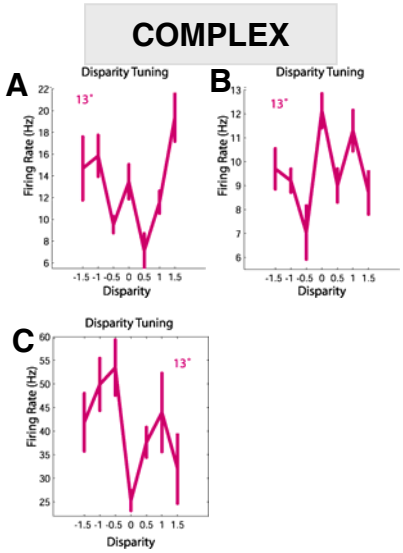

Figure 4-21 Complex tuning from different neurons during movement planning. These neurons exhibit multimodal tuning, that can exhibit tuning features for both crossed and uncrossed disparity.

4.5 Disparity and Vergence Interaction – Gain Models

The nature of coupled reach target disparity and vergence angle interaction was explored with a gain model. Previous quantitative approaches to gain models have used an explicit model using the 2 effectors under investigation (such as horizontal and vertical eye position, or neck rotation and horizontal eye position), and employing linear regressions of the firing rate on the effectors (Andersen, Bracewell et al. 1990; Brotchie, Andersen et al. 1995; Snyder, Grieve et al. 1998). A measure of linearity analogous to regression is the Pearson Correlation coefficient (Zar 1999)[5], where large values (±1) indicate a high degree of linearity, and values near 0 indicate non-linearity. Figure 4-22A shows the correlations of planning period responses with disparity (from all vergence angles) against the correlations with vergence angle (from all disparities). Figure 4-22B shows the correlations of planning period responses with disparity at each level of vergence. Taken together, it is evident that a low correlation exists between planning period firing rate and coupled reach target disparity. Consequently, a variety of models for disparity were tested, such as cubic, cosine, Gaussian, and Gabor tuning models. We chose not to model disparity responses explicitly since a single model with adequate flexibility was not found to describe the responses from all neurons well ($R^2<0.2$; data not shown; no single model described a significant number of neurons, e.g., $n < 15$ significantly fit neurons), and more complex models (*e.g.*, spline) were often unwieldy.

[5] The coefficient of determination r^2 reported for linear regressions is the square of the Pearson correlation coefficient.

We employed a nonparametric approach of transforming disparity responses using vergence as a linear operator. This method did not constrain disparity tuning to any functional form, and instead regressed on disparity tuning curves from different fixation depths to produce a model of disparity with multiplicative and additive gain by vergence angle. (See Methods) Simulated examples of pure additive gain and pure multiplicative gain by vergence are shown in Figure 4-23. A pure additive gain on disparity by vergence angle does not change the shape of tuning (Figure 4-23A). A multiplicative gain on disparity tuning by vergence angle can describe a change in profile shape of disparity tuning, *e.g.*, the "sharpening" of disparity tuning as previously described pure qualitatively for V1 neurons by Trotter et al., illustrated in Figure 4-23B. An example of a PRR neuron with a significant gain on disparity by vergence angle is shown in Figure 4-11D, where a "far" disparity tuned neuron exhibits a significant multiplicative gain on disparity tuning at increasing fixation depth (R^2=0.48). Another example is shown in Figure 4-24A.

26% (20/76) of disparity sensitive neurons (Experiment 1, n = 76) exhibit a significant gain model with an average R^2=0.35 (σ=0.1). A histogram of the r-squared values (averaged from the bootstrap iterations) for the significant gain model relations is shown in Figure 4-24B. From the population of neurons which had significant disparity tuning at multiple vergence angles (Experiment 1, n = 23), 65% (15/23) exhibit a gain model where the interaction between disparity tuning curves can be accounted for by vergence acting as a linear operator. Significant additive gain by vergence is exhibited in 58% of significant gain model interactions. The magnitude values of significant multiplicative

and additive gains are shown in Figure 4-24C. Most multiplicative gains are clustered around +1, which indicates that disparity tuning shape is mostly unchanged between vergence angles. An analysis that specifically looks at interactions that involve a change in the location (in disparity) of a peak tuning feature due to vergence is detailed in the subsequent section.

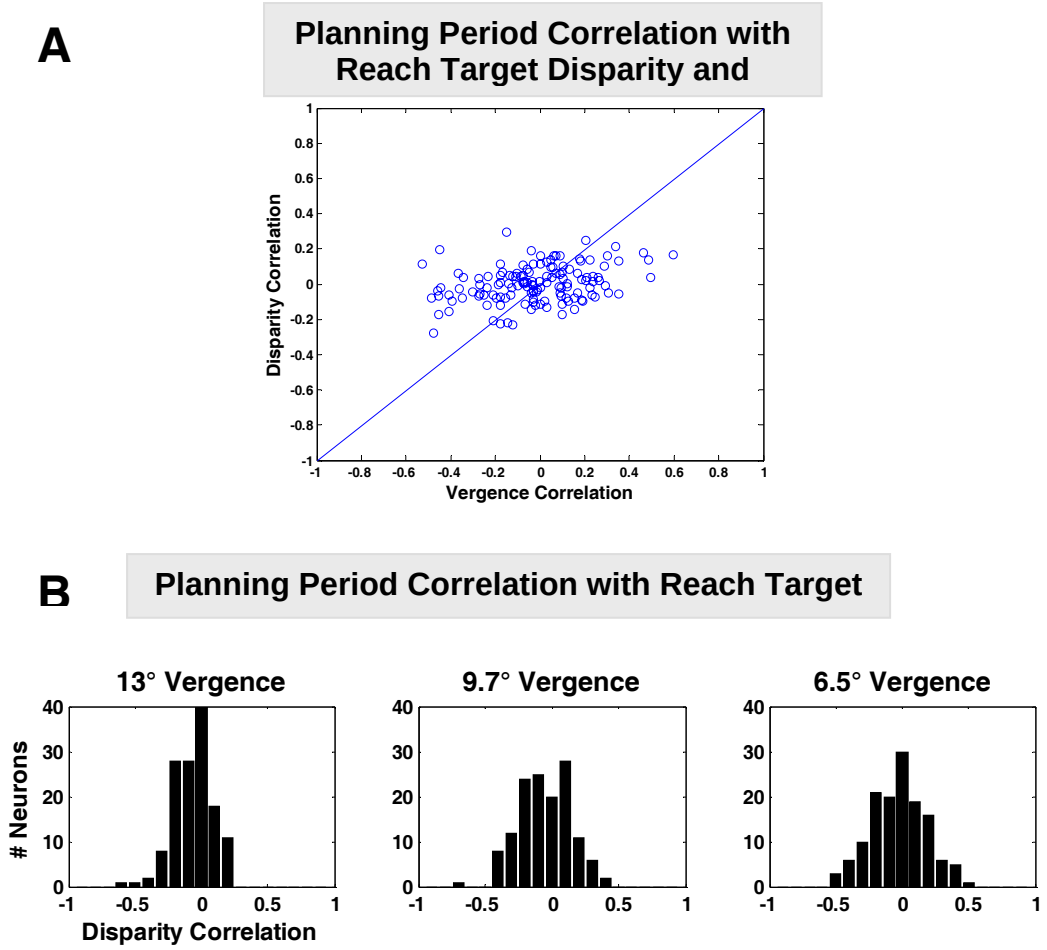

Figure 4-22 - Correlations for disparity from coupled reach targets (Experiment 1). A: The correlations of disparity response (averaged across vergence angle) plotted against the correlations with vergence angle for each neurons in the population. The mean correlations from disparity and vergence are similar ($\mu_{disparity} = 0.002$, $\mu_{vergence} = -0.02$), however the spread in vergence correlation is much larger, and makes for a significantly different distribution of correlation coefficients (Komolgorov-Smirnov test, $P < 5.5e\text{-}4$). B: The correlations of planning period responses with coupled reach target disparity at each level of vergence for all neurons in the population. It is visible at all levels of vergence that large correlations for disparity do not exist, and modest ones are rare (e.g., correlation = ±0.4). There is no difference in mean disparity correlation due to vergence angle (Kruskal-Wallis ANOVA $P = 0.35$), and no difference between the distributions at 13° and 9.7° (KS test $P=0.1$), 9.7° and 6.5° ($P > 0.54$), however a difference exists between 13° and 6.5° ($P = 0.0371$). Further testing using the Wilcoxon rank sum test yields that the medians of the distributions of the disparity correlations at each vergence angle are the same ($P > 0.51$, $P=0.15$, $P > 0.41$).

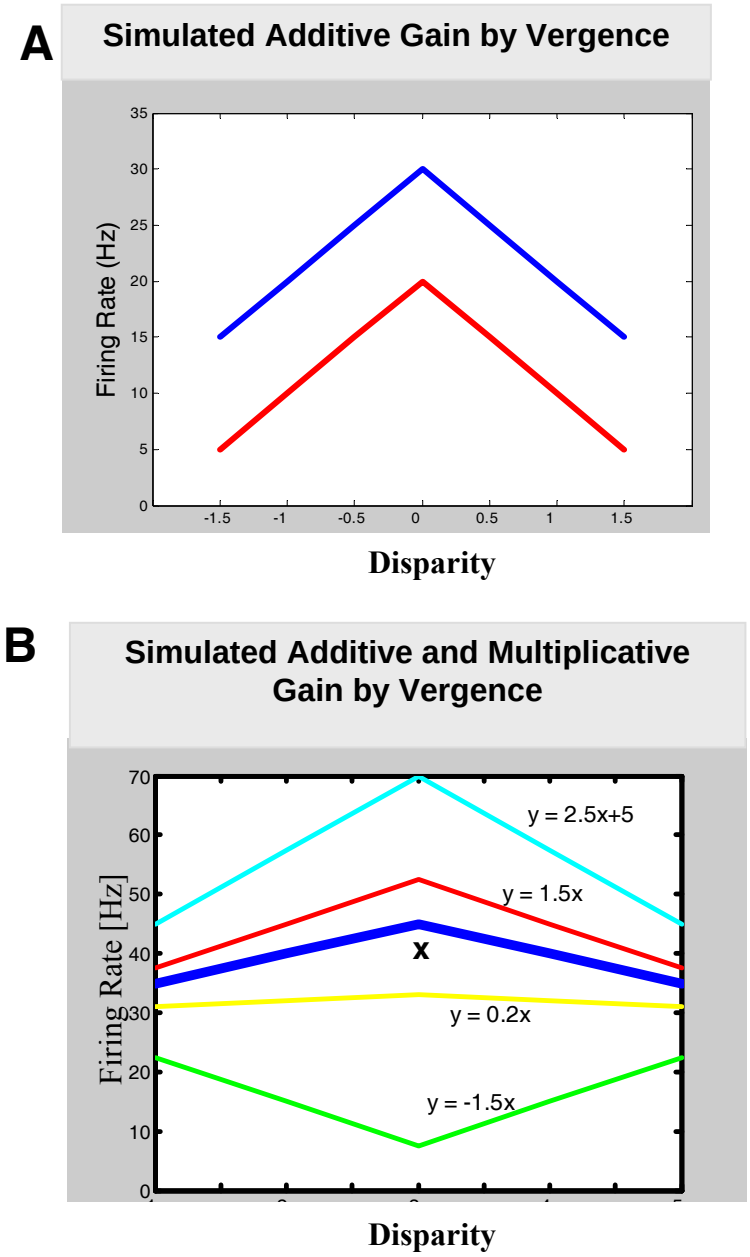

Figure 4-23 - Simulated hypothetical gain responses. The different colors represent disparity tuning from different fixation depths. A: A vergence gain on disparity tuning that is purely additive. Y = X + C., where Y and X are disparity tuning curves at different vergence angles, and C is a constant. B: A vergence gain on disparity which is purely multiplicative. The shape of the disparity tuning profile can change form excitatory to inhibitory. This relationship can change shape, but preserves the location (in disparity) of peak tuning features.

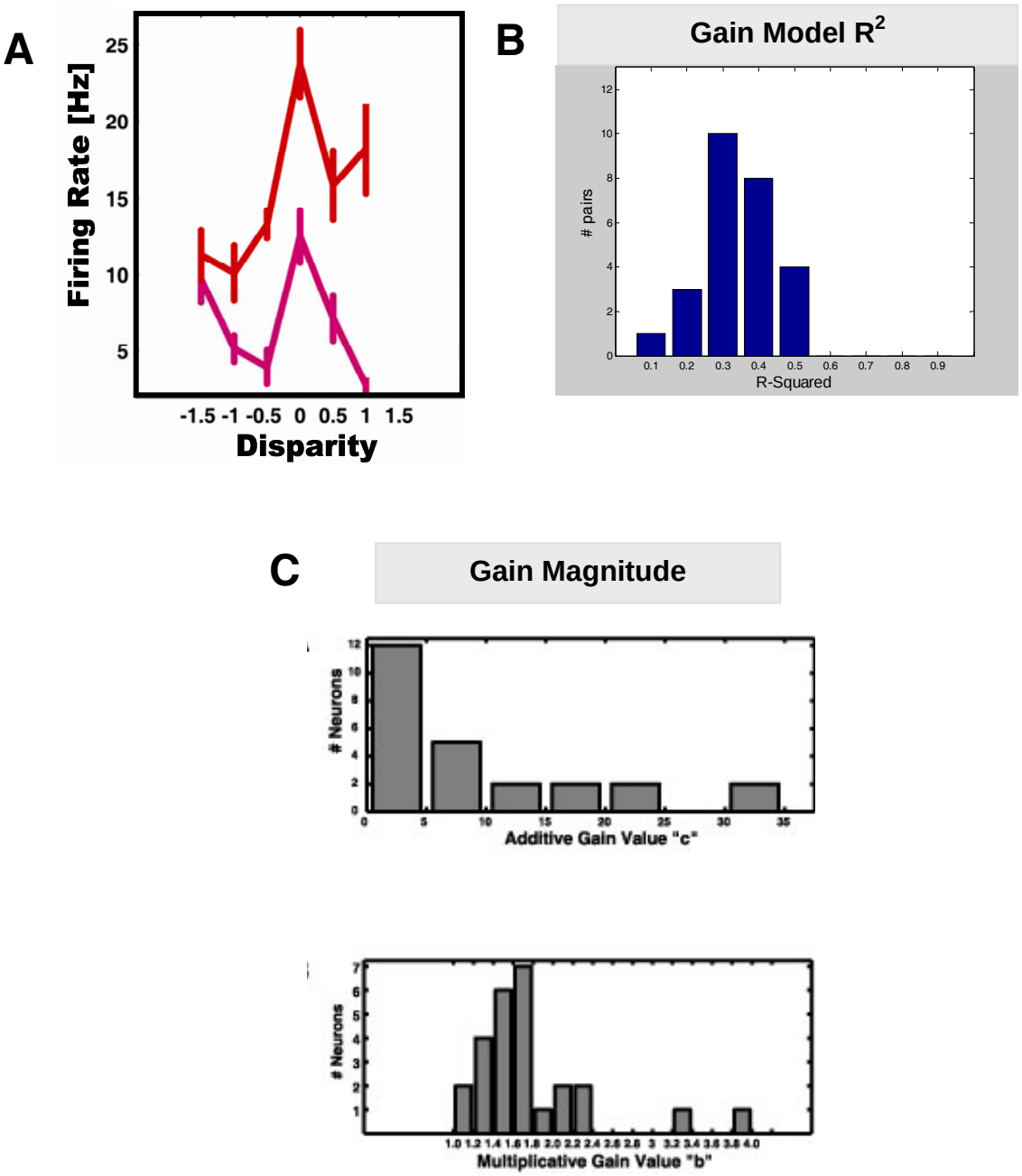

Figure 4-24 - A: Neuron expressing disparity tuning gain modulation by fixation distance. B: Histogram of R_squared values from significant gain models in the population. C: Histograms of the magnitude of additive gains ("c") and multiplicative gains ("b"); the average value for multiplicative gain b is 1.77, and for additive gain c is 14.6.

4.6 Shifting of Disparity Responses by Vergence Angle

A shift in disparity tuning due to vergence angle is a nonlinear and nonseparable interaction that is exclusive of a gain model. We examined whether PRR neurons exhibited disparity tuning shifts from one level of vergence to another. Shifting responses were measured using cross correlations for coupled reach target disparities, where neurons with a significant cross correlation between a pair of disparity tuning curves (3 possible pairings/shifts) were considered to have measurable shift(s) in disparity tuning by vergence angle (see Methods). This operation calculates the optimal shift that aligns the peak features of the tuning profiles, and is insensitive to changes in magnitude/gain between disparity tuning curves. We identified neurons (n = 120) which had significant cross correlations (n = 219). There were 65 significant shifts observed between disparity tuning curves at 13° vergence angle and 9.7° vergence angle, 77 between 13° and 6.5°, and 77 between 9.7° and 6.5°. 55 cells had one significant shift, 31 had 2, and 34 had all 3 pairs of disparity tunings significantly shifted from each other.

The majority of significant shifts in the population were 0°, indicating that disparity tuning profiles at different vergence angles were precisely aligned (Figure 4-25B, 26%). Figure 6-26A shows the planning period response of a neuron with a significant cross correlation of shift 0° for Zero-Tuned disparity responses at 13° and 9.7° of vergence angle. 58% (128/219) of all shifts were in the range of ±0.5°; whereas large shifts of ±1.5° in disparity tuning were less frequent (less than 20% of shifts). The average value

from the unimodal distribution of shifts was -0.03°±0.87°. The distribution of significant shifts from the disparity sensitive population (n = 76, Experiment 1) is similar to that for the entire population shown in Figure 4-25B (Komolgorov-Smirnov test; P=0.88). These results suggest that modulation by vergence angle on average preserves the location of peak features in the disparity tuning of PRR neurons across fixation depth.

The shift of a response to one effector by another is a method of integrating the encoding of variables that is commonly found in the parietal cortex. We can see in Figure 4-25B that approximately 74% of disparity responses do exhibit a shift by vergence angle that is non-zero. These shifts in disparity tuning may be a mechanism that encodes the vergence angle in planning period responses. Shifting responses can also indicate whether a response is indicative of a coordinate frame for encoding an effector (Shenoy, Bradley et al. 1999; Xing and Andersen 2000; Buneo, Jarvis et al. 2002). In the case of disparity tuning, alignment indicates that a retinal reference frame is used. If neurons were encoding target location in a body or limb centered reference frame, the disparity tuning would shift to compensate for a change in vergence angle to preserve the encoding in such a reference frame. A limb or body centered reference frame would most likely encode the absolute depth of the target. We examine the shifting responses from such hypothetical neurons for comparison in the next section.

4.7 Disparity Tuning Shift from Hypothetical Absolute Depth Encoding Neurons

We compared the PRR shifting responses to shifts that would be observed in a hypothetical population of absolute depth encoding neurons. Coupled reach target disparities in Experiment 1 probed neural responses in adjacent, non-overlapping regions of space (Figure 3-3, Figure 3-6, Figure 3-7). A neuron encoding absolute target depth has a receptive field corresponding to a region of space instead of disparity. Figure 4-25C shows an example of a simulated gaussian spatial receptive field, where the disparity tuning curves that would have been sampled from it using coupled reach targets are shown in different colors and plotted as a function of absolute depth. The simulated responses from different vergence angles are paired and plotted as a function of disparity in Figure 4-25C. These disparity tuning curves were cross correlated to measure shifts by vergence, which resulted in a single significant shifting response of 1.5° between disparity tuning at 9.7° and 6.5° of vergence angle (Figure 6-26C, far right).

We simulated receptive fields in space for populations of absolute depth encoding neurons using gaussian functions with different means and widths. Figure 4-25D shows a histogram of the proportions of disparity tuning shifts observed in these simulated populations. The vast majority (>75%) of simulated absolute depth encoding neurons exhibit shifts that have a large value of ±1.5°. The large difference in shift distributions between the simulated neurons and those obtained from PRR neurons indicates that the PRR population does not encode absolute target depth (Komolgorov-Smirnov; P = 1.92e-4). The distribution of shifts shows most PRR neurons exhibit the alignment of disparity

tuning consistent with an eye centered reference frame that is gain modulated by vergence angle.

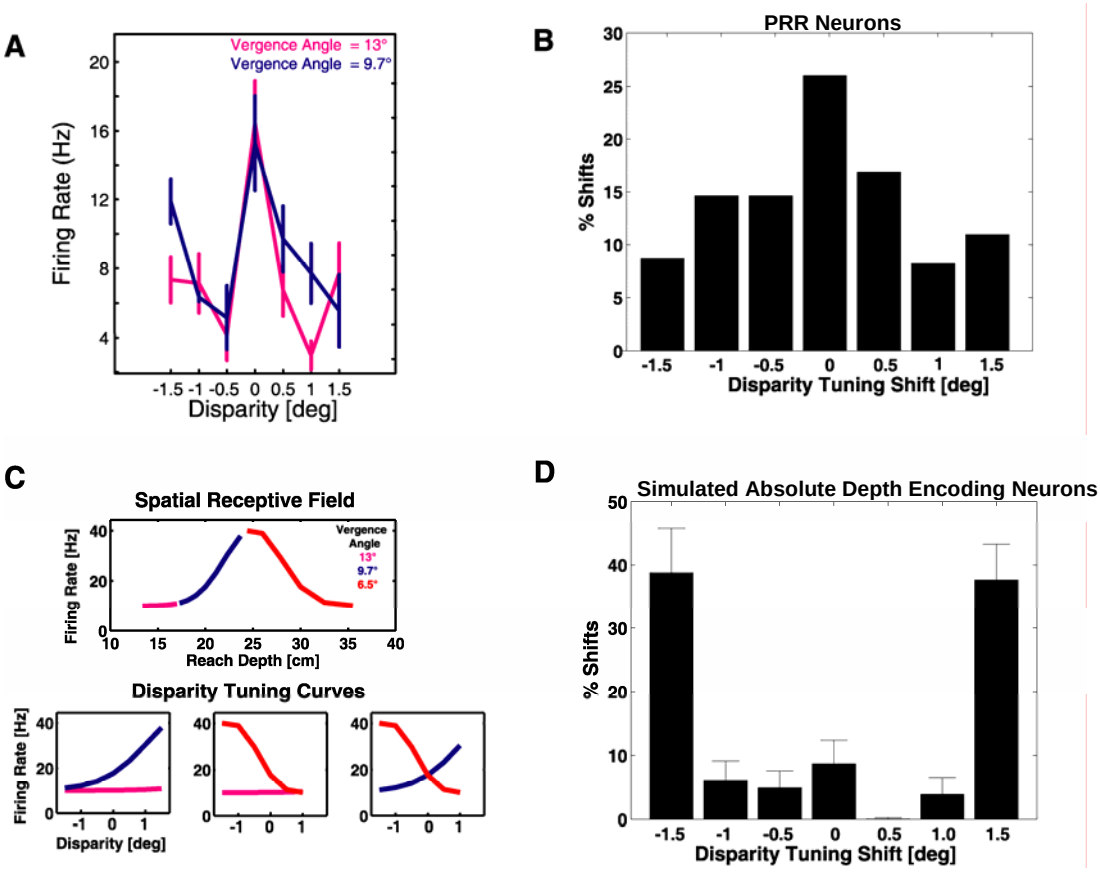

Figure 4-25– Disparity tuning shifts by vergence in PRR (top) and simulated absolute depth encoding neurons (bottom). A: Zero Tuned neuron exhibiting alignment of disparity tuning curves at 13° (magenta) and 9.7° (blue) of vergence angle. B: Significant disparity tuning shifts from neurons in Experiment 1. The majority of shifts are 0°, indicating precise alignment of disparity tuning at different fixation distances, and 58% of all shifts are in the range of ±0.5°. C: Simulated receptive field for a neuron encoding absolute target depth. Top - Spatial receptive field for a cell with a peak response at 25 cm and 6 cm width, sampled with the fixation and target configuration in Experiment 1 with vergence angle shown in color. Bottom - Disparity tuning curves from the different vergence angles obtained from the spatial receptive field above. Cross correlation yields only one significant shifting response in disparity tuning for disparity tuning curves from 9.7° and 6.5° vergence, shift =+1.5° (far right panel; P = 0). D: Disparity tuning shifts from simulated absolute depth encoding neurons, with the majority resulting in large shifts (±1.5°) in disparity tuning. Error bar indicates standard deviation from simulated populations.

4.8 Disparity Tuning Index

Modulation by coupled reach target disparity at each vergence angle was calculated using the Disparity Tuning Index (DTI, see Methods), where a DTI = 1 indicates a maximal response modulation occurs (with no spiking at the minimum response), DTI = 0 indicates that disparity does not modulate the response, and DTI = 0.33 indicates that the maximum disparity response is double the minimum response. The mean of the maximum planning period DTI from each neuron in the population (n = 137) is 0.4322 (±0.2374) with a median DTI of 0.3638, and indicates that the modulation of disparity response was large. The DTI of disparity sensitive neurons does not differ by the classification of the tuning (Kruskal-Wallis; $P > 0.19$). Based on the disparities at which the maximum and minimum responses were obtained at each vergence angle for the DTI, we find that the difference between these disparity values as a measure of disparity tuning width does not change with vergence angle across the PRR population (Kruskal-Wallis; $P > 0.99$). For comparison to other disparity responses, a table with the DTIs from other cortical areas was compiled in Table 4-1. The DTI measure is sometimes referred to as the binocular interaction index (BII) in other studies (Ohzawa and Freeman 1986). The responses in this table are from the period of stimulus presentation, and stimuli ranged from dynamic RDSs to stereograms presented binocularly (independently in each eye). It is interesting to note that the amount of disparity modulation during the working memory period is on average the same as that seen in the direct responses to stimuli during presentation in visual cortical areas.

The histogram of planning period DTIs for all neurons at each level of vergence is shown in Figure 4-27B, and the histogram of cue period DTIs is shown in Figure 4-26A for comparison. Cue period and planning period DTI is correlated across the population ($r = 0.75$ across all vergence; $r = 0.80$ at 13°, $r = 0.71$ at 9.7°, and $r = 0.74$ at 6.5° vergence angle; all $P < 1e\text{-}5$; Figure 4-26C), and although DTI is higher for the population during the cue period (Kruskal-Wallis; $P=0.0011$), the average reduction in DTI is only 13% during the planning period.

The DTI of the population does not change with fixation depth (Kruskal-Wallis; $P > 0.66$), and the distributions of DTI are the same at each vergence angle (Komolgorov-Smirnov test; $P > 0.54$ for 13° and 9.7° vergence; $P > 0.75$ for 13° and 6.5°; $P > 0.54$ for 9.7° and 6.5°). The Wilcoxon Rank Sum test for independent population medians confirmed the results from Kruskal-Wallis test ($P > 0.66$), yielding the same medians between vergence angles ($P > 0.36$ for 13° and 9.7°, $P > 0.53$ for 13° and 6.5°, $P > 0.87$ for 9.7° and 6.5°). In addition, we tested whether there was a difference in the median of paired observations for each neuron (DTI of a neuron at 2 levels of vergence) with the Wilcoxon Signed Rank Test and found no significant differences ($P > 0.57$ for 13° and 9.7°, $P > 0.09$ for 13° and 6.5°, $P > 0.14$ for 9.7° and 6.5°). This suggests that there is no change in DTI due to vergence for PRR neurons when considering the population as a whole or when considering changes for individual neurons when the DTI at different vergence levels are paired. We examine the DTI of the subpopulation of disparity sensitive neurons below.

There is an equal incidence of disparity tuning for coupled reach targets at each level of vergence (Figure 4-27A); however this might arise if neurons were encoding absolute depth with a distribution of tuning across space. If neurons were directly encoding the absolute depth of reach targets, or the distance between reach and fixation targets, the response modulation measured by DTI should increase with fixation depth due to the larger distance between reach targets (*e.g.*, inter-target distance changes by a factor of 3 between 13° and 6.5° of vergence angle). Instead, the DTIs for the significantly tuned responses at different fixation depths reveal that the response modulation does not increase with larger inter-target distances (Kruskal-Wallis; $P > 0.56$; Wilcoxon Rank Sum $P > 0.78$ for DTI of tuned responses at 13° and 9.7°, $P > 0.27$ for 13° and 6.5°, $P > 0.51$ for 9.7° and 6.5°).

The DTIs from significantly tuned responses at different vergence angles ensures that only DTIs from well modulated neural responses in comparison to firing rate variance are used for this comparison. The use of this selection process is thus similar to the idea of including a firing rate variance term in the DDI (below). The use of DTIs from all neurons yields the same qualitative result that DTI across the population does not change with fixation depth.

The DTIs from different vergence angles are paired and shown for individual neurons in Figure 4-27C. DTIs are correlated at different fixation depths across the population ($r = 0.70$ between 13° and 9.7°, $r = 0.76$ between 13° and 6.5°, $r = 0.76$ between 9.7° and

6.5°). In addition, we tested whether there was a difference in the median of paired observations for each neuron (DTI of a neuron at 2 levels of vergence) with the Wilcoxon Signed Rank Test and found no significant differences ($P > 0.57$ for 13° and 9.7°, $P > 0.09$ for 13° and 6.5°, $P > 0.14$ for 9.7° and 6.5°). The constancy of DTI despite large changes in inter-target distance implies that PRR neurons do not directly reflect the absolute depth of the reach target or the distance between reach and fixation targets. The results suggest that the planning activity encodes disparity with similar strength across vergence angle.

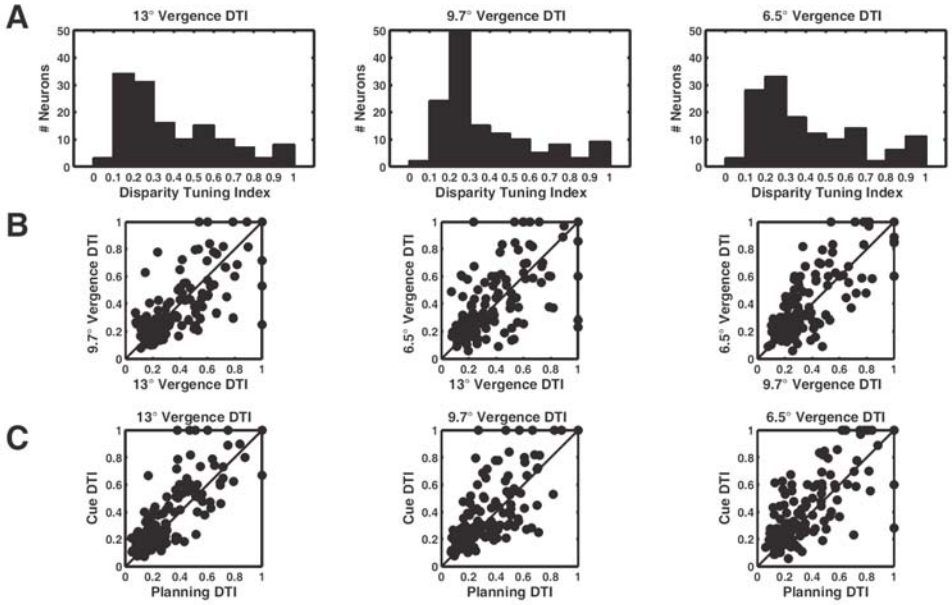

Figure 4-26 – Cue period DTI. The mean of the maximum cue period DTI from each neuron in the population (n = 137) is 0.4976 (±0.2679) with a median DTI of 0.4324. A: Histograms of cue period disparity tuning index (DTI) at each vergence angle for all neurons from Experiment 1 (n = 137). The mean of the DTI at each vergence angle does not differ (Kruskal-Wallis; P > 0.52), and the distributions of DTI at each vergence angle do not differ (Komolgorov-Smirnov test; P > 0.64 for 13° and 9.7° vergence; P > 0.54 for 13° and 6.5°; P > 0.36 for 9.7° and 6.5°). B: Cue period DTI from different vergence angles are paired for each neuron, shown for the population. Different pairings of vergence angle are shown from left to right. Cue period DTI is correlated at different fixation depths across the population (r = 0.75, 0.65, 0.79; P < 1e-5 for all r). C: Cue and planning period DTI at each vergence angle for all neurons (n = 137). Though there is a difference in magnitude between cue and planning period DTI (μ=0.0522, Kruskal-Wallis; P=0.0011), there is no effect of vergence angle in this difference (Kruskal-Wallis; P > 0.50). Cue and planning period DTI are correlated at each level of vergence across the population (r = 0.80 for 13°, 0.71 for 9.7°, 0.74 for 6.5°; P < 1e-5 for all r).

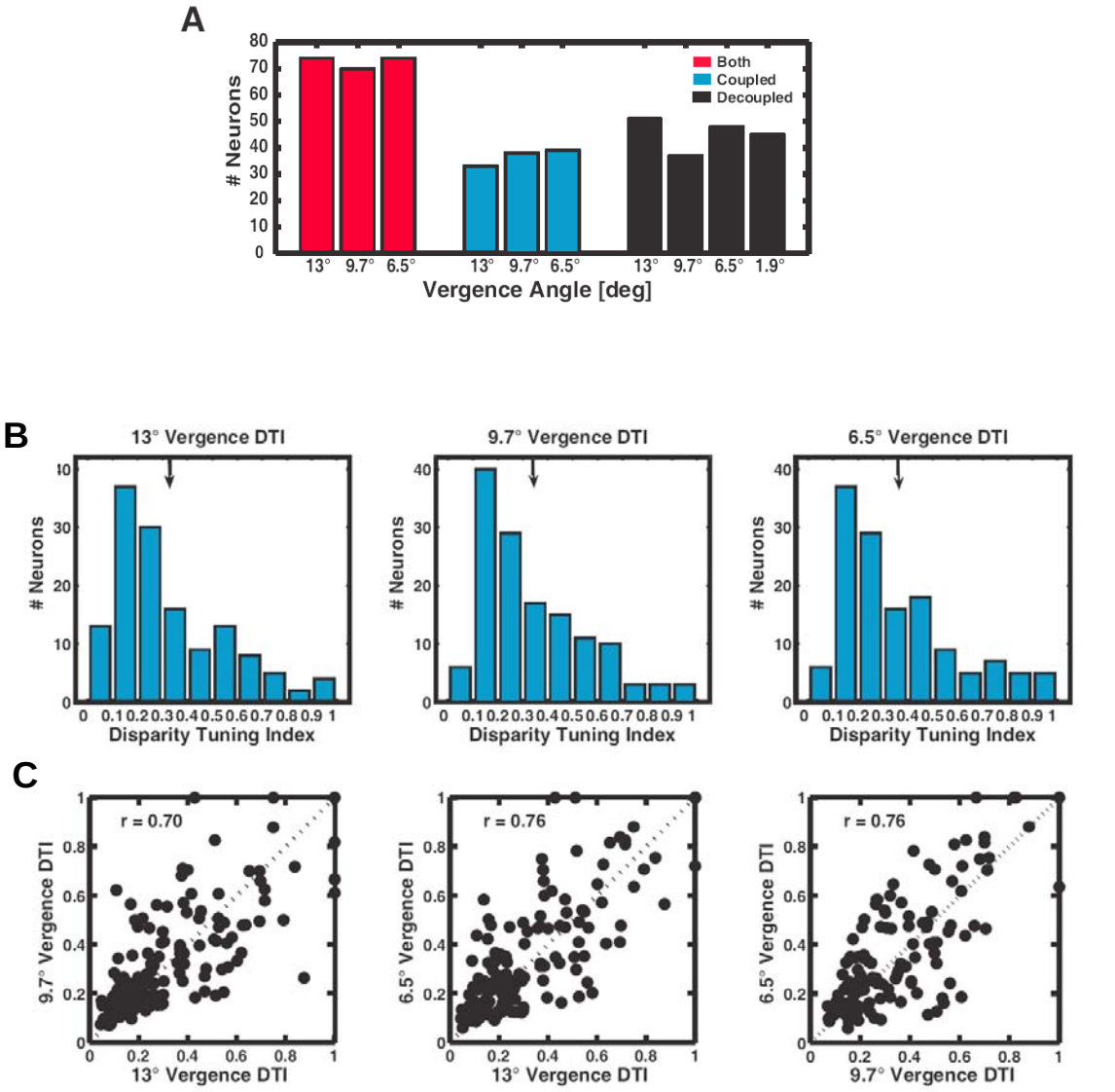

Figure 4-27 Population disparity tuning at each fixation depth, disparity tuning classification, and disparity tuning index for the neural population. A: Proportion of disparity tuning at each vergence angle from the disparity sensitive population of cells (n= 112). The proportions are shown separately for each experimental configuration due to the different disparity ranges tested. Coupled target disparities in Experiment 1(blue), decoupled target disparities in Experiment 2 (black), and for both (red). B: Histograms of disparity tuning index (DTI) at each vergence angle for all neurons from Experiment 1. C: DTI from different vergence angles are paired for each neuron, shown for the population. Different pairings of vergence angle are shown from left to right.

4.9 Disparity Discriminability Index

Previous studies have used the Disparity Discrimination Index (DDI) (Prince, Pointon et al. 2002; Uka and DeAngelis 2003) to measure the effect of disparity with reference to neuronal firing rate variance:

$$\mathrm{DDI} = \frac{\max - \min}{\max - \min + 2 * \sqrt{SSE/(N-M)}}$$

Where max and min are the maximum and minimum mean responses (trial averaged) to disparity at a single level of vergence, SSE is the sum of squared errors about the mean responses, N is the total number of trials, and M is the number of disparities tested. The term $\sqrt{SSE/(N-M)}$ is a measure of the firing rate variance, which was computed for mean subtracted responses for each disparity across the whole tuning curve. M was 6 for each vergence level, the disparities used for the calculation were [-1.5°:0.5°:1.0°] for each vergence as in DTI. A DDI of 0 indicates that response variability from trials dominated the response variability due to disparity, and a value of 1 indicates no trial variability occurred and all response variation was due to disparity. Figure 4-28 shows the DDI for PRR neurons at the different levels of vergence. The distributions of DDI are similar (Komolgorov-Smirnov test; $P > 0.07$ for 13° and 9.7° vergence; $P > 0.23$ for 13° and 6.5°; $P > 0.45$ for 9.7° and 6.5°). The mean DDI at each vergence angle is not different (μ=0.35 for 13° vergence, μ=0.36 for 9.7°, μ=0.37 for 6.5°; Kruskal Wallis ANOVA $P > 0.47$; Wilcoxon rank sum test, $P > 0.46$ for 13° and 9.7° vergence; $P > 0.25$ for 13° and 6.5°; $P > 0.51$ for 9.7° and 6.5°). The median across neurons for the

maximum DDI from vergence is 0.42, and is lower than that found in other areas (Table 4-1). The difference may be due to many other factors apart from the cortical response. Firstly the measurement here is taken for a planning response, and not the disparity stimulation period; secondly, the stimuli vary widely in the different experiments. The variance in the PRR responses may result from the stimulus location in frontoparallel space being non-optimal for a given neuron, and would bring the population average down. This is akin to DDI variation due to vergence angle, where a gain modulated response at optimal vergence will likely have a higher DDI than at non-optimal vergence. As a population, the results indicate that disparity discriminability is maintained across fixation depth. We tested whether individual PRR neurons had a relationship between DDI and vergence angle using the Wilcoxon sign rank test (paired observations of DDI at 2 levels of vergence), and found that no relation existed ($P > 0.25$ for 13° and 9.7°, $P > 0.09$ for 13° and 6.5°, $P > 0.34$ for 9.7° and 6.5°).

Figure 4-28B shows the DDI for neurons paired for different vergence angles. A DDI of 0 indicates the firing rate variance dominates response modulation, yielding no ability for an ideal observer to discriminate disparity. The values for PRR neurons have a grand median of 0.35 across all neurons and vergence angles, and yield a low correlation across neurons when DDI is paired for different vergence angles ($r = 0.31$ between 13° and 9.7°, $r = 0.43$ between 13° and 6.5°, $r = 0.28$ between 9.7° and 6.5°). This relates to the earlier point that discriminability may be higher at optimal vergence, which would predict a lower correlation for DDI at different vergence angles across neurons. In fact, examining the DDI at each vergence angle for cells with significant tuning at each level of vergence

yields that DDI does not change (Kruskal Wallis ANOVA, $P > 0.61$; $\mu=0.47$ for cells tuned for disparity at 13° vergence, $\mu=0.45$ for 9.7° vergence, and $\mu=0.47$ for 6.5°). DDI for cells tuned to disparity at each level of vergence is significantly higher than the DDI for the overall population ($P < 1e\text{-}7$ at each vergence angle) as expected. Figure 4-28C shows the relationship of DDI and DTI for neurons across the population. Across values of DTI, it can be seen that DDI remains similar, and also has a modest correlation (correlations are shown on the plot). DDI and DTI present complimentary information about response modulation and do not have a simple one-to-one relationship, and thereby have been presented together often in the disparity literature. The DDI has typically been used with the square root of firing rates in the literature to adjust for the mean-variance relationship from Poisson like firing (Prince, Pointon et al. 2002). The DDI using the square root of firing rates for PRR neurons remains very similar to the DDI without such transformation ($\mu=0.3614$ with transformation vs. $\mu=0.3606$ without), and does not effect the significance results.

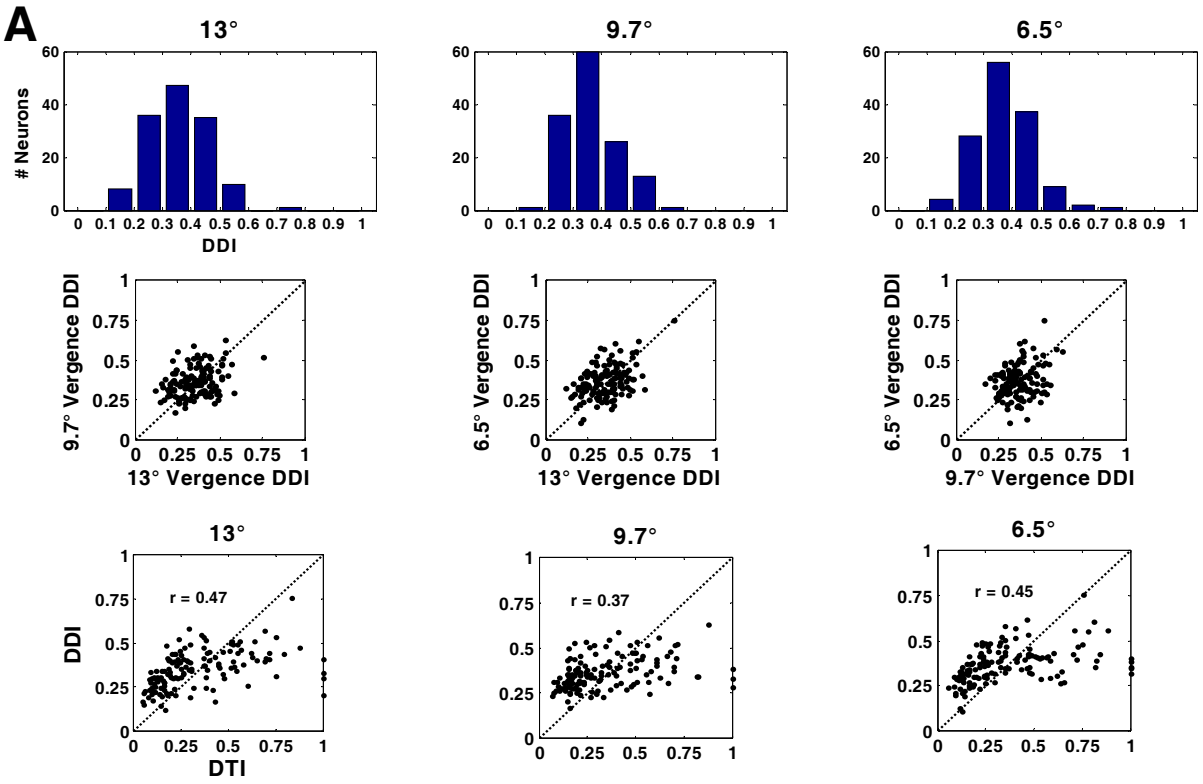

Figure 4-28 – DDI for PRR population (n = 137). A: Histograms of DDI at different vergence angles. B: DDI is paired at different vergence angles and plotted for all neurons. C: DTI and DDI is paired and plotted for all neurons, with correlations shown in the plot.

B Area	Mean DTI	Median DTI	Median DDI
PRR	0.43	0.36	0.42
V1	0.38	NA	0.54
V4	0.45	0.41	0.56
IT	NA	0.36	NA

Table 4-1– DTI and DDI from different cortical areas. DTIs from V1, V4, IT is during stimulus presentation for different types of stimuli. (Uka, Tanaka et al. 2000; Hinkle and Connor 2005) (NA = not available)

4.10 Absolute Target Depth and Disparity Modulation

In Experiment 2, we explored whether PRR neurons directly encode absolute depth by using decoupled reach targets that were fixed in space but represented different values of disparity at each level of vergence. We would expect that an absolute depth encoding neuron would not change firing rate for a reach target at a constant absolute depth. We found that 70% (96/137) of neurons have a significant change in firing rate during movement planning, and 80% (110/137) during movement execution, for a reach target at the same absolute depth but at different disparities and fixation depths (ANOVA; $P < 0.05$). We examined the remaining population of neurons without modulation in movement planning ($n = 41$) to see whether these neurons encoded the absolute depth of the reach target. 41% (17/41) of this subpopulation was modulated by the absolute depth of the reach target at any level of vergence (ANOVA; $P < 0.05$). An absolute depth encoding neuron would encode the absolute depth of the reach target independent of fixation depth, however none of the neurons in this subpopulation (0/17) demonstrated target depth modulation across all vergence angles tested. We observed that for the 9 neurons that were modulated at > 1 vergence angle ($n = 7$ for 2 vergence angle, $n = 2$ for 3 vergence angles), most (6/9) came close to significant modulation (6/9 ANOVA $P < 0.1$) for a reach target at constant absolute depth, and likely do not encode the absolute depth of the reach target. This suggests that PRR encodes target location in an eye centered reference frame, and this change in firing rate reflects both retinal location and eye position.

The disparity of the reach target, vergence angle, and the absolute depth of the reach target are related in 3 ways: A) disparity and vergence angle covary for a reach target at a constant absolute depth, B) absolute depth of the reach target and vergence angle covary for a target at a constant disparity, and C) disparity and absolute depth covary when vergence angle remains constant. The reach targets in Experiment 1 were used to measure the last relation (C) as the DTI at 3 levels of vergence angle. In Experiment 2, several decoupled reach targets were used to test the covarying relations A and B with the same vergence angles (13°, 9.7°, 6.5°) during reach planning. In other words, it is possible to compare the strength of modulation by vergence when target disparity changes (A) to when it remains constant (B). We measured the firing rate modulation for 3 decoupled reach targets that were fixed in depth but with changing disparity and vergence angle (A). This measured modulation by the same vergence angles for each decoupled reach target, however each target had different ranges of disparity (Figure 4-29). Interestingly, the strength of modulation in PRR neurons when absolute target depth remained constant (A) is similar to when it varied (C, DTI). The median of the maximum modulation from the 3 targets with changing disparity and vergence angle was similar to the DTI for coupled reach targets when vergence angle was held constant (0.33 vs. 0.36). We subsequently averaged the modulation from the 3 decoupled reach targets for each neuron (Index A) to compare to other quantities.

In contrast to Index A, we used decoupled reach targets in Experiment 2 to measure the change in planning period firing rate when target disparity remained constant (B). A measure of modulation due to changing reach target depth and vergence angle for targets

at the same disparity was calculated (Figure 4-30). This modulation was computed at 3 different disparity levels and averaged for each neuron (Index B). We subtracted Index B from Index A for each neuron. A value of zero indicates that the modulation by vergence angle is unaffected by changes in retinal location of the target; negative values indicate that vergence angle modulation has more influence than disparity, whereas positive values indicate that changes in disparity affect planning period firing more than changes in fixation depth. Overall, 65% of neurons have a difference between Index B and Index A that is >0. The distribution of the difference between the Index A and Index B for all neurons is unimodal and concentrated to the right of zero (Figure 4-31), with a population average indicating a larger Index A than Index B.

If the encoding of egocentric distance in an eye centered reference frame is achieved with divergent populations of vergence and disparity encoding neurons, we would expect a bimodal distribution with peaks at negative and positive differences corresponding to the two populations. PRR contains a homogenous gradient where the average response is influenced more by disparity than fixation depth. In summary, most PRR neurons have changes in planning activity for a reach target at a constant absolute depth due to different target disparities and vergence angles. The strength of modulation during reach planning was greater by disparity and vergence angle for a decoupled reach target fixed in depth (A) than by targets at different absolute depths (B) (Wilcoxon signed rank test, P=3.0e-6).

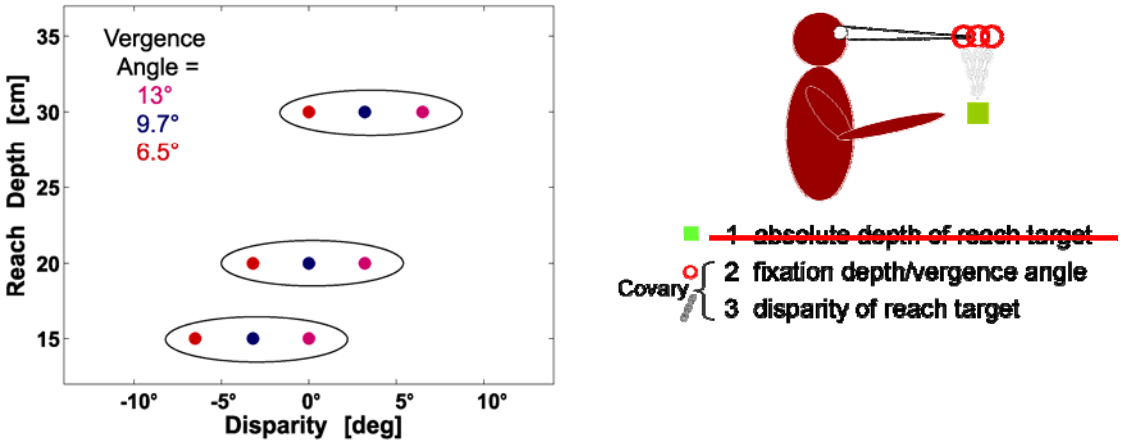

Figure 4-29– Target sampling for Index A, calculating modulation by reach target disparity and fixation depth. This was calculated for targets at fixed absolute target depth, circled in the figure. The vergence angles for the disparity modulation were the same as those used for Index B. The modulation for the three targets was averaged to Index B.

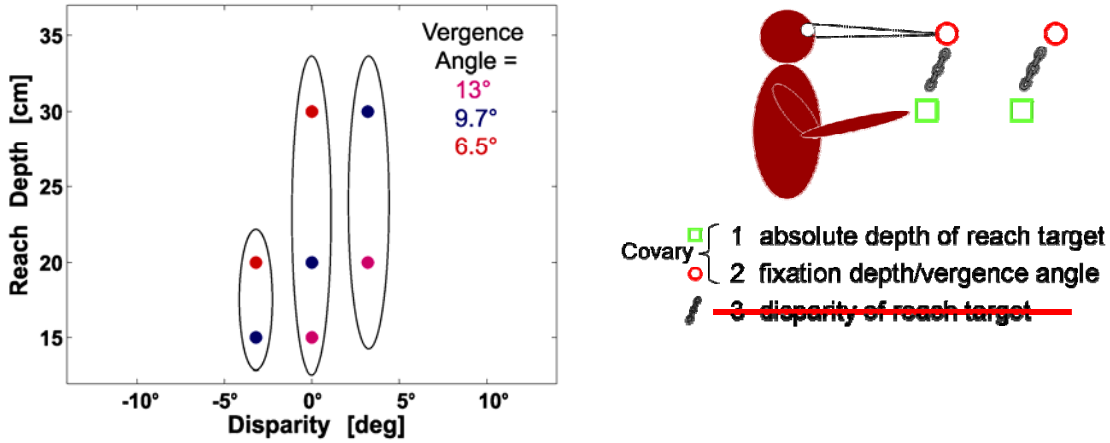

Figure 4-30– Target sampling for Index B calculating modulation by fixation depth at constant reach target disparity. The modulation ((max-min)/(max+min)) was measured for each group of circled targets, and then averaged.

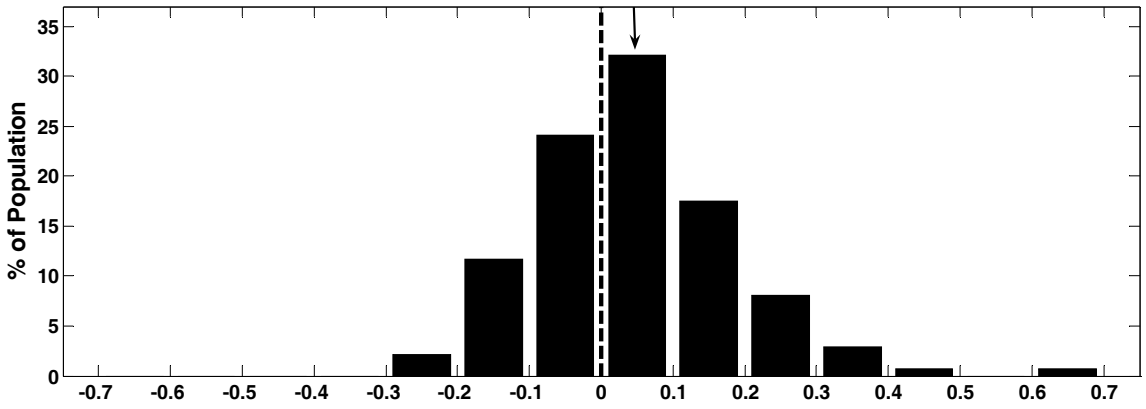

Figure 4-31– Histogram of difference in tuning indices (Index A-Index B) from Experiment 2. Index B measures modulation strength by vergence angle for targets at constant disparity during movement planning. Index A measures modulation strength by both disparity and vergence. A difference of zero indicates that disparity does not modulates a neuron's response more than disparity, a negative difference indicates a greater strength of modulation by vergence than disparity, and a positive difference indicates a greater modulation by disparity. The arrow indicates mean difference in population (μ=0.05, σ=0.11)

4.11 Mutual Information

Mutual information measures the overlap in entropy of signals. It is generally measured for 2 signals, however measures of information for >2 signals are being developed (Bell). For the data in this experiment, it is possible to measure the mutual information between firing rate and disparity or vergence angle. We employed a variant of the direct method for computing mutual information from the mean firing rates during movement planning (see Methods). Our goal was to compare the information encoded in firing rates for disparity and vergence angle. We were not interested in the absolute value of information (bits/sec). Instead, we computed the mutual information and normalized it

by the sum of the entropy of the firing rate and the entropy of the signal in question, referred to as the symmetric uncertainty.

The entropy of firing rate varied for each neuron, however the entropy of disparity and vergence angle remained largely the same between sessions/neural recordings since trial conditions for disparity and vergence were balanced in each experiment (*e.g.*, 5 trials/condition). There was a magnitude difference since disparity had 6-7 levels ($H(S) \sim 2.72$), whereas vergence had 3 levels ($H(S) \sim 1.58$), and so was the reason to use the symmetric uncertainty computation. The entropies for disparity and vergence stimuli are binned, and their histograms are plotted in Figure 4-32 B and C.

Planning period firing rate entropy was binned for all neurons, and the histogram is shown in Figure 4-32A. These entropies are for coupled reach target disparities and corresponding fixation points; entropies from other stimuli (decoupled reach targets and fixation points) may be different. Most neural entropies are larger than the stimulus entropies, which may be taken as a baseline for variability in this case. We measured the mutual information, or overlap of these 2 entropies, and normalized it by the stimulus entropies (see Methods) to obtain a symmetric uncertainty (SU) values. Permutation tests were used to obtain significance for each SU value. Figure 4-32D shows the SU values for neurons where the SU for both disparity and vergence angle were significant. A high correlation ($r = 0.7959$, $p < 0.0001$) exists between symmetric uncertainty for disparity and vergence angle for PRR neurons.

It is possible that separate subpopulations exist in PRR, one of which encodes primarily disparity, and the other which encodes vergence angle. This plot of SU and the correlation shows a single homogenous gradient of SU for disparity and vergence angle exists, and a single population exists in PRR which carries information for both disparity and vergence angle. A significant linear trend shows that neurons have a larger SU for disparity than vergence (ANOVA $p < 1.1e-16$; slope from regression $b = 1.22$), and hence encode ~ 20% more information about coupled reach target disparity than vergence angle.

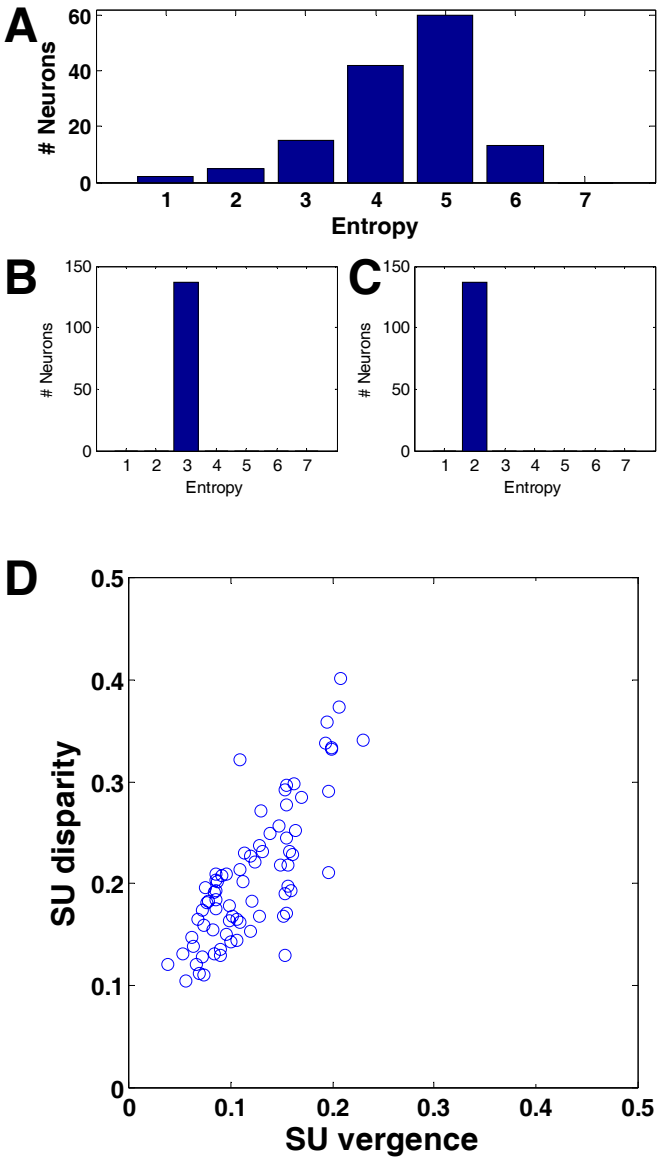

Figure 4-32 Entropy of neural responses and stimuli. A: Entropy of planning period responses for all neurons for coupled reach targets. B: Entropy of coupled reach target stimuli, which all fell into a single bin for all sessions/neurons. C: Entropy of fixtation stimuli, which all fell into a single bin for all sessions/neurons. D: Symmetric uncertainty (SU) for neurons that contained significant information for both coupled reach target disparity and vergence angle. There was significantly more information (normalized; symmetric uncertainty) about disparity than vergence in the planning period responses across the population of PRR neurons. The difference between the SU for disparity (μ=0.2080, σ=0.0685, median = 0.1945) and the SU for vergence angle (μ=0.1202, σ=0.0446, median = 0.1108) was significant (ANOVA; $p = 1.1102e\text{-}106$). Regressing SU disparity on SU vergence yields a significant slope of β=1.2232 ($p < 0.0017$), the Pearson correlation coefficient is $r = 0.7959$ ($p < 0.0001$).

4.12 Decoding PRR Responses

Previous studies have decoded the responses of PRR neurons to reaches made in the frontoparallel plane with central fixation (Shenoy, Meeker et al. 2003; Musallam, Corneil et al. 2004). The sophisticated decode methods employed in these studies transformed planning period responses using wavelets, and built databases of these responses during the initial portion of each experimental session for online decoding using a Bayesian framework. Studies by Gail et al. and Quian-Quiroga et al. have applied nearest neighbor methods for decoding planning period activity in PRR neurons (Gail and Andersen 2006; Quian Quiroga, Snyder et al. 2006). These methods do not transform spiking responses, and instead use firing rates averaged across the entire memory period, or firing rates over trial time (estimated from PSTHs). Again, a database of trials are used as a training set, and the relevant parameters are decoded from test trials by obtaining the class of the training trial firing rate nearest (by Euclidean distance) to the test trial firing rate. The nearest neighbor method is easily implemented, however does not take into account the variability in the firing rate in the relation to the classes of data during which linear discriminant analysis does by classifying data based on within-class and between-class variance (Bishop 1995; Hastie, Tibshirani et al. 2001).

In this work, we have performed some preliminary decode analyses on decoding reach target disparity, fixation depth, and absolute depth from the decoupled reach target experiment (Experiment 2). We have employed both nearest neighbor and linear discriminant decodes, as they yield different results. Figure 4-33 illustrates a neuron dropping curve using the nearest neighbor decode on reach target depth when the monkey

fixated at 13° of vergence angle. (Neuron dropping curves at other vergence angles are nearly identical, not shown.) Cross validation was performed on 100 sets of randomly selected neurons (without replacement) for each number of neurons used in the decode analysis, and the mean and standard deviation of performance is shown on the plot. Chance level performance is 20%, and is exceeded reliably (lower bound of performance using one standard deviation) with as little as 10 neurons. As documented in numerous studies, decode performance follows a near log function with the number of neurons.

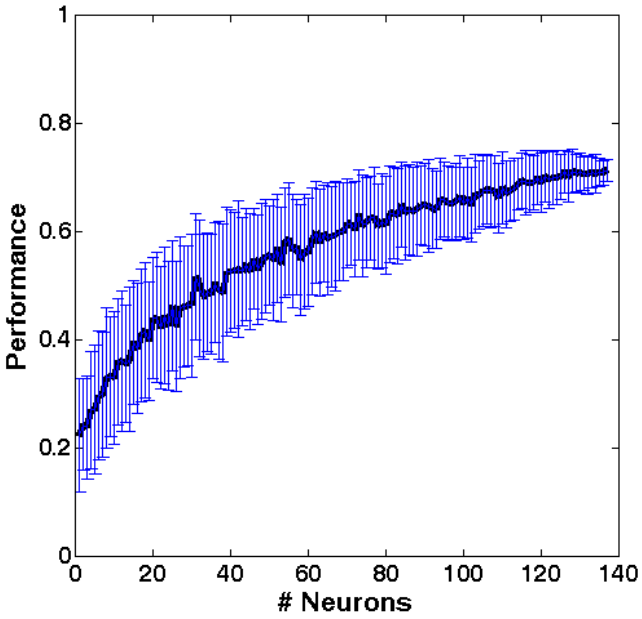

Figure 4-33 Neuron dropping curve using the nearest neighbor decode., plotting the average decode performance for reach target disparity at 13° of vergence angle against the number of neurons. Error bars indicate standard deviation from 100 cross validation sets, where neurons were selected at random without replacement.

Decode performance for both reach target disparity and fixation depth over trial time is shown in Figure 4-34. Reach target disparity is decoded using all fixation depths. Decode performance for reach target disparity rises significantly above chance level once the cue is flashed as expected (vertical line shows cue offset/memory begin). Decode performance dips slightly (~5% averaged across the memory period decode compared to

the peak decode performance during cue presentation) during the planning period, however remains well above chance performance. The decode performance for vergence angle remains constant across trial time, as expected since vergence angle is maintained. Other parameters in the nearest neighbor decode were employed – it is possible to use the n nearest neighbors to determine the task condition, however using n = 2,… 7 did not yield significant performance improvements. In addition, other distance measures can be used – interestingly, city block distance yielded some improvements in decode performance (~5%) when all neurons are used in the decode (performance difference decreases with fewer neurons), and indicate that the distance measure has a measurable dependence on when the dimensionality of the input vector becomes large (number of neurons in the population).

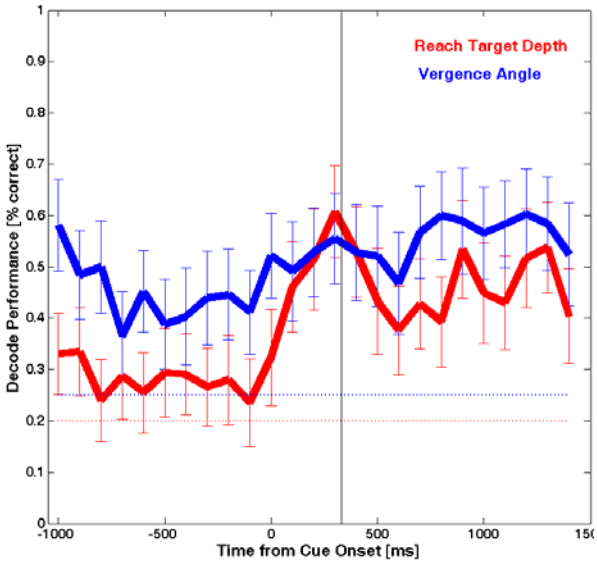

Figure 4-34 Decode performance using the nearest neighbor decode across trial time using all neurons. All conditions in Experiment 2 were included, and reach target depth and vergence angle were separately decoded. Chance levels are indicated by the dotted lines.

As a comparison, Figure 4-35 shows the decode performance across trial time using the linear discriminant. The same parameters for obtaining the firing rate from trials and cross validation are used. A diagonal covariance matrix was used since enough training

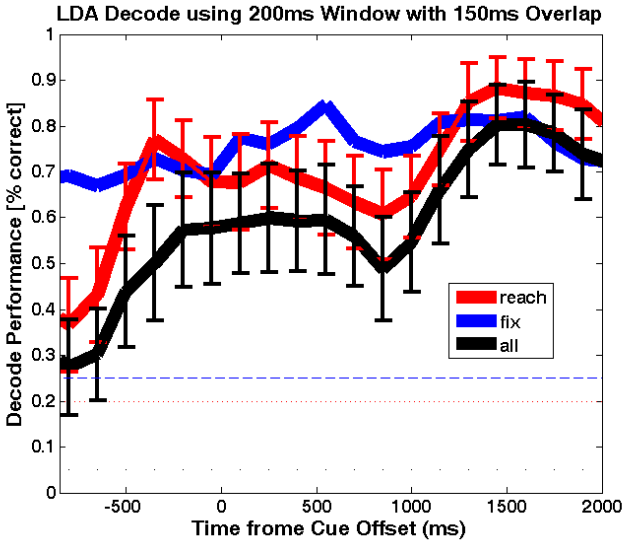

Figure 4-35 Decode performance using linear discriminant analysis across trial time using all neurons. All conditions in Experiment 2 were included and decoded; reach target depth (reach), vergence angle(fix), and the combination of reach target depth and vergence angle (all).

trials were not available for estimating a pooled covariance matrix with the total population of neurons. A large increase in decode performance is realized with this method, and shows that the use of class variability in the decode is an important factor. The same trend over trial time for decode performance exists between decode methods – vergence angle decode performance remains constant, and reach target disparity decodability rises with the presentation of the cue and persists through the planning period. There is a marked difference in decode performance between the methods in the motor period (the reach occurs approximately 1400 – 1600ms after cue offset); a peak is observed using LDA which is absent in the nearest neighbor method, again indicating that accounting for response variability between classes is an important feature in decoding firing rates in this task. Lastly, the combination of reach target disparity and vergence angle, which indicates the absolute depth of the target in eye centered coordinates, is decoded (black trace). Though chance level for decoding both parameters

is 5% (1/20; vs. 20%, 1/5 for disparity and 25%, 1/4 for vergence angle), the performance nearly tracks the decode of disparity alone. The results illustrate that the activity of population of PRR neurons can be used to decode the absolute depth or a reach target during movement planning.

Chapter 5 Discussion

5.1 Egocentric Distance and Reference Frames

The alignment of disparity tuning curves and gain modulation by vergence angle during movement preparation illustrates that neural activity encodes egocentric distance and implicates PRR in the early stages of reach planning. The processes underlying visual perception and action in visually guided reach movements require the coordination of information in multiple reference frames across the cerebral cortex. Our perceptual experience when scanning a visual scene and selecting a goal from multiple targets may occur in a world (allocentric) or object centered reference frame, where target distances are referenced to each other or a landmark in space. Once a goal is selected, its spatial parameters must be estimated with reference to the subject to prepare and execute a movement. The egocentric distance of the goal is represented in many ways throughout the reaching network at various stages of processing.

The egocentric distance could represent the distance of the target from the hands in a limb centered reference frame in cortical areas that are involved in the final stages of processing. The distribution of the preferred directions of neurons in the motor cortex during the execution of arm movements in three dimensional space contain an enhanced representation for the forward and backward directions, and shows a specialization in

motor control for reaches in depth (Naselaris, Merchant et al. 2006). Stimulated ensembles of neurons in primary motor cortex encode arm postures that can place the hand at proximal or distal locations from the trunk that are suited for reaching to targets in depth (Graziano 2006). Intermediate stages in processing use mixtures of limb and eye centered reference frames, such as in area 5 in the posterior parietal cortex (Buneo, Jarvis et al. 2002). We have shown that reach plans encoded in PRR contain a representation of egocentric distance that is eye centered, modulated by vergence angle, and reflects the initial processing stages in goal directed reaching in depth.

5.2 Visual, Planning and Movement Response in PRR

Spiking activity in PRR neurons represents egocentric distance by encoding the disparity of the reach target and fixation depth in movement plans. PRR neurons often have a visual response during stimulus presentation modulated by target disparity and vergence eye position that is likely to be strongly associated with the activity in the visual cortices through feedforward and feedback connections (34% (46/137) disparity sensitive in Experiment 1; 44% (60/137) vergence main effect; ANOVA $P < 0.05$). In this study we examined neural activity after the visual response from the stimulus and before movement execution to assess whether PRR neurons represented the depth of the target in the formation of movement plans. These signals emerge during movement preparation more frequently than during the presentation of the reach target stimulus (34% (46/137) are disparity sensitive during stimulus presentation vs. 56% (76/137) during planning). Reach target disparity tuning during the cue, planning, and movement epochs from

Experiment 1 were similar; however, it is difficult to distinguish disparity responses during the movement because they are confounded by motor related signals from motor efference and/or proprioception. The design of reach and fixation target configurations in Experiment 2 enabled the testing of the motor and visual components separately during movement execution by keeping the motor component (target depth) constant and varying the visual component (target disparity and vergence angle). Neural activity during the execution of the reach movement is strongly modulated by vergence angle for reaches to targets at constant absolute depth in 80% (110/137) of the population (ANOVA $P < 0.05$), and indicates that PRR neurons do not represent pure proprioceptive or motor commands (efference or feedback), but a visuomotor representation of hand guidance.

Human performance in memory reaches subsequent to intervening vergence eye movements are consistent with an egocentric reference frame that is referenced to gaze position, or retinally based (Van Pelt and Medendorp 2008). PRR neurons compensate for conjugate eye movements during reach planning (Batista 1999). The integration of these depth cues in the neural activity could mean that PRR plays a role in updating early reach plans due to vergence gaze shifts as well.

5.2.1 Disparity Tuning Classification

The shapes of significantly tuned disparity tuning profiles during movement planning in PRR are diverse, and a number of functional forms (e.g., linear, gaussian, sine, gabor,

polynomials up to 3rd degree, etc.) were explored to fit the disparity responses in the population and found to be insufficient (R^2>0.2; data not shown) in summarizing the disparity tuning shapes for a significant number of neurons (n > 15). The large number of neurons in the Complex tuned group in this data indicates that a coarser approach of subjective disparity response classification into previously described discrete classes does not play a significant role in separating the functions of PRR neurons. It remains possible that a finer sampling of disparity could reveal a functional form that models the disparity tuning as well as reveal a role for discrete classes of disparity tuning.

5.3 Vergence Angle and Disparity Gain Modulation

Fixation depth is recoverable directly from vergence angle and is a veridical depth cue, influencing neural activity in the oculomotor pathways extending from the midbrain through neocortex (Judge and Cumming 1986; Kurkin, Takeichi et al. 2003; Akao, Kurkin et al. 2005; Akao, Mustari et al. 2005), as well as visual cortical areas beginning at the level of primary visual cortex (Trotter, Celebrini et al. 1992; Uka, Tanaka et al. 2000; Rosenbluth and Allman 2002). Vergence angle strongly affected the response of the majority of PRR neurons for coupled reach targets at constant disparity during movement planning, however since the fixation target was fixed in azimuth and elevation, it is likely that the optimal response to vergence was not examined for many of the neurons. In addition, the sparse sampling of vergence angle taken at constant target disparity for Experiment 1 probably also underestimates the degree of modulation by vergence angle (VTI) in the population. The DTI of the population, however, does not

change with fixation depth and is well correlated between vergence angles, indicating that the strength of modulation by disparity is preserved across fixation depth in the population activity. The DTI of PRR neurons during movement planning is notably similar to that seen in the visual responses to various stimuli in areas V1, IT, and V4 (Table 4-1) (Uka, Tanaka et al. 2000; Hinkle and Connor 2005). Most PRR neurons were sensitive to both disparity and vergence angle, and the correlation between DTI and VTI in Experiment 1 and the unimodal distribution of (Index A – Index B) from Experiment 2 indicate the PRR population is not subdivided into discrete and separate subpopulations of vergence sensitive and disparity sensitive neurons.

Vergence angle was sampled in >3° steps, and a population of neurons exhibited gain modulation of disparity tuning by vergence angle acting as a linear operator. We believe that neurons express this relationship more frequently for smaller changes in vergence than those tested in this study. Nonlinear gain mechanisms based on fixation depth may play a role in transforming disparity responses as well. Two dimensional limb position gain fields have been found in reach related areas in the PPC that underlie the coordinate transformation process. Initial hand location on a frontoparallel plane is encoded in an eye centered reference frame in PRR (Buneo, Jarvis et al. 2002) , and it is likely that a similar gain mechanism may exist to encode the initial egocentric distance of the hand during movement planning. If so, the population activity in PRR could contain more than the goal of a reach in planning activity, but a complete representation of a movement plan from initiation to target acquisition for reaches in three dimensions in visual coordinates.

5.4 Depth Responses in the IPS

Previous studies have shown the influence of depth cues during visuospatial tasks on neural activity throughout the intraparietal sulcus (IPS) (Sakata, Taira et al. 1997). For example, neurons in the anterior region of the lateral bank of the IPS, area AIP, have been shown to have a role in grasping, and vary their response to the presentation of three dimensional disparity defined shape of target objects of manipulation (Murata, Gallese et al. 1996). The caudal region of the IPS, area CIP, has been shown to be sensitive to different surface orientations in depth as prescribed by diverse depth cues such as binocular disparity, texture, and linear perspective (Sakata, Tsutsui et al. 2005). It has been shown that neurons in Area 7a are tuned to stimulus disparity as well as relative size (Sakata, Shibutani et al. 1985). Area LIP has been shown to have modulation by stimulus blur, vergence angle, and binocular disparity during the planning of eye movements in depth (Gnadt and Mays 1995; Genovesio and Ferraina 2004). Human subjects have the ability to perceive and estimate the depth of targets with large disparities, which is necessary for performing reaches without foveating the target (or fixating at the same distance as the target) and for planning eye movements to locations far outside of the plane of fixation (Westheimer and Tanzman 1956; Ziegler and Hess 1997). LIP neurons support large vergence eye movements in behavior with sensitivity to large disparities (ranging from -7° to +10°) during saccade planning (Gnadt and Mays 1995; Genovesio and Ferraina 2004).

5.5 Decoupled Reach and Fixation Depth

Reaches can be performed with steady decoupled fixation throughout the movement, or more commonly planned with decoupled fixation to first bring the hand to the "ballpark" of the object before it is foveated and grasped (Johansson, Westling et al. 2001; Heath and Binsted 2007). Both scenarios initially require the representation of the depth of a reach target that is highly decoupled or "far" from fixation depth to plan the reach movement. The majority of PRR neurons (69%, 95/137) are sensitive to large target disparities that were tested with decoupled reach targets in Experiment 2 during reach planning. The functional similarity between PRR and LIP responses (Snyder, Batista et al. 2000) and anatomical connectivity (Lewis and Van Essen 2000) may suggest that a parallel neural architecture evolved in both areas to coordinate saccades and reaches in the same reference frame. Damage to the parietal cortex is known to cause limb specific deficits in decoupling a reach movement from gaze (Jackson, Newport et al. 2005). In Experiment 2, 40% (45/112) of the disparity sensitive population (including target disparities from both Experiments 1 and 2) encoded the disparity of highly decoupled targets (Experiment 2) when fixation depth was 1m. These results show that movement planning activity in PRR contains a neural correlate of decoupled reaching that supports hand-eye coordination.

5.6 Depth Specific Deficits and Relation to Reference Frames

Damage to the parietal cortices can create specific depth related visuomotor deficits that cause errors in visually guided reaching movements. Baylis et al. tested a patient with bilateral parietal lobe damage using a delayed reach task with targets at different azimuthal locations and depths (Baylis and Baylis 2001). The patient exhibited significantly more errors in depth than direction during visually guided reaching with either arm. This depth specific deficit in reaching vanished when reaches were guided without vision based on verbal instructions. These findings suggest that damage to the parietal lobe can disturb the representation of depth specific to reaches planned using vision. Visual form agnosia patient D.F. was tested with a reach to grasp and perceptual distance estimation task in depth (Carey, Dijkerman et al. 1998). D.F.'s performance in reaching to targets in depth under visual guidance was indistinguishable from normal subjects, however D.F.'s verbal estimates of target depth exhibited an above normal error rate, suggesting that the neural mechanism for visuomotor control in depth was intact and separate from those required in making perceptual judgments of depth. This may reflect the fact that the neural substrates for perceptual processes that may use a world or object centered frame of reference to estimate target depth are disturbed. A similar study examined how the expectation of target distance affects perception and visuomotor control, and found the perceptual estimates were effected by expectation, however reach performance was not (Pagano and Isenhower 2008). Taken together, the implications of these studies are that the parietal cortex is essential in the coordinate transformations that create early movement plans in an eye centered reference frame used in planning reaches in depth. The integration of depth cues central to representing egocentric distance of a

target place PRR at the early foundations of planning and making reaches in a three dimensional world.

5.7 Future Experiments

This thesis has examined egocentric distance encoding in the PPC and found that early reach plans in PRR employ a retinally based reference frame by directly encoding reach target disparity and vergence angle. The diversity of disparity tuning profile shapes among PRR neurons may reflect the effect of 2 unexplored variables discussed above: the frontoparallel location of the fixation target and reach target. A subsequent experiment that compares disparity tuning by systematically probing disparity in different locations in the frontoparallel plane could shed light on whether disparity receptive fields have a unimodal distribution in the frontoparallel field, as seen in area LIP for saccadic target location (Gnadt and Mays 1995), or a more complex relationship. In addition, it is unknown whether a cortical organization based on receptive field properties in 2D and 3D exists in the PRR. If it does, cortical microstimulation may provide input to a coherent population of similarly tuned neurons that may bias the subsequent reach behavior (*e.g.*, the amplitude/distance of the reach).

Previously, it has been that directional tuning of PRR neurons can undergo plasticity (increased tuning depth, or "sharpening" of the tuning curve) directed by reward modulation (Musallam, Corneil et al. 2004). Does the plasticity induced for reach target direction (frontoparallel location of the reach target) also effect disparity tuning in that

frontoparallel location? Likewise, it would be interesting to explore whether disparity tuning is capable of similar plasticity. In conjunction with 2D reach target location, is it possible to induce plasticity and sharpen disparity tuning curves in a nonpreferred frontoparallel location, and does it resemble disparity tuning in the preferred frontoparallel location (in effect, can disparity tuning be "transferred" from the preferred frontoparallel location to an arbitrary one)?

It has been shown that PRR neurons encode the location of auditory reach targets in an eye centered reference frame (Cohen and Andersen 2000; Cohen and Andersen 2000; Cohen 2002) and LIP neurons encode auditory saccadic targets in eye centered (and in addition head centered and intermediate) reference frames (Stricanne, Andersen et al. 1996; Stricanne, Andersen et al. 1996; Andersen, Grunewald et al. 1997). Neurons in the primary auditory cortex encode the azimuth and elevation of auditory stimuli (Ahissar, Ahissar et al. 1992; Recanzone, Guard et al. 2000), and it is clear that such a representation can be readily transformed into retinal coordinates. Though humans perceive the egocentric distance of sound sources (Mershon and Bowers 1979), the neural mechanisms are highly dependent on the environmental reverberations and their spatiotemporal effect on sound pressure levels (SPL) (Nelson 2000; Zahorik and Wightman 2001). We would expect PRR neurons to encode the egocentric distance of auditory reach targets in an eye-centered reference frame, and consequently transform this auditory distance into a target disparity referenced to the vergence angle.

Target location in a retinal reference frame changes when an eye movement causes a shift in the retinal location. PRR neurons show compensation when intervening conjugate eye movements occur after a cue is shown, but before the reach is made (Batista 1999). Intervening disjunctive saccades (vergence eye movements) after the cue and before the reach should also cause compensatory activity in PRR neurons, where the activity is updated to reflect the new disparity value of the target with reference to the new vergence angle. The psychophysical performance in reaching (in terms of endpoint errors) when humans perform a memory reach with an intervening vergence eye movement indicate that this occurs – endpoint errors are consistent with the updating of remembered location based on it's disparity value instead of it's absolute depth, and is consistent with the encoding of egocentric distance in a retinal reference frame (Van Pelt and Medendorp 2008). If compensatory activity for intervening vergence eye movements exists in PRR neurons, it indicates that PRR is crucial in the pathway for updating spatial representations that directly underlie reaching performance and eye-hand coordination when targets are dynamic.

Area LIP contains a body referenced signal that reflects the position of saccadic targets during eye movement planning that modulates the retinal coordinates of the target by eye position and head position (from neck proprioception) (Brotchie, Andersen et al. 1995; Andersen, Snyder et al. 1997; Snyder, Grieve et al. 1998). Activity in the PRR is modulated by the initial location of the hand in the frontoparallel plane (encoded in eye centered coordinate) (Buneo, Jarvis et al. 2002), and indicates that this area also contains a body referenced signal in visual coordinates that can be used in the relative encoding

schemes for eye, hand, and target position used in downstream areas such as Pmd (Pesaran, Nelson et al. 2006). We believe that PRR activity may also be modulated by the egocentric distance of the hands. It is possible that the activity is modulated by the proprioceptive position of the hands, which would be indicate that firing rates would encode the egocentric hand location as an absolute depth/distance, however it is more likely that this distance is again represented in visual coordinates as the retinal disparity. This body referenced signal would provide complete support for encoding these relative locations in 3D in downstream areas if a gain modulation by the disparity of the hands from the point of gaze exists. If a body referenced modulation by the egocentric distance of the hands exists in a population of PRR neurons, would intervening movements of the hands after the cue is shown but before the reach to the target is executed (analogous to the intervening conjugate saccades and vergence eye movements discussed above) cause compensatory activity to update the new body referenced location of the target? It is possible that multiple populations exist in PRR, some of which contain such body referenced signals that may compensate despite the fixed egocentric location of the target with respect to gaze, and others which do not contain modulation of hand location and maintain a stable activity that reflects target position only. Lastly, if divergent populations as described exist, it would be interesting to see if they are spatially segregated in the cortex, receive different afferent inputs, and project to different areas.

The local field potential (LFP) in PRR and LIP reflects aspects of movement planning such as directional tuning and state transitions (Pesaran, Pezaris et al. 2002; Buneo, Jarvis et al. 2003; Scherberger 2005). The power spectral densities of LFPs were examined in

this thesis work (not included) for modulation during movement planning by target disparity and vergence angle, and found to rarely exhibit significant modulation (8/48 recordings**)**. Studies have shown the synchronization of neurons to LFP activity, and between LFP activity at different sites (phase synchronization of oscillatory activity) across wide cortical areas, often occurring in the gamma band in motor areas (Murthy and Fetz 1996; Murthy and Fetz 1996; Donoghue, Sanes et al. 1998) and early visual cortex (Friedman-Hill, Maldonado et al. 2000; Maldonado, Friedman-Hill et al. 2000; Fries, Reynolds et al. 2001; Womelsdorf 2005). The synchronization of oscillatory activity, both in the spiking of single neurons and the LFPs, could be used to study the transfer of information from parietal areas such as PRR that encode target location in egocentric coordinates, to areas in the hippocampal and parahippocampal formations that represent the same information in allocentric coordinates.

Long term memories are formed for habitually performed actions/reaches in allocentric coordinates, and must be transformed into motor coordinates to perform the non-visually guided reach (*e.g.*, we have memories that enable us to reach for the radio without looking while driving). It is unknown which neuronal mechanisms function in the consolidation of short term memories (or working memory) in egocentric coordinates and their transformation into allocentric coordinates (and long term memories). Likewise, it is unknown whether and how the recall of long term allocentric memories are manifested in areas that represent movement intentions in egocentric coordinates. A study indicates that PRR activity reflects high level cognitive plans that contain the intended reach location, where abstract rules are used to transform the reach location (rotational) based

on the cue location in an eye centered reference frame (egocentric) (Gail and Andersen 2006). PRR neurons may also reflect the egocentric location of a plan initially formed using allocentric coordinates, and the dynamics of neural activity between PRR and area 7a (which encodes location in an allocentric reference frame) may be an important mechanism subserving reaches initially planned in an allocentric reference frame.

Areas in the IPS are sensitive to a wide variety of depth cues (see Chapter 1, 1.4.1.1, 2.2, 5.4). PRR neurons have been shown to be sensitive to horizontal binocular disparity and vergence angle in this work, however it is possible that other depth cues could be integrated in PRR to specify the egocentric distance of targets. Vertical disparity, or the differential angular subtense of surfaces projected onto the retina based on eccentricity and distance of the surface, is a veridical depth cue and may be used to calibrate horizontal disparities to produce absolute depth information without extraretinal information (Bishop 1989; Berends and Erkelens 2001). [6] Receptive fields for vertical disparity alone, and stimuli that contain both horizontal and vertical disparity may exist for PRR neurons. It is unknown whether PRR neurons integrate high level depth cues, such as the pictorial depth cues that can be tested monocularly. Other areas in the IPS are sensitive diverse monocular depth cues such as texture, perspective, slant, blur, and relative size. If PRR is sensitive to pictorial depth cues, it may receive an input from these areas that already integrate these depth cues, or receive input that is commonly

[6] Whereas the extraretinal signal of vergence angle produces horizontal disparity calibration in PRR, LIP, V1, and other areas (see 3.1 and 4.4.2). The effect of vergence angle on oculomotor control is ~20x stronger than depth cues such as vertical and horizontal disparity, though these depth cues effect perceptual estimates (sensory) strongly Wei, M., G. C. DeAngelis, et al. (2003). "Do visual cues contribute to the neural estimate of viewing distance used by the oculomotor system?" J Neurosci **23**(23): 8340-50..

received *by* these areas and integrate the information in coordination with these areas, to compute the egocentric distance of reach targets. Motion parallax has been shown to provide depth information (see 1.4.4) The PPC contains vestibular inputs, and it would be interesting to see whether PRR computes depth from motion parallax and integrates pictorial depth cues, and how PRR represents this depth information. One possibility is that this information is transformed and represented as "equivalent" binocular disparities. In this case, a similar updating of gaze referenced location in the presence of intervening eye movements may take place.

References

Afraz, S. R., R. Kiani, et al. (2006). "Microstimulation of inferotemporal cortex influences face categorization." Nature 442(7103): 692-5.

Ahissar, M., E. Ahissar, et al. (1992). "Encoding of sound-source location and movement: activity of single neurons and interactions between adjacent neurons in the monkey auditory cortex." J Neurophysiol 67(1): 203-15.

Akao, T., S. A. Kurkin, et al. (2005). "Visual and vergence eye movement-related responses of pursuit neurons in the caudal frontal eye fields to motion-in-depth stimuli." Exp Brain Res 164(1): 92-108.

Akao, T., M. J. Mustari, et al. (2005). "Discharge characteristics of pursuit neurons in MST during vergence eye movements." J Neurophysiol 93(5): 2415-34.

Albert, M. K. (2006). "Lightness and perceptual transparency." Perception 35(4): 433-43.

Allman, J. M. (1999). Evolving brains. New York, Scientifc American Library : Distributed by W.H. Freeman and Co.

Andersen, R. A. (1985). The neurobiological basis of spatial cognition: Role of the parietal lobe. The Development of Spatial Cognition. U. Bellugi, M. Kritchevski and J. Stiles-Davis. Chicago, University of Chicago Press: 57-80.

Andersen, R. A. (1988). Visual and visual-motor functions of the posterior parietal cortex. Neurobiology of Neocortex. P. Rakic and W. Singer. New York, Wiley: 285-295.

Andersen, R. A. (1994). Coordinate transformations and motor planning in posterior parietal cortex. The Cognitive Neurosciences. M. S. Gazzaniga, MIT Press: 519-532.

Andersen, R. A. (1997). "Multimodal integration for the representation of space in the posterior parietal cortex." Phil. Trans. Royal Soc. Bio. Sci. B(352): 1421-1428.

Andersen, R. A., and C.A. Buneo (2002). "Intentional maps in the posterior parietal cortex." Annual Review of Neuroscience 25: 189-220.

Andersen, R. A., and C.A. Buneo (2003). Sensorimotor integration in posterior parietal cortex. The Parietal Lobes. A. M. Siegel, R.A. Andersen, H-J Freund, and D.D. Spencer, Lippincott Williams and Wilkins. 93: 159-177.

Andersen, R. A., R. M. Bracewell, et al. (1990). "Eye position effects on visual, memory, and saccade-related activity in areas LIP and 7a of macaque." J Neurosci 10(4): 1176-96.

Andersen, R. A., Essick, G.K., and Siegel, R.M. (1985). "The encoding of spatial location by posterior parietal neurons." Science 230:456-458.

Andersen, R. A., A. Grunewald, et al. (1997). The processing of auditory stimuli for eye movements in the posterior parietal cortex of monkeys. Central Auditory Processing and Neural Modeling. P. Poon and J. Brugge. New York, Plenum Press.

Andersen, R. A., L. H. Snyder, et al. (1997). "Multimodal representation of space in the posterior parietal cortex and its use in planning movements." Annu Rev Neurosci 20: 303-30.

Andersen, R. A., L. H. Snyder, et al. (1993). "Coordinate transformations in the representation of spatial information." Current Opinion in Neurobiology 3: 171-176.

Andersen, R. A. and D. Zipser (1988). "The role of the posterior parietal cortex in coordinate transformations for visual-motor integration." Can J Physiol Pharmacol 66(4): 488-501.

Arnheim, R. (2004). Art and visual perception : a psychology of the creative eye : the new version. Berkeley, Calif., University of California Press.

Backus, B. T., D. J. Fleet, et al. (2001). "Human cortical activity correlates with stereoscopic depth perception." J Neurophysiol 86(4): 2054-68.

Banks, M. S., B. T. Backus, et al. (2002). "Is vertical disparity used to determine azimuth?" Vision Res 42(7): 801-7.

Batista, A. P., C. A. Buneo, et al. (1999). "Reach plans in eye-centered coordinates." Science 285: 257-260.

Batista, A. P., Buneo, C.A., Snyder, L.H., Andersen, R.A. (1999). "Reach plans in eye-centered coordinates." Science 285: 257-260.

Baylis, G. C. and L. L. Baylis (2001). "Visually misguided reaching in Balint's syndrome." Neuropsychologia 39(8): 865-75.

Bell, A. J. "The Co-Information Lattice."

Berends, E. M. and C. J. Erkelens (2001). "Strength of depth effects induced by three types of vertical disparity." Vision Res 41(1): 37-45.

Bingham, G. P. and C. C. Pagano (1998). "The necessity of a perception-action approach to definite distance perception: monocular distance perception to guide reaching." J Exp Psychol Hum Percept Perform 24(1): 145-68.

Bishop, C. (1995). Neural networks for pattern recognition. Oxford

Oxford ; New York, Clarendon Press ;

Oxford University Press.

Bishop, P. O. (1989). "Vertical disparity, egocentric distance and stereoscopic depth constancy: a new interpretation." Proc R Soc Lond B Biol Sci 237(1289): 445-69.

Bradshaw, M. F., K. M. Elliott, et al. (2004). "Binocular cues and the control of prehension." Spat Vis 17(1-2): 95-110.

Brotchie, P. R., R. A. Andersen, et al. (1995). "Head position signals used by parietal neurons to encode locations of visual stimuli." Nature 375(6528): 232-235.

Brouwer, G. J., R. van Ee, et al. (2005). "Activation in visual cortex correlates with the awareness of stereoscopic depth." J Neurosci 25(45): 10403-13.

Bulthoff, H. H., S. Y. Edelman, et al. (1995). "How are three-dimensional objects represented in the brain?" Cereb Cortex 5(3): 247-60.

Buneo, C. A., A. P. Batista, et al. (2008). "Time-invariant reference frames for parietal reach activity." Exp Brain Res 188(1): 77-89.

Buneo, C. A., M. R. Jarvis, et al. (2002). "Direct visuomotor transformations for reaching." Nature 416:632-636.

Buneo, C. A., M. R. Jarvis, et al. (2003). "Properties of spike train spectra in two parietal reach areas." Exp Brain Res 153(2): 134-9.

Buschman, T. J. and E. K. Miller (2007). "Top-Down Versus Bottom-Up Control of Attention in the Prefrontal and Posterior Parietal Cortices." Science 315(5820): 1860.

Carey, D. P., H. C. Dijkerman, et al. (1998). "Perception and action in depth." Conscious Cogn 7(3): 438-53.

Churchland, M. M., G. Santhanam, et al. (2006). "Preparatory activity in premotor and motor cortex reflects the speed of the upcoming reach." J Neurophysiol 96(6): 3130-46.

Cisek, P. and J. F. Kalaska (2002). "Simultaneous encoding of multiple potential reach directions in dorsal premotor cortex." J Neurophysiol 87(2): 1149-54.

Clower, D. M., J. M. Hoffman, et al. (1996). "Role of posterior parietal cortex in the recalibration of visually guided reaching." Nature 383(6601): 618-21.

Cohen, Y. E. and R. A. Andersen (2000). "Eye position modulates reach activity to sounds." Neuron 27(3): 647-52.

Cohen, Y. E. and R. A. Andersen (2000). "Reaches to sounds encoded in an eye-centered reference frame." Neuron 27(3): 647-52.

Cohen, Y. E., Batista, A.P. and Andersen R.A. (2002). "Comparison of neural activity preceding reaches to auditory and visual stimuli in the parietal reach region." NeuroReport 13:891-894.

Connolly, J. D. and M. A. Goodale (1999). "The role of visual feedback of hand position in the control of manual prehension." Exp Brain Res 125(3): 281-6.

Constantinidis, C. and M. A. Steinmetz (2005). "Posterior Parietal Cortex Automatically Encodes the Location of Salient Stimuli." Journal of Neuroscience 25(1): 233.

Cui, H. and R. A. Andersen (2007). "Posterior parietal cortex encodes autonomously selected motor plans." Neuron 56(3): 552-9.

Cumming, B. (2002). "Stereopsis: where depth is seen." Curr Biol 12(3): R93-5.

DeAngelis, G. C. (2000). "Seeing in three dimensions: the neurophysiology of stereopsis." Trends Cogn Sci 4(3): 80-90.

DeAngelis, G. C. and T. Uka (2003). "Coding of Horizontal Disparity and Velocity by MT Neurons in the Alert Macaque." J Neurophysiol 89(2): 1094-1111.

DeLucia, P. R. (2005). "Does binocular disparity or familiar size information override effects of relative size on judgements of time to contact?" Q J Exp Psychol A 58(5): 865-86.

Dias, E. C., T. McGinnis, et al. (2006). "Changing plans: neural correlates of executive control in monkey and human frontal cortex." Experimental Brain Research 174(2): 279-291.

Dijkerman, H. C., A. D. Milner, et al. (1996). "The perception and prehension of objects oriented in the depth plane. I. Effects of visual form agnosia." Exp Brain Res 112(3): 442-51.

Donoghue, J. P., J. N. Sanes, et al. (1998). "Neural discharge and local field potential oscillations in primate motor cortex during voluntary movements." J Neurophysiol 79(1): 159-73.

Dorris, M. C. a. G., P.W. (2004). "Activity in posterior parietal cortex is correlated with the relative subjective desirability of action." Neuron 44: 365-378.

Durand, J. B., K. Nelissen, et al. (2007). "Anterior regions of monkey parietal cortex process visual 3D shape." Neuron 55(3): 493-505.

Ebenholtz, S. M. and J. M. Ebenholtz (2003). "Distance perception for points at equiconvergence and equidistance loci." Perception 32(6): 707-16.

Edward H. Yeterian, D. N. P. (1985). "Corticothalamic connections of the posterior parietal cortex in the rhesus monkey." The Journal of Comparative Neurology 237(3): 408-426.

Efron, B. and R. J. Tibshirani (1993). An introduction to the bootstrap. London, Chapman and Hall.

Ellison, A. and A. Cowey (2007). "Time course of the involvement of the ventral and dorsal visual processing streams in a visuospatial task." Neuropsychologia 45(14): 3335-3339.

Erens, R. G., A. M. Kappers, et al. (1993). "Perception of local shape from shading." Percept Psychophys 54(2): 145-56.

Ferris, S. H. (1972). "Motion parallax and absolute distance." J Exp Psychol 95(2): 258-63.

Fisher, S. K. and K. J. Ciuffreda (1988). "Accommodation and apparent distance." Perception 17(5): 609-21.

Friedman-Hill, S., P. E. Maldonado, et al. (2000). "Dynamics of striate cortical activity in the alert macaque: I. Incidence and stimulus-dependence of gamma-band neuronal oscillations." Cereb Cortex 10(11): 1105-16.

Fries, P., J. H. Reynolds, et al. (2001). "Modulation of oscillatory neuronal synchronization by selective visual attention." Science 291(5508): 1560-3.

Gail, A. and R. A. Andersen (2006). "Neural Dynamics in Monkey Parietal Reach Region Reflect Context-Specific Sensorimotor Transformations." J. Neurosci. 26(37): 9376-9384.

Galati, G., E. Lobel, et al. (2000). "The neural basis of egocentric and allocentric coding of space in humans: a functional magnetic resonance study." Exp Brain Res 133(2): 156-64.

Genovesio, A. and S. Ferraina (2004). "Integration of retinal disparity and fixation-distance related signals toward an egocentric coding of distance in the posterior parietal cortex of primates." J Neurophysiol 91(6): 2670-84.

Georgopoulos, A. P., Kalaska, J.F., Caminiti, R., and Massey, J.T. (1982). "On the relations between the direction of two-dimensional arm movements and cell discharge in primate motor cortex." J Neurosci 2(11): 1527-1537.

Georgopoulos, A. P., Kettner, R.E., and Schwartz, A.B. (1988). "Primate motor cortex and free arm movements to visual targets in 3-dimensional space. 2. Coding of the direction of movement by a neuronal population." J Neurosci 8(8): 2928-2937.

Georgopoulos, A. P., A. Schwartz, et al. (1986). "Neuronal population coding of movement direction." Science 233`: 1416-1419.

Gilaie-Dotan, S., S. Ullman, et al. (2002). "Shape-selective stereo processing in human object-related visual areas." Hum Brain Mapp 15(2): 67-79.

Gillam, B. J. and M. L. Cook (2001). "Perspective based on stereopsis and occlusion." Psychol Sci 12(5): 424-9.

Gleason, T. C. and L. A. Rothblat (1994). "Landmark discrimination in the rat: a measure of allocentric spatial ability." Behav Neurosci 108(1): 206-9.

Gnadt, J. W. and L. E. Mays (1995). "Neurons in monkey parietal area LIP are tuned for eye-movement parameters in three-dimensional space." J Neurophysiol 73(1): 280-97.

Gogel, W. C. and J. D. Tietz (1979). "A comparison of oculomotor and motion parallax cues of egocentric distance." Vision Res 19(10): 1161-70.

Goodale, M. A. and A. D. Milner (1992). "Separate visual pathways for perception and action." Trends in Neuroscience 15: 20-25.

Graziano, M. (2006). "The Organization of Behavioral Repertoire in Motor Cortex." Annu Rev Neurosci.

Greene, E. and S. Gentner (2001). "Further consideration of size illusions in random dot stereograms." Percept Mot Skills 93(1): 205-12.

Gross, C. G., C. E. Rocha-Miranda, et al. (1972). "Visual properties of neurons in inferotemporal cortex of the Macaque." Journal of Neurophysiology 35(1): 96-111.

Hartley, T., C. M. Bird, et al. (2007). "The hippocampus is required for short-term topographical memory in humans." Hippocampus 17(1): 34-48.

Hasegawa, R. P., M. Matsumoto, and A. Mikami (2000). "Search target selection in monkey prefrontal cortex." J. Neurophysiol. 84: 1692-1996.

Hastie, T., R. Tibshirani, et al. (2001). The elements of statistical learning : data mining, inference, and prediction : with 200 full-color illustrations. New York, Springer.

He, Z. J. and K. Nakayama (1994). "Perceiving textures: beyond filtering." Vision Res 34(2): 151-62.

Heath, M. and G. Binsted (2007). "Visuomotor memory for target location in near and far reaching spaces." J Mot Behav 39(3): 169-77.

Himmelbach, M. and H. O. Karnath (2005). "Dorsal and Ventral Stream Interaction: Contributions from Optic Ataxia." Journal of Cognitive Neuroscience 17(4): 632-640.

Hinkle, D. A. and C. E. Connor (2005). "Quantitative characterization of disparity tuning in ventral pathway area V4." J Neurophysiol 94(4): 2726-37.

Hogervorst, M. A. and E. Brenner (2004). "Combining cues while avoiding perceptual conflicts." Perception 33(10): 1155-72.

Holscher, C., W. Jacob, et al. (2004). "Learned association of allocentric and egocentric information in the hippocampus." Exp Brain Res 158(2): 233-40.

Hoshi, E. and J. Tanji (2002). "Contrasting neuronal activity in the dorsal and ventral premotor areas during preparation to reach." J Neurophysiol 87(2): 1123-8.

Ishai, A., L. G. Ungerleider, et al. "Distributed representation of objects in the human ventral visual pathway." Proc. Natl. Acad. Sci. US A 96: 9379–9384.

Jackson, S. R., R. Newport, et al. (2005). "Where the eye looks, the hand follows; limb-dependent magnetic misreaching in optic ataxia." Curr Biol 15(1): 42-6.

Jeannerod, M. (1997). The cognitive neuroscience of action, Blackwell Oxford.

Johansson, R. S., G. Westling, et al. (2001). "Eye-hand coordination in object manipulation." J Neurosci 21(17): 6917-32.

Judge, S. J. and B. G. Cumming (1986). "Neurons in the monkey midbrain with activity related to vergence eye movement and accommodation." J Neurophysiol 55(5): 915-30.

Judge, S. J., B. J. Richmond, et al. (1980). "Implantation of magnetic search coils for measurement of eye position: an improved method." Vision Res 20(6): 535-8.

Julesz, B., T. V. Papathomas, et al. (2006). Foundations of cyclopean perception. Cambridge, Mass., MIT Press.

Kalaska, J. F. (1996). "Parietal cortex area 5 and visuomotor behavior." Can J Physiol Pharmacol 74(4): 483-98.

Kandel, S., Jessell (2000). "Principles of Neural Science."

Kesner, R. P., G. Farnsworth, et al. (1989). "Double dissociation of egocentric and allocentric space following medial prefrontal and parietal cortex lesions in the rat." Behav Neurosci 103(5): 956-61.

Kiani, R., H. Esteky, et al. (2005). "Differences in onset latency of macaque inferotemporal neural responses to primate and non-primate faces." J Neurophysiol 94(2): 1587-96.

Kitagawa, N. and S. Ichihara (2002). "Hearing visual motion in depth." Nature 416(6877): 172-4.

Knill, D. C. (2003). "Mixture models and the probabilistic structure of depth cues." Vision Res 43(7): 831-54.

Koechlin, E., C. Ody, et al. (2003). "The Architecture of Cognitive Control in the Human Prefrontal Cortex." Science 302(5648): 1181-1185.

Koenderink, J. J. and A. J. van Doorn (1981). "Exterospecific component of the motion parallax field." J Opt Soc Am 71(8): 953-7.

Koike, Y., H. Hirose, et al. (2006). "Prediction of arm trajectory from a small number of neuron activities in the primary motor cortex." Neurosci Res 55(2): 146-53.

Krigolson, O., N. Clark, et al. (2007). "The proximity of visual landmarks impacts reaching performance." Spat Vis 20(4): 317-36.

Kudoh, N. (2005). "Dissociation between visual perception of allocentric distance and visually directed walking of its extent." Perception 34(11): 1399-416.

Kurkin, S., N. Takeichi, et al. (2003). "Neurons in the caudal frontal eye fields of monkeys signal three-dimensional tracking." Ann N Y Acad Sci 1004: 262-70.

Lacquaniti, F., E. Guigon, et al. (1995). "Representing spatial information for limb movement: role of area 5 in the monkey." Cereb Cortex 5(5): 391-409.

Landy, M. S., L. T. Maloney, et al. (1995). "Measurement and modeling of depth cue combination: in defense of weak fusion." Vision Res 35(3): 389-412.

Lappin, J. S. and M. A. Fuqua (1983). "Accurate visual measurement of three-dimensional moving patterns." Science 221(4609): 480-2.

Lewis, J. W. and D. C. Van Essen (2000). "Corticocortical connections of visual, sensorimotor, and multimodal processing areas in the parietal lobe of the macaque monkey." J Comp Neurol 428(1): 112-37.

Livingstone, M. (1990). "Segregation of form, color, movement, and depth processing in the visual system: anatomy, physiology, art, and illusion." Res Publ Assoc Res Nerv Ment Dis 67: 119-38.

Loftus, A., P. Servos, et al. (2004). "When two eyes are better than one in prehension: monocular viewing and end-point variance." Exp Brain Res 158(3): 317-27.

Maguire, E. A., C. D. Frith, et al. (1998). "Knowing where things are parahippocampal involvement in encoding object locations in virtual large-scale space." J Cogn Neurosci 10(1): 61-76.

Makino, Y. and M. Yano (2006). "Pictorial cues constrain depth in da Vinci stereopsis." Vision Res 46(1-2): 91-105.

Maldonado, P. E., S. Friedman-Hill, et al. (2000). "Dynamics of striate cortical activity in the alert macaque: II. Fast time scale synchronization." Cereb Cortex 10(11): 1117-31.

Marotta, J. J. and M. A. Goodale (1998). "The role of learned pictorial cues in the programming and control of grasping." Exp Brain Res 121(4): 465-70.

Marr, D. and T. Poggio (1979). "A computational theory of human stereo vision." Proc R Soc Lond B Biol Sci 204(1156): 301-28.

Mather, G. and D. R. Smith (2004). "Combining depth cues: effects upon accuracy and speed of performance in a depth-ordering task." Vision Res 44(6): 557-62.

McKee, S. P. and P. Verghese (2002). "Stereo transparency and the disparity gradient limit." Vision Res 42(16): 1963-77.

Melmoth, D. R. and S. Grant (2006). "Advantages of binocular vision for the control of reaching and grasping." Exp Brain Res 171(3): 371-88.

Mershon, D. H. and J. N. Bowers (1979). "Absolute and relative cues for the auditory perception of egocentric distance." Perception 8(3): 311-22.

Miller, E. K. a. C., J.D. (2001). "An integrative theory of prefrontal cortex function." Ann. Rev. Neurosci. 24: 167-202.

Milner, A. D. and M. A. Goodale (1995). The visual brain in action. New York, Oxford University Press.

Mon-Williams, M. and J. R. Tresilian (2000). "Ordinal depth information from accommodation?" Ergonomics 43(3): 391-404.

Morris, R. G., J. J. Hagan, et al. (1986). "Allocentric spatial learning by hippocampectomised rats: a further test of the "spatial mapping" and "working memory" theories of hippocampal function." Q J Exp Psychol B 38(4): 365-95.

Murata, A., V. Gallese, et al. (1996). "Parietal neurons related to memory-guided hand manipulation." J Neurophysiol 75(5): 2180-6.

Murthy, V. N. and E. E. Fetz (1996). "Oscillatory activity in sensorimotor cortex of awake monkeys: synchronization of local field potentials and relation to behavior." J Neurophysiol 76(6): 3949-67.

Murthy, V. N. and E. E. Fetz (1996). "Synchronization of neurons during local field potential oscillations in sensorimotor cortex of awake monkeys." J Neurophysiol 76(6): 3968-82.

Musallam, S., B. D. Corneil, et al. (2004). "Cognitive Control Signals for Neural Prosthetics." Science 305(5681): 258-262.

Mushiake, H., Y. Tanatsugu, et al. (1997). "Neuronal activity in the ventral part of premotor cortex during target-reach movement is modulated by direction of gaze." J Neurophysiol 78(1): 567-71.

Nakayama, K. and S. Shimojo (1990). "da Vinci stereopsis: depth and subjective occluding contours from unpaired image points." Vision Res 30(11): 1811-25.

Naselaris, T., H. Merchant, et al. (2006). "Large-Scale Organization of Preferred Directions in the Motor Cortex. I. Motor Cortical Hyperacuity for Forward Reaching." Journal of Neurophysiology 96(6): 3231.

Neely, K. A., M. Heath, et al. (2008). "Egocentric and allocentric visual cues influence the specification of movement distance and direction." J Mot Behav 40(3): 203-13.

Nefs, H. T. and J. M. Harris (2008). "Induced motion in depth and the effects of vergence eye movements." J Vis 8(3): 8 1-16.

Neggers, S. F., R. H. Van der Lubbe, et al. (2006). "Interactions between ego- and allocentric neuronal representations of space." Neuroimage 31(1): 320-31.

Nelson, B. S. (2000). "Avian dependence on sound pressure level as an auditory distance cue." Anim Behav 59(1): 57-67.

Nishida, Y., O. Hayashi, et al. (2001). "Stereopsis-processing regions in the human parieto-occipital cortex." Neuroreport 12(10): 2259-63.

O'Brien, J. and A. Johnston (2000). "When texture takes precedence over motion in depth perception." Perception 29(4): 437-52.

O'Kane, L. M. and P. B. Hibbard (2007). "Vertical disparity affects shape and size judgments across surfaces separated in depth." Perception 36(5): 696-702.

O'Keefe, J. (1991). "An allocentric spatial model for the hippocampal cognitive map." Hippocampus 1(3): 230-5.

Ogle, K. N. (1954). "Stereopsis and vertical disparity." AMA Arch Ophthalmol 53(4): 495-504.

Ohzawa, I. and R. D. Freeman (1986). "The binocular organization of simple cells in the cat's visual cortex." J Neurophysiol 56(1): 221-42.

Ono, H. and H. Ujike (2005). "Motion parallax driven by head movements: conditions for visual stability, perceived depth, and perceived concomitant motion." Perception 34(4): 477-90.

Ono, H. and N. J. Wade (2005). "Depth and motion in historical descriptions of motion parallax." Perception 34(10): 1263-73.

Ono, M. E., J. Rivest, et al. (1986). "Depth perception as a function of motion parallax and absolute-distance information." J Exp Psychol Hum Percept Perform 12(3): 331-7.

Orban, G. A., P. Janssen, et al. (2006). "Extracting 3D structure from disparity." Trends Neurosci 29(8): 466-73.

Pagano, C. C. and G. P. Bingham (1998). "Comparing measures of monocular distance perception: verbal and reaching errors are not correlated." J Exp Psychol Hum Percept Perform 24(4): 1037-51.

Pagano, C. C. and R. W. Isenhower (2008). "Expectation affects verbal judgments but not reaches to visually perceived egocentric distances." Psychon Bull Rev 15(2): 437-42.

Palmer, S. E. (1999). Vision science : photons to phenomenology. Cambridge, Mass., MIT Press.

Panerai, F., V. Cornilleau-Peres, et al. (2002). "Contribution of extraretinal signals to the scaling of object distance during self-motion." Percept Psychophys 64(5): 717-31.

Paninski, L., M. R. Fellows, et al. (2004). "Spatiotemporal tuning of motor cortical neurons for hand position and velocity." J Neurophysiol 91(1): 515-32.

Parslow, D. M., R. G. Morris, et al. (2005). "Allocentric spatial memory in humans with hippocampal lesions." Acta Psychol (Amst) 118(1-2): 123-47.

Peh, C. H., F. Panerai, et al. (2002). "Absolute distance perception during in-depth head movement: calibrating optic flow with extra-retinal information." Vision Res 42(16): 1991-2003.

Pesaran, B., M. J. Nelson, et al. (2006). "Dorsal premotor neurons encode the relative position of the hand, eye, and goal during reach planning." Neuron 51(1): 125-34.

Pesaran, B., J. Pezaris, et al. (2002). "Temporal structure in neuronal activity during working memory in Macaque parietal cortex." Nature Neuroscience 5: 805-811.

Piaget, J. (1930). The Child's Conception of Physical Causality New York, Harcourt, Brace.

Ping-Sung Liao, S.-M. G., Zung-En Tsai (2006). "Feature Selection Strategy for Mass Detection in Mammograms." 2006 19th IPPR Conference on Computer Vision, Graphics, and Image Processing: 862-868.

Platt, M. L. and P. W. Glimcher (1999). "Neural correlates of decision variables in parietal cortex." Nature 400(6741): 233-8.

Poggio, G. E. (1995). "Mechanisms of stereopsis in monkey visual cortex." Cereb Cortex 5(3): 193-204.

Poggio, G. F. and B. Fischer (1977). "Binocular interaction and depth sensitivity in striate and prestriate cortex of behaving rhesus monkey." J Neurophysiol 40(6): 1392-405.

Poggio, G. F. and T. Poggio (1984). "The analysis of stereopsis." Annu Rev Neurosci 7: 379-412.

Press, W. H., S. A. Teukolsky, et al. (1992). Numerical Recipes. Cambridge, Cambridge University Press.

Prince, S. J., A. D. Pointon, et al. (2002). "Quantitative analysis of the responses of V1 neurons to horizontal disparity in dynamic random-dot stereograms." J Neurophysiol 87(1): 191-208.

Quian Quiroga, R., L. H. Snyder, et al. (2006). "Movement intention is better predicted than attention in the posterior parietal cortex." J Neurosci 26(13): 3615-20.

Quiroga, R. Q., L. Reddy, et al. (2005). "Invariant visual representation by single neurons in the human brain." Nature 435(7045): 1102-7.

Rauschecker, A. M., S. G. Solomon, et al. (2006). "Stereo and motion parallax cues in human 3D vision: can they vanish without a trace?" J Vis 6(12): 1471-85.

Recanzone, G. H., D. C. Guard, et al. (2000). "Correlation between the activity of single auditory cortical neurons and sound-localization behavior in the macaque monkey." J Neurophysiol 83(5): 2723-39.

Rizzuto, D. S., A. N. Mamelak, et al. (2005). "Spatial selectivity in human ventrolateral prefrontal cortex." Nature Neuroscience 8: 415-417.

Rogers, B. and M. Graham (1979). "Motion parallax as an independent cue for depth perception." Perception 8(2): 125-34.

Rogers, B. and M. Graham (1982). "Similarities between motion parallax and stereopsis in human depth perception." Vision Res 22(2): 261-70.

Rogers, B. J. and M. F. Bradshaw (1995). "Disparity scaling and the perception of frontoparallel surfaces." Perception 24(2): 155-79.

Rolls, E. T., R. G. Robertson, et al. (1997). "Spatial view cells in the primate hippocampus." Eur J Neurosci 9(8): 1789-94.

Rose, D., M. F. Bradshaw, et al. (2003). "Attention affects the stereoscopic depth aftereffect." Perception 32(5): 635-40.

Rosenbluth, D. and J. M. Allman (2002). "The effect of gaze angle and fixation distance on the responses of neurons in V1, V2, and V4." Neuron 33(1): 143-9.

Sakata, H., H. Shibutani, et al. (1994). "Functional properties of rotation-sensitive neurons in the posterior parietal association cortex of the monkey." Exp Brain Res 101(2): 183-202.

Sakata, H., H. Shibutani, et al. (1980). "Spatial properties of visual fixation neurons in posterior parietal association cortex of the monkey." J Neurophysiol 43(6): 1654-72.

Sakata, H., H. Shibutani, et al. (1985). "Neural mechanisms of space vision in the parietal association cortex of the monkey." Vision Res 25(3): 453-63.

Sakata, H., M. Taira, et al. (1997). "The TINS Lecture. The parietal association cortex in depth perception and visual control of hand action." Trends Neurosci 20(8): 350-7.

Sakata, H., M. Taira, et al. (1998). "Neural coding of 3D features of objects for hand action in the parietal cortex of the monkey." Philos Trans R Soc Lond B Biol Sci 353(1373): 1363-73.

Sakata, H., M. Taira, et al. (1999). "Neural representation of three-dimensional features of manipulation objects with stereopsis." Exp Brain Res 128(1-2): 160-9.

Sakata, H., M. Taira, et al. (1995). "Neural mechanisms of visual guidance of hand action in the parietal cortex of the monkey." Cereb Cortex 5(5): 429-38.

Sakata, H., K. Tsutsui, et al. (2005). "Toward an understanding of the neural processing for 3D shape perception." Neuropsychologia 43(2): 151-61.

Scheidt, R. A., M. A. Conditt, et al. (2005). "Interaction of visual and proprioceptive feedback during adaptation of human reaching movements." J Neurophysiol 93(6): 3200-13.

Schenk, T. (2006). "An allocentric rather than perceptual deficit in patient D.F." Nat Neurosci 9(11): 1369-70.

Scherberger, H., Jarvis, M.R., and Andersen, R.A. (2005). "Cortical Local Field Potential Encodes Movement Intentions in the Posterior Parietal Cortex." Neuron 46: 347-354.

Schwartz, A. B., R. E. Kettner, et al. (1988). "Primate motor cortex and free arm movements to visual targets in 3-dimensional space. 1. Relations between single cell discharge and direction of movement." J Neurosci 8(8): 2913-2927.

Seltzer, B. and D. N. Pandya (1980). "Converging visual and somatic sensory cortical input to the intraparietal sulcus of the rhesus monkey." Brain Res 192(2): 339-51.

Seltzer, B. and D. N. Pandya (1986). "Posterior parietal projections to the intraparietal sulcus of the rhesus monkey." Exp Brain Res 62(3): 459-69.

Shenoy, K. V., D. C. Bradley, et al. (1999). "Influence of gaze rotation on the visual response of primate MSTd neurons." J Neurophysiol 81(6): 2764-86.

Shenoy, K. V., D. Meeker, et al. (2003). "Neural prosthetic control signals from plan activity." Neuroreport 14(4): 591-6.

Shikata, E., F. Hamzei, et al. (2001). "Surface orientation discrimination activates caudal and anterior intraparietal sulcus in humans: an event-related fMRI study." J Neurophysiol 85(3): 1309-14.

Shimono, K. (1984). "Evidence for the subsystems in stereopsis: fine and coarse stereopsis." Japanese Psychological Research 26(3): 168-172.

Shipp, S., M. Blanton, et al. (1998). "A visuo-somatomotor pathway through superior parietal cortex in the macaque monkey: cortical connections of areas V6 and V6A." Eur J Neurosci 10(10): 3171-93.

Snyder, L. H., A. P. Batista, et al. (1997). "Coding of intention in the posterior parietal cortex." Nature 386(6621): 167-70.

Snyder, L. H., A. P. Batista, et al. (2000). "Intention-related activity in the posterior parietal cortex: a review." Vision Res 40: 1433-1441.

Snyder, L. H., K. L. Grieve, et al. (1998). "Separate body- and world-referenced representations of visual space in parietal cortex." Nature 394(6696): 887-91.

Sobel, E. C. (1990). "The locust's use of motion parallax to measure distance." J Comp Physiol [A] 167(5): 579-88.

Sober, S. J. and P. N. Sabes (2005). "Flexible strategies for sensory integration during motor planning." Nat Neurosci 8(4): 490-7.

Sperling, G. and M. S. Landy (1989). "Kinetic depth effect and identification of shape." J Exp Psychol Hum Percept Perform 15(4): 826-40.

Stevens, K. A. and A. Brookes (1987). "Probing depth in monocular images." Biol Cybern 56(5-6): 355-66.

Stricanne, B., R. A. Andersen, et al. (1996). "Auditory signals are transformed to eye-centered coordinates in posterior parietal cortex." J Neurophysiol 76: 2071-2075.

Stricanne, B., R. A. Andersen, et al. (1996). "Eye-centered, head-centered, and intermediate coding of remembered sound locations in area LIP." J Neurophysiol 76(3): 2071-2076.

Taira, M., K. I. Tsutsui, et al. (2000). "Parietal neurons represent surface orientation from the gradient of binocular disparity." J Neurophysiol 83(5): 3140-6.

Tamura, R., T. Ono, et al. (1990). "Recognition of egocentric and allocentric visual and auditory space by neurons in the hippocampus of monkeys." Neurosci Lett 109(3): 293-8.

Trotter, Y., S. Celebrini, et al. (1992). "Modulation of neural stereoscopic processing in primate area V1 by the viewing distance." Science 257(5074): 1279-81.

Tsutsui, K., M. Jiang, et al. (2001). "Integration of perspective and disparity cues in surface-orientation-selective neurons of area CIP." J Neurophysiol 86(6): 2856-67.

Tsutsui, K., H. Sakata, et al. (2002). "Neural correlates for perception of 3D surface orientation from texture gradient." Science 298(5592): 409-12.

Uka, T. and G. C. DeAngelis (2003). "Contribution of middle temporal area to coarse depth discrimination: comparison of neuronal and psychophysical sensitivity." J Neurosci 23(8): 3515-30.

Uka, T., H. Tanaka, et al. (2000). "Disparity selectivity of neurons in monkey inferior temporal cortex." J Neurophysiol 84(1): 120-32.

van Ee, R. and C. M. Schor (2000). "Unconstrained stereoscopic matching of lines." Vision Res 40(2): 151-62.

Van Pelt, S. and W. P. Medendorp (2008). "Updating target distance across eye movements in depth." J Neurophysiol 99(5): 2281-90.

Watt, S. J. and M. F. Bradshaw (2003). "The visual control of reaching and grasping: binocular disparity and motion parallax." J Exp Psychol Hum Percept Perform 29(2): 404-15.

Wei, M., G. C. DeAngelis, et al. (2003). "Do visual cues contribute to the neural estimate of viewing distance used by the oculomotor system?" J Neurosci 23(23): 8340-50.

Westheimer, G. and I. J. Tanzman (1956). "Qualitative depth localization with diplopic images." J Opt Soc Am 46(2): 116-7.

Wheatstone, C. (1838). "Contributions to the Physiology of Vision.—Part the First. On some remarkable, and hitherto unobserved, Phenomena of Binocular Vision." Philosophical Transactions of the Royal Society of London 128: 371-394.

Wilcox, L. M., J. H. Elder, et al. (2000). "The effects of blur and size on monocular and stereoscopic localization." Vision Res 40(26): 3575-84.

Womelsdorf, T., Fries, P., Mitra, P.P., and Desimone, R. (2005). "Gamma-band synchronization in visual cortex predicts speed of change detection." Nature 439: 733-736.

Wu, B., Z. J. He, et al. (2007). "The linear perspective information in ground surface representation and distance judgment." Percept Psychophys 69(5): 654-72.

Wurger, S. M. and M. S. Landy (1989). "Depth interpolation with sparse disparity cues." Perception 18(1): 39-54.

Xing, J. and R. A. Andersen (2000). "Models of the posterior parietal cortex which perform multimodal integration and represent space in several coordinate frames." J Cogn Neurosci 12(4): 601-14.

Zaehle, T., K. Jordan, et al. (2007). "The neural basis of the egocentric and allocentric spatial frame of reference." Brain Res 1137(1): 92-103.

Zahorik, P. and F. L. Wightman (2001). "Loudness constancy with varying sound source distance." Nat Neurosci 4(1): 78-83.

Zar, J. H. (1999). Biostatistical Analysis. New Jersey, Prentice Hall.

Ziegler, L. R. and R. F. Hess (1997). "Depth perception during diplopia is direct." Perception 26(10): 1125-30.